Journal of Medicinal Chemistry



# An Efficient Buchwald-Hartwig/Reductive Cyclization for the Scaffold Diversification of Halogenated Phenazines: Potent Antibacterial Targeting, Biofilm Eradication and Prodrug Exploration

Aaron T. Garrison, Yasmeen Abouelhassan, Dimitris Kallifidas, Hao Tan, Young Sik Kim, Shouguang Jin, Hendrik Luesch, and Robert William Huigens III

*J. Med. Chem.*, **Just Accepted Manuscript** • DOI: 10.1021/acs.jmedchem.7b01903 • Publication Date (Web): 11 Apr 2018



ACS Publications

is published by the American Chemical Society. 1155 Sixteenth Street N.W., Washington, DC 20036

# An Efficient Buchwald-Hartwig/Reductive Cyclization for the Scaffold Diversification of Halogenated Phenazines: Potent Antibacterial Targeting, Biofilm Eradication and Prodrug Exploration

Aaron T. Garrison[†], Yasmeen Abouelhassan[†], Dimitris Kallifidas[†], Hao Tan[‡], Young S. Kim[‡], Shouguang Jin[‡], Hendrik Luesch[†], Robert W. Huigens III[†*]

[†]*Department of Medicinal Chemistry, Center for Natural Products, Drug Discovery and Development (CNPD3), College of Pharmacy, University of Florida, Gainesville, Florida 32610, United States*

[‡]*Department of Molecular Genetics & Microbiology, College of Medicine, University of Florida, Gainesville, Florida 32610, United States*

* Corresponding author E-mail: rhuigens@cop.ufl.edu

**Abstract:**

Bacterial biofilms are surface-attached communities comprised of non-replicating persister cells housed within a protective extracellular matrix. Biofilms display tolerance towards conventional antibiotics, occur in ~80% of infections and lead to >500,000 deaths annually. We recently identified halogenated phenazine (HP) analogues which demonstrate biofilm-eradicating activities against priority pathogens; however, the synthesis of phenazines presents limitations. Herein we report of a refined HP synthesis which expedited the identification of improved biofilm-eradicating agents. 1-Methoxyphenazine scaffolds were generated through a Buchwald-Hartwig cross-coupling (70% average yield) and subsequent reductive cyclization (68% average yield), expediting the discovery of potent biofilm-eradicating HPs (e.g. **61;** MRSA BAA-1707 MBEC = 4.69 μM). We also developed bacterial-selective prodrugs (reductively-activated quinone-alkyloxycarbonyloxymethyl moiety) to afford HP **87**, which demonstrated excellent antibacterial and biofilm eradication activities against MRSA BAA-1707 (MIC = 0.15 μM, MBEC = 12.5 μM). Furthermore, active HPs herein exhibit negligible cytotoxic or hemolytic effects, highlighting their potential to target biofilms.

**Introduction:**

New antibacterial agents that operate through unique mechanisms of action are of significant importance to combat the emergence of antibiotic-resistant and tolerant bacteria. Bacteria utilize multiple mechanisms (e.g., target modification, drug inactivation, overexpression of efflux pumps) to acquire, or gain, resistance to antibiotics following drug exposure during treatment.[1] In contrast to acquired antibiotic resistance, free-floating bacteria can collectively form surface-attached biofilm communities resulting in an innate tolerance towards antibiotic therapies due to metabolically dormant persister cells (non-replicating bacteria).[2–4] Persistent biofilms are credited as the underlying cause of chronic and recurring bacterial infections, which is recognized as a major clinical problem resulting in an estimated 17 million new biofilm infections and >500,000 deaths each year.[5,6]

Each of our conventional antibiotic classes was initially discovered as growth-inhibiting agents that targeted rapidly-dividing planktonic bacteria in phenotypic screens/assays. In addition, the large majority of our antibiotic classes were discovered pre-1970, which was 25 years before bacterial biofilms were recognized as medically relevant.[7] As such, it should be no surprise that our clinically used antibiotic growth inhibitors have essentially no effect on non-replicating biofilm bacteria. Unfortunately, biofilm-associated infections remain an unanswered clinical problem as there are currently no biofilm-eradicating agents available to treat persistent and chronic biofilm-associated infections.[7] Biofilm-associated infections are highly prevalent, occurring in ~80% of all bacterial infections, and play a critical role in numerous infections and diseases, including: hospital-acquired infections, implanted medical device infections (e.g., prosthetic joint replacement), catheter-based infections, skin/burn wounds, endocarditis, periodontitis, caries (tooth decay) and lung infections in Cystic Fibrosis patients.[7]

Innovative strategies are needed to address the many concerns that drug-resistance and antibiotic-tolerance (biofilm infections) have placed on mankind. With the large majority of clinically used antibiotics being products of microbial warfare (e.g., penicillin, streptomycin, vancomycin), we reasoned that biofilm-eradicating microbial compounds exist and had likely not been identified or harnessed therapeutically. It is known that young Cystic Fibrosis (CF) patients endure persistent *Staphylococcus aureus* lung infections.[8] As these CF patients age, *Pseudomonas aeruginosa* co-infects the lungs of these patients and eradicates *S. aureus*. It is known that *P.*

*aeruginosa* is able to kill *S. aureus* through the use of phenazine antibiotics, which established the framework for our biofilm eradication strategy design as the initial *S. aureus* infections were likely biofilm-associated.[8–10]

We discovered that halogenated phenazine (HP) analogues of the marine phenazine 2-bromo-1-hydroxyphenazine **1** demonstrate potent antibacterial and biofilm-killing activities (Figure 1) against drug-resistant, Gram-positive pathogens (e.g. methicillin-resistant *Staphylococcus aureus* isolates) and *Mycobacterium tuberculosis*, which is responsible for 1.5 million deaths globally each year.[11–14] With the dual planktonic and biofilm-killing activity demonstrated by select halogenated phenazines, we find this class of natural product derived compounds to be exciting and unique. The majority of biofilm-eradicating agents operate through the destruction of bacterial membranes; however, halogenated phenazines operate through a metal(II)-dependent mechanism that enables a high degree of bacterial targeting.[12,15] Through the course of our investigations, we have found the chemical synthesis of halogenated phenazines, and highly substituted phenazines in general, to be quite challenging. Synthetic challenges related to scaffold diversification of biologically active heterocycles remain, yet motivated these studies and enabled us to generate novel halogenated phenazines that displayed an array of antibacterial and biofilm-eradicating activities. Here we report an efficient Buchwald-Hartwig/Reductive Cyclization (BH-RC) route enabling extensive biological investigations of novel HP analogues not readily accessed using previous routes (Figure 2). In addition, we report our investigations regarding the exploration of several phenolic-based prodrug strategies in an attempt to improve water solubility and target bacteria to avoid off-target metal-cation binding of HP analogues. Together, these investigations demonstrate the potential for halogenated phenazine analogues to be developed using multiple medicinal chemistry strategies.

**Results and Discussion:**

*Construction of the Halogenated Phenazine (HP) Scaffold:*

Although our previous HP analogues show great promise as antibacterial and biofilm-eradicating agents, a major hindrance in the rapid assembly of HP libraries was the inherently poor means of synthesizing the phenazine heterocycle. The reported phenazine syntheses by which the aforementioned halogenated phenazines were generated are not without shortcomings (Figure 2A). The phenylenediamine-quinone condensation used previously by our group suffers from a lack of regioselectivity with regard to substituents at

the 6-, 7-, 8-, and 9-positions of the phenazine heterocycle.[11,12] This leads to complications when structural fine-tuning is necessary for optimization of structure activity relationship (SAR) profiles. The regioisomers obtained from the condensation of an *ortho*-quinone and a mono-substituted phenylenediamine yields a mixture of products that are often not easily separable. Furthermore, structural characterization of the two resulting methoxyphenazine isomers is no trivial task. The Wohl-Aue reaction, at present, also leaves much to be desired in terms of synthetic efficiency to afford halogenated phenazine compounds.[15] The yields for phenazines synthesized from the Wohl-Aue reaction are often low, owing to the formation of diphenylamine and nitroso compounds as the major products.[16–18] Additionally, the conditions by which cyclization occurs in the Wohl-Aue reaction are very harsh (e.g. refluxing in a highly alkaline chemical environment).

There are a handful of remaining phenazine syntheses reported in literature; however, most either utilize homocoupling or offer little to no regioselectivity for asymmetric phenazines.[19–21] Perhaps the most elegant phenazine synthesis, reported by the Ellman group, incorporated a rhodium(III)-catalyzed [3 + 3] annulation by C−H amination with aromatic azides and diazobenzenes.[22] Using this route, phenazines with asymmetric substitution can be obtained in good yield but for our purposes, the synthesis would necessitate the preparation of either a diazobenzene or aryl azide diversity-incorporating coupling partner for each analogue. Consequently, improved methods by which halogenated phenazines can be rapidly synthesized needed to be developed. A primary goal of this work was to develop a modular methodology such that phenazine scaffolds could be generated using readily available materials (e.g. anilines, aryl halides), permitting a high degree of diversity with no additional synthetic steps.

One of the few synthetic methods known to regioselectively afford phenazine compounds is the reductive cyclization of 4-amino-2-nitrodiphenylamines under basic conditions using sodium borohydride.[23–25] This protocol has the potential to incorporate a multitude of commercially available anilines, nitrobenzenes, and aryl halides into the synthesis of the diarylamine intermediate via one of several well-described methods (e.g. Buchwald-Hartwig amination, Jourdan-Ullman coupling, nucleophilic aromatic substitution).[26–32] Thus, reductive cyclization was selected for the synthesis of halogenated phenazines to accommodate diverse substitution at the 6-, 7-, 8-, and 9-positions. We envisioned 1-methoxyphenazine intermediates could be obtained via reductive cyclization through two orientations of diarylamine intermediates: **2** and **3** (Figure 2B). In addition to expanding the scope of this synthesis, the use of two orientations of diarylamine intermediates can ostensibly

remedy one caveat with the synthesis: C2 rotation of the phenyl moiety housing the $R^1$ through $R^3$ substituents of intermediate **2** inverts the orientation of the $R^1$ and $R^3$ substituents such that two regioisomers can form in the reductive cyclization. In the case of singly *ortho*-substituted anilines, cyclization can only occur through one position (the remaining *ortho* position), which makes these substrates a non-issue for the proposed reactions. However, in the case where a *meta*-substituted aniline is used as the diversity-housing coupling partner, two regioisomers can form following reductive cyclization of the diarylamine intermediate (6- and 8-substituted phenazines). Fortunately, the use of both "standard" and "inverted" diarylamines as shown in Figure 2B paired with careful selection of coupling partners can, in theory, provide complete regioselectivity at the 6- through 9-positions.

Our synthesis commenced with investigation into coupling conditions for the generation of diarylamine intermediates. A copper-catalyzed Ullmann coupling, although frequently used to couple anilines to aryl halides, yielded no desired product in the reaction between anilines and 2-bromo-1-methoxy-3-nitrobenzene (**4**, Figure 3A).[28–30] With this shortcoming in mind, we then turned our attention toward a palladium-catalyzed Buchwald-Hartwig (BH) amination reaction as this chemistry has been very useful due to typical high yields and a broad substrate scope of coupling partners.[26,27] Initially, we attempted a BH cross-coupling between iodobenzene and 2-amino-1-methoxy-3-nitrobenzene (**5**), but observed no product formation (Figure 3B). We suspect this result is due to the electron-poor nature of the aniline coupling partner when positioned *ortho* to the nitro group on substrate **5**, although others have reported success with similar BH couplings using electron-poor anilines.[33,34] We also sought to design the synthesis such that a TBS-protected hydroxyphenazine could be generated from the reductive cyclization. Since we anticipated the necessity for demethylation of every successfully cyclized phenazine, this strategy would allow for far simpler deprotections en route to the corresponding HP target structures. However, the attempt to couple anilines to (2-bromo-3-nitrophenoxy)(*tert*-butyl)dimethylsilane (**8**) were also met with failure (Figure 3C).

To our delight, simple inversion of the anilinic and aryl halide coupling partners from the example shown in Figure 3B (e.g., from **5** and aryl halides to **4** and anilines) cleanly afforded both orientations of desired diarylamine intermediates in good yield (**2** and **3**, Figures 3D and 3E). Anilines were coupled to 2-bromo-1-methoxy-3-nitrobenzene (**4**) using 6 mol % tris(dibenzylideneacetone)dipalladium(0) with 18 mol % (±)-2,2′-bis(diphenylphosphino)-1,1′-binaphthalene (rac-BINAP) as a ligand to afford **2**-series diarylamines in 71%

average yield and inverted **3**-series diarylamine intermediates in 25% average yield. With diarylamine intermediates in hand, the reductive cyclization (RC) reactions were conducted using a procedure adapted from previously reported syntheses.[24] Using six equivalents of sodium borohydride in ethanolic solutions of 2 N sodium ethoxide, the reductive cyclizations proceeded smoothly for the **2**-series diarylamines, affording 1-methoxyphenazines in 70% average yield (22 examples; Figure 4). Interestingly, the **3**-series diarylamines yielded no desired 1-methoxyphenazine products from reductive cyclization. This is likely due to electron donation from the *ortho*-positioned anisole oxygen, rendering the nitro group nitrogen atom much less electrophilic.

Nonetheless, the successful formation of 17 1-methoxyphenazine scaffolds was achieved as planned (Figure 4). In several cases, unexpected 1-methoxyphenazine products (**31**, **41**, **44**, **45**) were obtained following reductive cyclization of the corresponding diarylamines (**19**, **22**, **23**, **24**). From these examples, it is apparent that select halogenated anilines are subject to substitution or over-reduction during cyclization and, as such, may not be ideal substrates for BH-RC. This result was initially surprising as analogous reductive ring closures have been previously reported to yield halogen-bearing phenazine products.[24,25] However, there is also literature precedence for the selective displacement of fluorine atoms during reductive ring closures en route to phenazine scaffolds.[35] Although initially discouraging, it is likely that this fluorine displacement could be utilized in future studies for regioselective cyclization from asymmetrical anilines or the introduction of nucleophilic groups during cyclization, as observed in the formation of 7-ethoxy-1-methoxyphenazine (**41**). In the case of the trifluoromethylated diarylamine **23**, formation of an orthoester was observed during reductive cyclization, which could be isolated under basic workup conditions. Although acid-promoted hydrolysis of this orthoester afforded the corresponding ethyl 6-methoxyphenazine-2-carboxylate (**44**) in quantitative yield, we found that direct conversion from diarylamine **23** to this ethyl ester analogue via standard reductive cyclization conditions followed by acidic workup afforded **44** in an improved 84% yield following column chromatography. However, despite these synthetic challenges related to halogenated aniline substrates, we were able to synthesize 7-chloro-1-methoxyphenazine **42** and 7,9-dichloro-1-methoxyphenazine **43** using this BH-RC route.

It was also noted, however, that silyl ethers were unstable toward these reductive cyclization conditions (Figure 4). Ring closure of diarylamine intermediate **24** afforded 1-methoxyphenazine **45** with loss of the silyl protecting group as the sole product in 64% yield. Anticipating the difficulty in selectively brominating the demethylated

1,7-diol counterpart of this analogue, we discontinued its advancement. Although desired TBS-protected products could be obtained in low yield (e.g. **49** was obtained from **28** in 31% yield), it was found that removal of the TBS group prior to reductive cyclization allowed for substantial improvements in 1-methoxyphenazine yields (e.g. a 31% yield for TBS-containing **49** compared to a 64**%** yield for the corresponding alcohol **50**).

Shortcomings notwithstanding, this two-step Buchwald-Hartwig/reductive cyclization (BH-RC) protocol yielded 21 discrete 1-methoxyphenazines with an average coupling yield of 70% and an average reductive cyclization yield of 68% (Figure 4). With this collection of 1-methoxyphenazines in hand, we advanced analogues toward HP final products for biological evaluation. Of the 21 novel 1-methoxyphenazines generated, 13 were demethylated using boron tribromide to afford 1-hydroxyphenazines in 89% average yield (Figure 5). Several 1-methoxyphenazines presented difficulty with this demethylation reaction, resulting in decomposition (**40**, **51**; structures found in Figure 4) or formation of unexpected products. Surprisingly, demethylation of 1-methoxyphenazines **48** and **50** resulted in concomitant bromide displacement of the primary alcohol or silyl ether to afford alkyl bromides **70** and **71** in 87% and 53% yield, respectively (Figure 6). Initially, this result was discouraging as the intention was to utilize the desired primary alcohol products for late-stage derivatization. These transformations, however, were perhaps fortuitous as reactions of the primary bromides with nucleophiles are likely preferable to attempting to selectively react the primary alcohols without undesired side reactions at the 1-position phenol.

Dibromination reactions of 1-hydroxyphenazines were conducted using 2.2 equivalents of *N*-bromosuccinimide in dichloromethane to afford HP target structures in 69% average yield (Figure 5A; analogues **52**-**65**). It should be noted that attempts to dibrominate the 1-hydroxyphenazine obtained from **47** at only the 2- and 4-positions were unsuccessful, as reactions using NBS or bromine in acetic acid both yielded 2,4,6-tribrominated HP **64** (and to a lesser extent, dealkylated side products). Despite this complication, the tribrominated analogue **64** was advanced to biological studies.

In our previous work, we disclosed 4-position halogenated HPs (i.e. without 2-position halogenation) to demonstrate excellent antibacterial activities against *Mycobacterium tuberculosis.*[11,12] These findings motivated the synthesis of a small sub-set of HPs for investigations into novel anti-MtB agents (**66** – **69**, Figure 5B). These four target analogues were chosen on the basis of the highly potent MIC activity (versus *S. aureus*) of the corresponding 2,4-dibrominated counterparts **52**, **53**, **56**, and **61** (vide infra). The chosen 1-

methoxyphenazines were selectively brominated at the 4-position using *N*-bromosuccinimide in refluxing dichloromethane to afford 4-bromo-1-methoxyphenazines which subsequently underwent boron tribromide demethylation to afford 4-bromo-1-hydroxyphenazine anti-MtB designed analogues **66** – **69** in 72% average yield over two steps.

Initially, the structure-activity relationships of this new BH-RC HP series (antibacterial activity discussed in the next section) suggested that structural modifications could be made to select positions of the phenazine scaffold (particularly the 7-position) that would result in activity gains against bacterial pathogens. This BH-RC synthetic route grants the opportunity to introduce functional groups to the phenazine scaffold, which can be used as handles for late-stage derivatization and development (e.g. **70** and **71**, Figure 6). To this end, we sought to utilize alkyl bromide compounds **70** and **71** for analogue synthesis with the goal of using functionalized 2,4-dibrominated HPs as starting materials. A last-step copper-catalyzed click reaction was chosen as the derivatization step due to generally high reaction yields and broad range of viable alkyne substrates.[36,37]

Although 7-(2-bromoethyl)phenazin-1-ol (**71**) was prone to elimination of HBr (likely owing to favorable conjugation of the resulting olefin with the phenazine heterocycle), **70** proved to be an robust analogue to functionalize. A reaction of sodium azide with **70** in *N*,*N*-dimethylformamide afforded a primary azide in quantitative yield. However, subsequent 2,4-dibromination of this product proved troublesome, yielding the desired product in only 31% yield (best of three attempts). To circumvent this issue, **70** was first brominated at the 2- and 4-positions, generating HP **65** in 73% yield (Figure 6). This dibrominated product was then subjected to azide displacement, yielding the crude azidophenazine **72**. To avoid complications arising from undesired hydroxyphenazine-copper chelation during the last-step click reaction, the phenol of crude **72** was protected using acetyl chloride and a catalytic amount of DMAP in dichloromethane to afford the acylated azidophenazine **73** in 59% yield over two steps. The final click reaction proceeded smoothly, reacting azidophenazine **73** with 1-pentyne, copper(II) sulfate, and sodium ascorbate in *tert*-butanol:water:dichloromethane (1:2:1) to afford triazole-HP **74** in 96% yield. For a full library of HP analogues synthesized in this study, see Supporting Information Figure 1.

*Antibacterial Investigations:*

Following the chemical synthesis of our new series of halogenated phenazine small molecules, we began antibacterial investigations using minimum inhibitory concentration (MIC) assays[11,12,15] to determine the growth-inhibitory activities against planktonic bacteria. MIC assays are operationally simple and provide a rapid approach to generating antibacterial profiles of HPs that allow for the identification of compounds to select for further investigation. We have found this to be a useful approach as HPs that demonstrate potent antibacterial activities in MIC assays typically perform well at eradicating biofilms using Calgary Biofilm Device (CBD) assays (discussed in later section).[11,12,15]

The 17 novel HP analogues obtained from these BH-RC studies were first evaluated for antibacterial activities against several drug-resistant strains of major bacterial pathogens (Table 1). This library of HPs hosts several analogues which demonstrate improved MIC activity from that of previous lead HPs.[11,12] Halogenated phenazines **61** and **63**, particularly, report MIC activity of <0.1 μM against methicillin-resistant *Staphylococcus aureus* (0.038 μM and 0.075 μM, respectively against MRSA BAA-1707) while also demonstrating potent activity against methicillin-resistant *S. epidermidis* (MRSE 35984; MIC 0.1 μM for **61** and **63**) and vancomycin-resistant *Enterococcus faecium* (VRE 700221; MIC 0.39 μM and 0.2 μM for **61** and **63**, respectively).

From mechanistic investigations regarding HP analogues, which are able to chelate select metal(II) cations[12,15], we suspected that substitution of the 9-position of the HP scaffold would not be well tolerated in terms of antibacterial activities due to steric interference with chelating metal(II)-cations. Expectedly, 9-alkylated HP analogues **57** and **58** were completely inactive against MRSA, MRSE, and VRE (MICs >100 μM). To further evaluate the nature of metal interaction observed from these inactive HPs, UV-vis determination of chelation kinetics was conducted. Therein, we observed little to no loss of absorbance at the $\lambda_{max}$ wavelength for HPs **57** and **58** following addition of ammonium iron(II) sulfate hexahydrate (see Supporting Information). In contrast, addition of iron(II) to active HP **61** presents a distinct loss of absorbance at the $\lambda_{max}$. To supplement kinetic chelation experiments, UV-vis evaluation of HP:metal(II) stoichiometry was conducted, wherein it was found that inactive HP **58** exhibited no chelation to copper(II) in contrast to active HP **61**, which chelates copper(II) in a manner representative of expected 2:1 HP:metal(II) stoichiometry (see Supporting Information). Thus, it was concluded that inactive HP analogues **57** and **58** were unable to chelate metal(II) cations due to 9-position steric bulk perturbing the metal-binding site of the HP scaffold, whereas potent antibacterial agent HP **61**

efficiently chelated iron(II) and copper(II) at rates analogous to those observed with previously reported active HPs.[12,15]

We were surprised to learn that mono-halogenated HPs **66** – **69** reported only good to moderate activity (MICs of 6.25 – 50 μM; Figure 5B) against MtB, suggesting this new series did not conform to our previously established predictive method for MtB activities (i.e. active dibrominated HPs against MRSA would correlate to active mono-halogenated counterparts against MtB).[11,12,15] Fortunately, we were pleased to learn that dihalogenated HP **61** (lead agent versus MRSA in MIC assays) reported excellent MIC activity against MtB (3.13 μM), proving to be equipotent to our previously reported anti-MtB lead.[11,12,15]

It was also discovered that triazole-HP **74** showed very poor activity against all bacterial pathogens tested against during these studies, with the most potent MIC being 18.8 μM against MRSE (Table 1). The analogue was tested as the acetylated HP as our previous reports have shown good activity from acetylated HP **1** as well as structurally-related halogenated quinolines.[24,38,39] These MIC results precluded further analogue synthesis from the HP click chemistry protocol.

*HeLa Cytotoxicity and Hemolysis Assessment:*

Several HPs that demonstrated potent antibacterial activities against MRSA BAA-1707, or proved to have anti-MtB activities, were evaluated for mammalian cytotoxicity against HeLa cells in LDH-release assays (Table 1). Cytotoxicity from HeLa cells generated from these assays were used to provide selectivity indexes (SI) for these HPs to quantify the targeting of bacterial cells. This series of HPs demonstrated excellent cytotoxicity profiles using this approach. Despite HPs **53** and **54** reporting cytotoxicity against HeLa cells at 100 μM (highest concentration tested; $IC_{50}$ >50 μM), the remaining 11 HP analogues tested (**52**, **55**, **56**, **59**, **61**, **63**, **64**, **66**, **67-69**) reported minimal, if any, cytotoxicity against HeLa cells ($IC_{50}$ >100 μM). Using these results, selectivity indices were generated (HeLa cell $IC_{50}$ divided by MRSA BAA-1707 MIC) for these HPs to quantify their high degree of selectivity and bacterial targeting relative to HeLa cells (SI >169 to >2,632 for HPs active against MRSA BAA-1707; Table 1).

In addition to mammalian cytotoxicity assessment, we conducted hemolysis assays with human red blood cells (RBCs). No HP analogue exceeded 3% hemolysis at 200 μM (Table 2). Most importantly, this finding (in addition to demonstrating a favorable safety profile) suggests that our new HP analogues act through a

mechanism that does not involve membrane lysis. QAC-10 is a known membrane-lysing agent that demonstrates antibacterial activities in addition to biofilm eradication. When tested alongside with our HP small molecules, QAC-10 served as a positive-control and demonstrated >99% hemolysis of RBCs at 200 μM.

*Biofilm Eradication Activities:*

Nine potent HPs (**52 – 56**, **59**, **61**, **63**, **64**; Table 2) were identified during initial MIC studies and advanced to biofilm eradication assays against MRSA, MRSE and VRE using Calgary Biofilm Devices (CBD; several potent HPs presented in Figure 7 to illustrate SAR and antibacterial profiles). CBDs are specialized 96-well plates that have lids containing pegs designed to sit down in microtiter wells (one peg per microtiter well) and provide bacteria with a surface for biofilm formation.[40,41] Biofilm eradication assays have three distinct phases, which include: 1) biofilm establishment (media and bacteria only, biofilms are established on CBD pegs), 2) compound treatment (compounds in media; test compounds have the chance to eradicate biofilms during this phase), and 3) growth and dispersion of viable biofilms (media only). Each of these phases involves static incubation (24 hours at 37 °C), a wash of the CBD pegs containing biofilms with subsequent lid transfer to new 96-well plate at the end of phases one and two; however, at the end of the final phase, the microtiter wells are evaluated for bacterial growth (turbidity). Upon completion of the assay, microtiter wells that are turbid from bacterial growth correspond to wells that contained viable biofilms that dispersed bacteria into the media followed by bacterial growth during phase 3. Microtiter wells without bacterial growth, or turbidity, at the end of the CBD assay corresponds to microtiter wells that contained eradicated biofilms (≥99.9% of biofilm cells eradicated based on previous studies[12,15]) that were unable to grow and disperse viable bacteria during phase 3 (see Figure 8A and supporting information for CBD plate images). HPs and control compounds were tested in 2-fold serial dilution and the lowest test concentration of a compound that is required to eradicate biofilms (from non-turbid microtiter wells) is known as the minimum biofilm eradication concentration (MBEC) value. The Calgary Biofilm Device also allows for planktonic toxicity (determination of minimum bactericidal concentration or MBC values) to be evaluated alongside the biofilm eradication activity, providing ideal information regarding planktonic and biofilm killing dynamics (MBC:MBEC ratios) from a single bacterial culture under the same experimental conditions.[11,12,15]

During these investigations, we identified several new HPs with potent biofilm eradication activities against MRSA, MRSE and VRE biofilms (Table 2). Against MRSA-1707 biofilms, 7-substituted HPs **55** (MBEC = 4.69

μM; 7-*tert*-butyl-HP), **61** (MBEC = 4.69 μM; 7-chloro-HP), **63** (MBEC = 2.35 μM; 7-phenoxy-HP) and **64** (MBEC = 4.69 μM; 7-diethylamine-6-bromo-HP) demonstrated potent killing activities (Figure 7). In addition, 6,8-dimethyl-HP **56** demonstrated potent MRSA BAA-1707 biofilm eradication (MBEC = 4.69 μM). Several HPs demonstrated excellent biofilm eradication activities against MRSA-2 (e.g., HP **55**; MBEC = 3.13 μM) and MRSA BAA-44 (e.g., HP **55**; MBEC = 9.38 μM). Multiple front-running MRSA antibiotics, including vancomycin, daptomycin and linezolid, demonstrated no biofilm eradication activities against MRSA biofilms at 2,000 μM (highest concentration tested) when tested alongside this series of halogenated phenazine small molecules. Against MRSE 35984 biofilms, HPs **55** (MBEC = 3.13 μM), **56** (MBEC = 4.69 μM) and **63** (MBEC = 4.69 μM) demonstrated highly potent eradication activities; however, several analogues reported MBEC values ≤ 25 μM against MRSE 35984 biofilms. In addition, several HPs from this series demonstrated potent, sub-micromolar MBEC activities against VRE 700221 biofilms with **55**, **61** (MBEC = 0.59 μM), **56**, **63** and **64** (MBEC = 0.78 μM) proving to be the most active agents against this pathogen. Viable biofilm cell counts were carried out using CBD pegs from select experiments with HP biofilm-eradicating agents and demonstrated ≥ 3 log reduction of viable biofilm cells at their corresponding MBEC values (≥99.9% biofilm cell killing), similar to previous findings (see supporting information).[12,15]

In addition to select antibiotic comparators, various biofilm eradication controls (e.g. QAC-10, CCCP)[11,12,15] along with metal-chelating agents (e.g. EDTA, TPEN)[12,15] were assayed alongside new halogenated phenazines. These comparator agents proved to be significantly less active, or inactive, in their ability to eradicate established biofilms in CBD assays when compared to these HPs. These data collectively point to the unique mechanism and biofilm-killing potency displayed by these HP small molecules. Similar to previous studies, the planktonic killing (MBC) to biofilm killing (MBEC) ratios generated from these Calgary Biofilm Device assays demonstrated that HPs have near equipotent killing activities against planktonic and biofilm bacteria (MBC:MBEC ratios 1-3; see Table 2), a profile that conventional antibiotic therapies do not possess.

Following biofilm eradication investigations in CBD assays, lead HP **61** was tested against biofilms of MRSE 35984 in live/dead staining experiments (Figure 8B). After a 24-hour biofilm establishment, HP **61** was added at 1, 5, and 10 μM then left to incubate against MRSE 35984 biofilms for an additional 24 hours at 37 °C. Images were then taken of treated and untreated biofilms using fluorescence microscopy to further demonstrate the highly potent eradication and clearance of MRSE 35984 biofilms with HP **61**.

*HP-Prodrug Strategy and Synthesis:*

Due to the inherently high CLogP values and potential for off-target metal-chelating events of lead HP analogues, we sought to preemptively address these concerns through the development of phenolic-based prodrug strategies (Figure 9). Although we were initially excited about the incorporation of water-soluble moieties at the 6- through 8-positions attainable by way of BH-RC, the lack of activity observed with triazole-HP **74** discouraged us from this endeavor. In lieu of 6- through 8-position modifications, prodrug strategies were sought wherein conjugation of water-soluble groups to the phenol group would afford HP analogues with reduced CLogP values. Although we initially devised our phenolic prodrug approach to attain improved water solubility and suppress off-target metal chelation, we realized the proposed functionalization strategy could ostensibly be used to impart bacterial selectivity onto our HP series. To this end, a library of bacterial-selective prodrugs (Figure 9F-I; HP-prodrugs synthesized using various alkylation reactions) was assembled (see Supporting Information for further descriptions of the employed prodrug strategies and proposed mechanisms of activation/HP release). Thus, a library of diverse, CLogP-guided prodrugs was synthesized from active HP scaffolds (Figure 9A-E; HP-prodrugs synthesized using acylation, alkylation and sugar-based syntheses).

*Biological Evaluation of HP-Prodrugs:*

We initiated the biological evaluation of this HP-prodrug library with MIC and MBEC assays against MRSA, MRSE, and VRE (Table 3). Among the CLogP-guided analogues, HP prodrugs **75**, **76**, **77**, and **78** were found to be active in MIC assays, reporting MICs between 0.0005 to 3.13 μM and MBECs of 0.78 to 75 μM against all strains (Table 3). Surprisingly, carbonate prodrugs **77** and **78** reported MICs of 0.0005 μM and 0.1 μM respectively against MRSA BAA-1707 (up to ~76-fold increase in potency relative to the corresponding HPs). As prodrug activity is not expected to exceed that of the active agent to which it is metabolized, we suspect the carbonate prodrugs temporarily protect HPs from ionization (phenolic pKa = ~6.7[12]), allowing for improved membrane permeability prior to intracellular activation of the prodrug (see Supporting Figures 4 and 5). Although these intriguing activities may warrant further investigation, the apparent susceptibility of prodrugs **75** – **78** to rapidly undergo enzymatic or chemical hydrolysis (implied by their highly potent antibacterial activities) may limit their utility *in vivo* in future endeavors.

Interestingly, the HP-glycoconjugate (**79**, Figure 9D) and HP-alkyloxycarbonyloxymethyl (AOCOM) prodrugs **80** and **82** (Figure 9E) demonstrated no activity in MIC assays. We suspect that differences in carbonate stability of the AOCOM series relative to HP-carbonates **77** and **78** are likely responsible for this activity disparity. Fortunately, human serum stability assays for HPs **80** and **82** reveal favorable serum half-lives ($t_{1/2}$) of 15.8 minutes and 7.3 minutes, respectively, which are in line with reported half-lives for structurally related prodrugs.[42] These data suggest the HP-AOCOM prodrugs could have potential for further *in vivo* experiments wherein host-dependent prodrug cleavage could occur.

In an effort to develop more stable HP prodrugs, we investigated ether-based prodrug moieties. We targeted the synthesis of boron-based ether **83** and beta-lactam **84**. Each of these HP-prodrugs were designed to target different host response/bacterial features relevant to infection. Pinacol boron-HP **83** was designed to undergo a host inflammation-induced oxidation of boron, followed by the liberation of an active HP compound at the site of bacterial infection.[43,44] Beta-lactam **84** was designed to target penicillin-binding proteins/beta-lactamases for an initial beta-lactam cleavage, followed by the liberation of the active HP compound.[45,46] Although we were able to isolate ether-linked prodrugs **83** and **84** (Figure 9F, 9G), we found them to be unstable and, thus, discontinued further investigations of these analogues.

We then moved to exploiting the bacterial cytoplasm for the intracellular release of active HPs.[47,48] The bacterial cytoplasm is a reductive environment and we drew inspiration from the natural product mitomycin C, a potent antibacterial agent and cytotoxin, that requires bioreductive activation of its quinone moiety before it can carry out its mode of action (DNA crosslinking).[47] Interestingly, reductively activated HP-disulfide prodrug **85** (Figure 9H) reported no antibacterial activity against any pathogen tested. We then designed two quinone-AOCOM (QuAOCOM) prodrugs **86** and **87** (Figure 9I) and found these agents to demonstrate antibacterial activities which were near equipotent to the corresponding HP counterparts with MICs = 2.35 μM and 0.15 μM, respectively, versus MRSA BAA-1707. The exceptional antibacterial activity of QuAOCOM **87** was confirmed via agar diffusion assay, wherein this prodrug reported activity near that of the parent HP **61** (Figure 8D). Additionally, the QuAOCOM prodrugs exhibited good to potent biofilm eradication activities against MRSA BAA-1707 (MBECs = 75 μM and 12.5 μM for **86** and **87**, respectively). To ensure this activity was not a result of prodrug activation in the assay medium, stability experiments were conducted in lysogeny broth (LB), wherein no loss of the prodrug moiety was observed at up to 16 hours at 37 °C (Figure 8C). Additionally,

serum stability assays for QuAOCOM prodrugs revealed half-lives of 6.3 ± 3.3 minutes and 11.4 ± 2.8 minutes for **86** and **87**, respectively (Table 3). Finally, QuAOCOM **87** proved to have an outstanding cytotoxicity ($IC_{50}$ >100 μM against HeLa cells; SI > 667) and hemolysis (2.7% hemolysis of RBCs at 200 μM) profile, similar to parent HPs identified during these studies. Based on our stability assays for this prodrug class along with the well-understood reductive conditions of the bacterial cytoplasm, we can conclude that the QuAOCOM prodrugs exhibit activities due to a bacterial-selective release mechanism. We are very encouraged by the initial activity profiles of these HP-QuAOCOM prodrugs and believe the reductive trigger of the quinone moiety in conjunction with the AOCOM linker to be an ideal platform for future developments regarding HP-based biofilm therapies.

**Conclusions:**

The design, optimization, and utilization of the BH-RC protocol reported herein has not only broadened the substrate scope for phenazine synthesis, but has also offered substantial improvement of regioselective control for modification at the 6- through 9-positions of the phenazine heterocycle. We have shown that intermediate 1-methoxyphenazines can be efficiently generated through a Buchwald-Hartwig cross-coupling (71% average yield) and a subsequent, relatively mild reductive cyclization (68% average yield) en route to final HP products. These disclosed syntheses have permitted the identification of novel HP agents which efficaciously eradicate biofilms of harmful, drug-resistant pathogens. We also now have an improved understanding of the importance of metal chelation in the antibacterial mode of action as demonstrated by the apparent liability of 9-position functionalization in HP analogues (HPs **57** and **58**). Novel lead HP **61** demonstrates the remarkable ability to eradicate biofilms of domestically-threatening MRSA (MBEC = 4.69 μM) while also reporting good activity in antibacterial susceptibility assays against the worldwide bacterial threat *Mycobacterium tuberculosis* (MIC = 3.13 μM).

Furthermore, prodrug investigations afforded the discovery of analogues with potential therapeutic utility. AOCOM prodrugs **80** and **82** are endowed with improved CLogP values and were shown to be activated in human serum. In addition, the bacterial-selective QuAOCOM prodrugs **86** and **87** were designed to target the reductive cytoplasm of bacteria for requisite bioreduction of their quinone moiety, which triggers HP release. Development of HP prodrugs herein has strengthened our understanding of what the synthetic capabilities are for phenolic functionalization of this compound class. Naturally, all prodrug avenues have not yet been

exhausted and further development of HP prodrugs will be forthcoming. The potent biofilm eradication activities of new halogenated phenazines in conjunction with negligible hemolytic toxicity or mammalian cytotoxicity represent a unique profile compared to our current antibiotic arsenal. Thus, halogenated phenazines and prodrugs thereof may prove to be invaluable agents for combatting the growing threat of biofilm-associated bacterial infections worldwide.

**Experimental:**

**I) General Information.** All synthetic reactions were carried out under an inert atmosphere of argon unless otherwise specified. All reagents for chemical synthesis were purchased from commercial sources and used without further purification. Reagents were purchased at ≥ 95% purity and commercially available controls were used in our biological investigations without further purification. All microwave reactions were carried out in sealed tubes in an Anton Paar Monowave 300 Microwave Synthesis Reactor. A constant power was applied to ensure reproducibility. Temperature control was automated via IR sensor and all indicated temperatures correspond to the maximal temperature reached during each experiment. Analytical thin layer chromatography (TLC) was performed using 250 μm Silica Gel 60 F254 pre-coated plates (EMD Chemicals Inc.). Flash column chromatography was performed using 230-400 Mesh 60Å Silica Gel from Sorbent Technologies. All melting points were obtained, uncorrected, using a Mel-Temp capillary melting point apparatus from Laboratory Services, Inc.

NMR experiments were recorded using broadband probes on a Varian Mercury-Plus-400 spectrometer via VNMR-J software (400 MHz for $^{1}$H and 100 MHz for $^{13}$C) and a Bruker Avance II (600 MHz for $^{1}$H NMR; 150 MHz for $^{13}$C NMR). All spectra are presented using MestReNova 11.0 (Mnova) software and are displayed without the use of the signal suppression function. Spectra were obtained in the following solvents (reference peaks also included for $^{1}$H and $^{13}$C NMRs): $CDCl_3$ ($^{1}$H NMR: 7.26 ppm; $^{13}$C NMR: 77.23 ppm) and $d_6$-DMSO ($^{1}$H NMR: 2.50 ppm; $^{13}$C NMR: 39.52 ppm). All NMR experiments were performed at room temperature. Chemical shift values (δ) are reported in parts per million (ppm) for all $^{1}$H NMR and $^{13}$C NMR spectra. $^{1}$H NMR multiplicities are reported as: s = singlet, br. s = broad singlet, d = doublet, t = triplet, q = quartet, m = multiplet. High-Resolution Mass Spectrometry (HRMS) were obtained for all new compounds from the Chemistry Department at the University of Florida.

All compounds evaluated in biological assays were determined to be ≥ 95% pure via LC-MS using a Shimadzu Prominence HPLC system, AB Sciex 3200 QTRAP spectrometer and a Kinetex C18 column (50 mm × 2.1 mm × 2.6 μm) with a 35-minute linear gradient from 10-65% acetonitrile in 0.5% formic acid at a flow rate of 0.25 mL/min. Bacterial strains used during these investigations include: methicillin-resistant *Staphylococcus aureus* (Clinical Isolate from Shands Hospital in Gainesville, FL: MRSA-2; ATCC strains: BAA-1707, BAA-44) methicillin-resistant *Staphylococcus epidermidis* (MRSE strain ATCC 35984), and vancomycin-resistant *Enterococcus faecium* (VRE strain ATCC 700221). All compounds were stored as DMSO stocks at room temperature in the absence of light for several months at a time without observing any loss in biological activity. To ensure compound integrity of our DMSO stock solutions, we did not subject DMSO stocks of our test compounds to freeze-thaw cycles.

**II) Chemistry.** This chemistry section includes the following items, in numerical order: (a) synthetic procedures, (b) compound characterization data for analogues synthesized via general procedures, (c) UV-vis experiments for HP complex formation with iron(II) and (d) spectroscopic determination of prodrug stability in LB media.

**II.a) Synthetic procedures**

**1) General Procedure for the Buchwald-Hartwig Amination (9-26, 28, 30).** To a stirring solution of **4** (436.2 mg, 1.88 mmol) and desired aniline (2.26 mmol) in toluene was added tris-(dibenzylideneacetone)dipalladium(0) (103.5 mg, 0.11 mmol), (±)-2,2′-Bis(diphenylphosphino)-1,1′-binaphthalene (210.5 mg, 0.34 mmol), and sodium tert-butoxide (234.6 mg, 2.44 mmol). The reaction was allowed to stir for 16 hours at 100 °C. The mixture was then allowed to cool to room temperature and transferred to a separatory funnel containing ethyl acetate and saturated sodium bicarbonate. The organic layer was sequentially washed with sodium bicarbonate and brine before the organic layer was collected. The organic layer was then dried with anhydrous sodium sulfate, filtered, and concentrated in vacuo. The crude solid was purified via flash column chromatography using hexanes:ethyl acetate (95:5 to 80:20) to elute pure diarylamines.

**2) General Procedure for the Removal of TBS Ethers (27, 29).** To a stirring solution of *tert*-butyl-di-methyl silyl ethers (561.7 mg, 1.45 mmol) in anhydrous tetrahydrofuran (15 mL) was added 2.17 mL (2.17 mmol) of a 1 M solution of tetrabutyl ammonium fluoride in tetrahydrofuran. The reaction mixture was allowed to stir for 2

hours at room temperature. The reaction was then quenched with water and transferred to a separatory funnel containing ethyl acetate and brine. The organic layer was sequentially washed with brine before the organic layer was collected. The organic layer was dried with anhydrous sodium sulfate, filtered, and concentrated in vacuo. The crude solid was purified via flash column chromatography using hexanes:ethyl acetate (99:1 to 85:15) to elute pure alcohols as red oily residues.

**3) General Procedure for Reductive Cyclization with Sodium Borohydride and Sodium Ethoxide (31-51).** To a stirring solution of diarylamine (1.27 mmol) in 2 N sodium ethoxide in ethanol (35 mL) was added sodium borohydride (290 mg, 7.66 mmol). The reaction was allowed to stir for 2 hours at 60 °C. The reaction was cooled to room temperature, quenched with water and then transferred to a separatory funnel containing ethyl acetate and brine. The organic layer was sequentially washed with brine before the organic layer was collected. The organic layer was dried with anhydrous sodium sulfate, filtered, and concentrated *in vacuo*. The crude solid was purified via flash column chromatography using hexanes:ethyl acetate (99:1 to 85:15) to elute pure 1-methoxyphenazine analogues.

**4) General Procedure for Dibromination of 1-Hydroxyphenazines (52-65):** Desired 1-hydroxyphenazines (0.24 mmol) and *N*-bromosuccinimide, (86.2 mg, 0.48 mmol) were dissolved in dichloromethane (15 mL) and allowed to stir at room temperature for 2 hours. The reaction was diluted with dichloromethane and quenched with brine (3 x 20 mL). The organic layer was dried with sodium sulfate, filtered and concentrated. The reaction contents were then concentrated, adsorbed onto silica gel and purified via column chromatography using dichloromethane to elute pure 2,4-dibromohydroxyphenazine analogues as yellow solids.

**5) General Procedure for Boron Tribromide Demethylation (66-71; 97-109 see ESI).** To a round bottom flask was added the desired 1-methoxyphenazine (1.07 mmol) dissolved in anhydrous dichloromethane (18 mL). The mixture was brought to -78 °C in a dry ice bath before dropwise addition of 1M boron tribromide solution in dichloromethane (6.4 mL, 6.41 mmol). The reaction was left to stir at -78 °C for 1 hour, and then allowed to reach ambient temperature for reaction overnight. The reaction was heated to reflux for 8 hours until complete (monitored by TLC). The solution was transferred to a separatory funnel containing an aqueous solution of saturated sodium bicarbonate, and then extracted with dichloromethane. Organic solvents were dried with sodium sulfate, filtered through cotton, and removed *in vacuo*. The resulting solid was purified via

column chromatography using dichloromethane to elute pure 1-hydroxyphenazines as yellow solids. Note: Analogous procedures were used for all demethylation reactions using boron tribromide ($BBr_3$).

**6) Synthesis of 7-(azidomethyl)-2,4-dibromophenazin-1-yl acetate (73)**: HP **65** (33.6 mg, 0.08mmol) was added to a round-bottom flask and dissolved in *N,N*-dimethylformamide (4 mL). Sodium azide (12.2 mg, 0.188 mmol) was added and the reaction was stirred at room temperature for 2 hours. Following completion by TLC, the reaction was diluted with ethyl acetate and quenched with brine (3 x 50 mL). The organic layer was dried with sodium sulfate, filtered and concentrated. The crude solid was then dissolved in dichloromethane (10 mL). Triethylamine (6 µL, 0.04 mmol), a catalytic amount of 4-dimethlyaminopyridine, then acetyl chloride (3 µL, 0.03 mmol) were added at room temperature. The reaction was allowed to stir for one hour before being quenched with an aqueous solution of saturated sodium bicarbonate. The resulting mixture was then transferred to a separatory funnel and extracted with dichloromethane. The organic layer was then dried with anhydrous sodium sulfate, filtered, and concentrated *in vacuo*. The crude solid was purified via flash column chromatography using dichloromethane as the eluent to afford **73** as a yellow oily residue (20.1 mg, 59% over two steps). $^1$H NMR (400 MHz, $CDCl_3$): δ 8.35 (s, 1H), 8.30 (m, 1H), 8.25 (d, *J* = 9.0 Hz, 1H), 7.83 (dd, *J* = 9.0, 1.9 Hz, 1H), 4.66 (s, 2H), 2.61 (s, 3H). $^{13}$C NMR (100 MHz, $CDCl_3$): δ 168.3, 145.2, 143.4, 143.1, 140.6, 139.9, 137.9, 136.1, 132.1, 130.7, 128.4, 122.3, 117.5, 54.7, 20.9. HRMS (ESI): calc. for $C_{15}H_{10}Br_2N_5O_2$ $[M+H]^+$: 451.9176, found: 451.9176.

**7) Synthesis of 2,4-dibromo-7-((4-propyl-1H-1,2,3-triazol-1-yl)methyl)phenazin-1-yl acetate (74)**: Anhydrous copper sulfate (2.2 mg, 0.01 mmol) and sodium ascorbate (8.0 mg, 0.04 mmol) were dissolved in a solution of *tert*-butanol:$H_2O$ (1:2, 300 µL) and was added to a round-bottom flask containing **73** (12.2 mg, 0.06 mmol). 1-Pentyne (16.0 µL, 0.16 mmol) was added, followed by dichloromethane (3.0 mL). The biphasic mixture was vigorously stirred at room temperature for 16 hours until starting material was fully consumed as determined by TLC analysis. The mixture was quenched with brine (2 x 50 mL) and the product was extracted with dichloromethane. The organics were collected, dried with sodium sulfate, filtered and concentrated to afford pure **74** (96%, 13.5 mg) as a yellow solid. $^1$H NMR (600 MHz, DMSO-$d_6$): δ 8.68 (s, 1H), 8.28 (d, *J* = 9.0 Hz, 1H), 8.08 – 8.06 (m, 2H), 7.93 (dd, *J* = 9.0, 1.9 Hz, 1H), 5.93 (s, 2H), 2.62 (t, *J* = 7.5 Hz, 2H), 2.57 (s, 3H), 1.62 (sextet, *J* = 7.4 Hz, 2H), 0.91 (t, *J* = 7.4 Hz, 3H). $^{13}$C NMR (150 MHz, DMSO-$d_6$): δ 168.0, 147.3, 144.5,

142.5, 142.1, 141.2, 139.7, 137.1, 135.8, 132.6, 129.9, 127.3, 122.7, 121.6, 117.2, 52.2, 27.1, 22.2, 20.4, 13.6. HRMS (ESI): calc. for $C_{20}H_{18}Br_2N_5O_2$ $[M+H]^+$: 519.9803, found: 519.9793. MP: 203 – 205 °C.

**8) General Procedure for the Synthesis of HP Esters/Carbamate Prodrugs (75, 76).** To a stirring solution HP **1** (62.0 mg, 0.18 mmol), triethylamine (48 µL, 0.35 mmol), and a catalytic amount of 4-dimethlyaminopyridine in dichloromethane (20 mL) was added the acid chloride or carbamoyl chloride reagent (0.35 mmol) at room temperature. The reaction was allowed to stir for two hours before being quenched with an aqueous solution of saturated sodium bicarbonate. The resulting mixture was then transferred to a separatory funnel and ethyl acetate was added to extract the product. The organic layer was sequentially washed with water and brine before being collected. The organic layer was then dried with anhydrous sodium sulfate, filtered, and concentrated *in vacuo*. The respective ester or carbamate derivative was purified via flash column chromatography using hexanes:ethyl acetate (99:1 to 80:20) to elute, yielding pure products as yellow solids.

**9) General Procedure for the Synthesis of HP-Carbonates (77, 78):** Tetraethyleneglycol monomethyl ether (101.4 µL, 0.48 mmol) was placed in an oven-dried round-bottomed flask and dissolved in anhydrous dichloromethane (2 mL) and cooled to 0 °C. Pyridine (46.4 µL, 0.58 mmol) and triethylamine (16.8 µL 0.12 mmol) was then added via syringe, followed by triphosgene (71.2 mg, 0.24 mmol) dissolved in dichloromethane (2 mL). The resulting mixture was stirred from 0 °C to room temperature and continued to stir at room temperature for 5 hours. The reaction was then cooled to 0 °C before the addition of solution of **61** (118.2 mg, 0.30 mmol) and triethylamine (63 µL 0.45 mmol) in anhydrous dichloromethane was added to the reaction dropwise. The reaction was allowed to reach ambient temperature for reaction overnight. After the reaction was complete by TLC, the reaction mixture was poured into a separatory funnel containing brine (20 mL). The organic layer was drawn and the extracts were collected, dried over sodium sulfate, filtered, and concentrated under vacuum. The resulting crude material was purified using flash column chromatography with 3:1 hexanes:ethyl acetate to 100% ethyl acetate as eluent to yield **77** (183.1 mg, 99% yield) as a yellow solid.

**10) Synthesis of HP-glucoconjugate prodrug 79 ((2*S*,3*R*,4*S*,5*S*,6*R*)-2-((2,4-dibromophenazin-1-yl)oxy)-6-(hydroxymethyl)tetrahydro-2H-pyran-3,4,5-triol):** To a sealed microwave vial was added HP **1** (50.0 mg, 0.14 mmol), potassium carbonate (39.0 mg, 0.28 mmol) in methanol (5 mL). The resulting mixture was heated to 80 °C in the microwave reactor for a single 5 minute cycle. After that time, acetobromo-α-D-glucose (145

mg, 0.35 mmol) was added to the reaction vial. The reaction was cooled to room temperature and the solvent was removed *in vacuo*. The crude residue was taken up in ethyl acetate, transferred to a separatory funnel and then washed with water and extracted with ethyl acetate three times. The organic layers were combined, dried with anhydrous sodium sulfate, filtered and concentrated *in vacuo*. The crude solid was dissolved in methanol (6 mL) and sodium ethoxide (40.8 mg, 0.60 mmol) was added. The reaction was allowed to stir for 16 hours, then was diluted with dichloromethane and transferred to a separatory funnel. The organic layer was drawn and the extracts were collected, dried over sodium sulfate, filtered, and concentrated under vacuum. The crude solid was rinsed with ice-cold water and methanol, then dried *in vacuo* to afford pure desired product as a pale yellow solid (17.7 mg, 24% over 2 steps). $^{1}$H NMR (600 MHz, DMSO-$d_6$): δ 8.56 (s, 1H), 8.38 – 8.26 (m, 2H), 8.14 – 8.02 (m, 2H), 6.03 (d, $J$ = 7.7 Hz, 1H), 5.57 (d, $J$ = 4.9 Hz, 1H), 5.11 (d, $J$ = 5.2 Hz, 1H), 4.98 (d, $J$ = 5.2 Hz, 1H), 4.20 (t, $J$ = 5.7 Hz, 1H), 3.59 – 3.40 (m, 2H), 3.38 – 3.25 (m, 2H, partially buried under water signal), 3.14 (m, 2H). $^{13}$C NMR (150 MHz, DMSO-$d_6$): δ 148.9, 142.3, 141.4, 139.8, 137.8, 136.4, 132.6, 132.5, 129.3, 129.3, 118.0, 115.8, 104.0, 77.8, 76.9, 74.8, 69.9, 60.8. HRMS (DART): calc. for $C_{18}H_{17}Br_2N_2O_6$ $[M+H]^+$: 516.9429, found: 516.9435. MP: 199 – 201 °C.

**11) Synthesis of alkyloxycarbonyloxymethyl ("AOCOM") carbonate prodrugs (80-81, 85-87):** To a stirring solution of the desired alkyloxy chloromethyl carbonate (0.08 mmol) in acetone (2 mL) was added sodium iodide (10.5 mg, 0.07 mmol). The reaction was allowed to stir for two hours at room temperature. Then, this mixture was added to a stirring solution of **1** (23.5 mg, 0.07 mmol) and potassium carbonate (11.0 mg, 0.08 mmol) in acetone (2 mL). After stirring for 14 additional hours, the reaction was quenched by addition of deionized water. The resulting mixture was then transferred to a separatory funnel and ethyl acetate was added to extract the product. The organic layer was sequentially washed with sodium bicarbonate and brine before being collected. The organic layer was then dried with anhydrous sodium sulfate, filtered, and concentrated *in vacuo*. The resulting crude material was purified using flash column chromatography with 3:1 hexanes:ethyl acetate to 100% ethyl acetate as eluent to yield AOCOM prodrugs as yellow solids.

**12) Synthesis of ((2,4-dibromophenazin-1-yl)oxy)methyl (2-(2-(2-(2-hydroxyethoxy)ethoxy)ethoxy)ethyl) carbonate (82):** To a stirring solution of **81** (25.8 mg, 0.03 mmol) at 0 °C in 6 mL of anhydrous tetrahydrofuran was added 34 µL of a 1 M solution of tetrabutylammonium fluoride (0.03 mmol). The reaction mixture was allowed to stir for 6 hours, slowly reaching ambient temperature. The reaction was then quenched with water

and transferred to a separatory funnel containing ethyl acetate and brine. The organic layer was sequentially washed with brine before the organic layer was collected. The organic layer was dried with anhydrous sodium sulfate, filtered, and concentrated *in vacuo*. The crude solid was purified via flash column chromatography using ethyl acetate to elute pure **82** as a yellow oily residue (60% yield, 11.0 mg). $^{1}$H NMR (400 MHz, $CDCl_3$): δ 8.37 (m, 1H), 8.32 (s, 1H), 8.28 (m, 1H), 7.97 – 7.89 (m, 2H), 6.26 (s, 2H), 4.39 – 4.23 (m, 2H), 3.73 – 3.68 (m, 4H), 3.68 – 3.54 (m, 10H). $^{13}$C NMR (100 MHz, $CDCl_3$): δ 154.7, 149.7, 143.5, 143.0, 140.7, 138.4, 136.5, 132.3, 132.0, 130.2, 129.8, 120.5, 116.7, 92.4, 72.7, 70.9, 70.9, 70.7, 70.5, 69.0, 67.7, 62.0. HRMS (ESI): calc. for $C_{22}H_{25}Br_2N_2O_8$ $[M+H]^+$: 604.9954, found: 604.9951.

**II.b) Compound characterization data for analogues synthesized via general procedures, in numerical order. Additional information can be found in the Supporting Information document.**

**2-Methoxy-6-nitro-*N*-phenylaniline** (**9**). Yield: 81%; 206.0 mg was isolated as a red oily residue. $^{1}$H NMR (400 MHz, $CDCl_3$): δ 8.18 (br. s, 1H), 7.71 (dd, *J* = 8.5, 1.4 Hz, 1H), 7.28 – 7.17 (m, 2H), 7.09 (dd, *J* = 8.0, 1.4 Hz, 1H), 7.01 (d, *J* = 8.3 Hz, 1H), 6.98 (tt, *J* = 7.2, 1.0 Hz, 1H), 6.85 – 6.79 (m, 2H), 3.75 (s, 3H). $^{13}$C NMR (100 MHz, $CDCl_3$): δ 152.7, 142.3, 140.5, 129.6, 128.7, 122.4, 120.7, 118.6, 118.1, 116.3, 56.3. MP: 55 – 57 °C. HRMS (ESI): calc. for $C_{13}H_{13}N_2O_3$ $[M+H]^+$: 245.0921, found: 245.0930. Note: Compound has been previously reported (CAS: 7575-27-1), but no spectra were found for comparison.

**2-Methoxy-6-nitro-*N*-(*p*-tolyl)aniline (10).** Yield: 94%; 460.8 mg was isolated as a red oily residue. $^{1}$H NMR (400 MHz, $CDCl_3$): δ 8.18 (br. s, 1H), 7.71 (dd, *J* = 8.5, 1.4 Hz, 1H), 7.08 (dd, *J* = 8.1, 1.4 Hz, 1H), 7.04 (d, *J* = 8.3 Hz, 2H), 6.97 (dd, *J* = 8.5, 8.0 Hz, 1H), 6.75 (d, *J* = 8.3 Hz, 2H), 3.75 (s, 3H), 2.31 (s, 3H). $^{13}$C NMR (100 MHz, $CDCl_3$): δ 152.4, 139.9, 139.8, 132.1, 130.4, 129.3, 120.1, 118.9, 118.2, 116.3, 56.4, 20.9. HRMS (ESI): calc. for $C_{14}H_{15}N_2O_3$ $[M+H]^+$: 259.1077, found: 259.1085. MP: 65 – 67 °C.

***N*-(4-Ethylphenyl)-2-methoxy-6-nitroaniline (11).** Yield: 71%; 83.3 mg was isolated as a red oily residue. $^{1}$H NMR (400 MHz, $CDCl_3$): δ 8.21 (br. s, 1H), 7.72 (dd, *J* = 8.5, 1.4 Hz, 1H), 7.12 – 7.05 (m, 3H), 6.98 (dd, *J* = 8.5, 8.0 Hz, 1H), 6.85 – 6.68 (m, 2H), 3.76 (s, 3H), 2.62 (q, *J* = 7.6 Hz, 2H), 1.23 (t, *J* = 7.6 Hz, 3H). $^{13}$C NMR (100 MHz, $CDCl_3$): δ 152.4, 139.9, 138.5, 130.3, 128.1, 120.1, 118.9, 118.1, 116.3, 56.3, 28.3, 15.8. Note: One $^{13}$C signal missing in the aromatic region, likely due to signal overlap. HRMS (ESI): calc. for $C_{15}H_7N_2O_3$ $[M+H]^+$: 273.1234, found: 273.1243.

**2-Methoxy-6-nitro-*N*-(4-propylphenyl)aniline (12)**. Yield: 71%; 453.3 mg was isolated as a red oily residue. $^1$H NMR (400 MHz, $CDCl_3$): δ 8.24 (br. s, 1H), 7.72 (dd, *J* = 8.5, 1.4 Hz, 1H), 7.14 – 7.03 (m, 3H), 6.98 (dd, *J* = 8.5, 8.0 Hz, 1H), 6.84 – 6.73 (m, 2H), 3.75 (s, 3H), 2.57 (dd, *J* = 8.5, 6.7 Hz, 2H), 1.76 – 1.44 (m, 2H), 0.97 (t, *J* = 7.3 Hz, 3H). $^{13}$C NMR (100 MHz, $CDCl_3$): δ 152.3, 139.9, 139.7, 136.8, 130.2, 128.6, 120.0, 118.7, 118.0, 116.2, 56.2, 37.4, 24.7, 13.9. HRMS (ESI): calc. for $C_{16}H_{19}N_2O_3$ $[M+H]^+$: 287.1390, found: 287.1398.

***N*-(4-(*tert*-Butyl)phenyl)-2-methoxy-6-nitroaniline (13).** Yield: 63%; 477.0 mg was isolated as a red oily residue. $^1$H NMR (400 MHz, $CDCl_3$): δ 8.22 (br. s, 1H), 7.73 (dd, *J* = 8.5, 1.4 Hz, 1H), 7.32 – 7.22 (m, 2H), 7.11 (dd, *J* = 8.1, 1.4 Hz, 1H), 6.99 (dd, *J* = 8.5, 8.0 Hz, 1H), 6.85 – 6.72 (m, 2H), 3.77 (s, 3H), 1.33 (s, 9H). $^{13}$C NMR (100 MHz, $CDCl_3$): δ 152.5, 145.3, 140.0, 139.7, 130.1, 125.4, 120.2, 118.3, 118.1, 116.3, 56.3, 34.3, 31.6. HRMS (ESI): calc. for $C_{17}H_{21}N_2O_3$ $[M+H]^+$: 301.1547, found: 301.1547.

***N*-(3,5-Dimethylphenyl)-2-methoxy-6-nitroaniline (14).** Yield: 67%; 366.1 mg was isolated as a red oily residue. $^1$H NMR (400 MHz, $CDCl_3$): δ 8.02 (br. s, 1H), 7.70 (dd, *J* = 8.5, 1.5 Hz, 1H), 7.11 (dd, *J* = 8.1, 1.4 Hz, 1H), 7.01 (dd, *J* = 8.5, 8.1 Hz, 1H), 6.65 (m, 1H), 6.48 (m, 2H), 3.79 (s, 3H), 2.27 (q, *J* = 0.7 Hz, 6H). $^{13}$C NMR (100 MHz, $CDCl_3$): δ 152.7, 142.1, 140.4, 138.4, 129.6, 124.2, 120.4, 118.0, 116.3, 116.1, 56.3, 21.5. HRMS (ESI): calc. for $C_{15}H_{17}N_2O_3$ $[M+H]^+$: 273.1234, found: 273.1237.

***N*-(2-Methoxy-6-nitrophenyl)-2,3-dimethylaniline (15).** Yield: 65%; 315.8 mg was isolated as a red oily residue. $^1$H NMR (400 MHz, $CDCl_3$): δ 8.10 (br. s, 1H), 7.74 (dd, *J* = 8.6, 1.4 Hz, 1H), 7.10 (dd, *J* = 8.0, 1.4 Hz, 1H), 7.00 – 6.94 (m, 2H), 6.91 (m, 1H), 6.56 (m, 1H), 3.74 (s, 3H), 2.38 (s, 3H), 2.35 (s, 3H). $^{13}$C NMR (100 MHz, $CDCl_3$): δ 152.1, 140.7, 139.3, 137.2, 131.4, 127.2, 125.0, 124.8, 119.5, 118.0, 116.7, 116.2, 56.3, 20.7, 13.7. HRMS (ESI): calc. for $C_{15}H_{17}N_2O_3$ $[M+H]^+$: 273.1234, found: 273.1233.

***N*-(2-Ethylphenyl)-2-methoxy-6-nitroaniline (16)**. Yield**:** 60%; 260.2 mg was isolated as a red oily residue. $^1$H NMR (400 MHz, $CDCl_3$): δ 8.17 (br. s, 1H), 7.68 (dd, *J* = 8.5, 1.5 Hz, 1H), 7.19 (dd, *J* = 7.4, 1.8 Hz, 1H), 7.06 – 6.94 (m, 3H), 6.91 (dd, *J* = 8.5, 7.9 Hz, 1H), 6.60 (dd, *J* = 7.9, 1.5 Hz, 1H), 3.65 (s, 3H), 2.75 (q, *J* = 7.6 Hz, 2H), 1.31 (t, *J* = 7.6 Hz, 3H). $^{13}$C NMR (100 MHz, $CDCl_3$): δ 152.2, 140.1, 139.5, 134.0, 131.1, 128.5, 125.8, 123.0, 119.8, 118.7, 118.0, 116.3, 56.2, 24.7, 13.8. HRMS (ESI): calc. for $C_{15}H_{17}N_2O_3$ $[M+H]^+$: 273.1234, found: 273.1233. Note: TMS used for reference of $^1$H NMR spectrum (0.00 ppm).

***N*-(2-Methoxy-6-nitrophenyl)-3,4,5-trimethylaniline (17)**. Yield**:** 61%; 427.6 mg was isolated as a red oily residue. $^{1}$H NMR (400 MHz, $CDCl_3$): δ 8.00 (br. s, 1H), 7.69 (dd, *J* = 8.5, 1.4 Hz, 1H), 7.09 (dd, *J* = 8.0, 1.4 Hz, 1H), 6.97 (dd, *J* = 8.6, 8.0 Hz, 1H), 6.52 (pentet, *J* = 0.6 Hz, 2H), 3.78 (s, 3H), 2.22 (s, 3H), 2.22 (s, 3H), 2.12 (s, 3H). $^{13}$C NMR (100 MHz, $CDCl_3$): δ 152.5, 139.9, 139.2, 136.9, 130.3, 129.4, 119.9, 118.2, 118.0, 116.1, 56.4, 20.9, 15.0. HRMS (ESI): calc. for $C_{16}H_{19}N_2O_3$ $[M+H]^+$: 287.1390, found: 287.1399.

***N*-(2-Methoxy-6-nitrophenyl)pyridin-3-amine (18)**. Yield**:** 76%; 249.1 mg was isolated as a yellow oily residue. $^{1}$H NMR (400 MHz, $CDCl_3$): δ 8.25 (br. s, 1H), 8.18 – 8.10 (m, 2H), 7.67 (dd, *J* = 8.4, 1.5 Hz, 1H), 7.15 – 7.05 (m, 2H), 7.05 – 6.94 (m, 2H), 3.70 (s, 3H). $^{13}$C NMR (100 MHz, $CDCl_3$): δ 152.5, 142.9, 140.8, 140.7, 138.7, 128.2, 124.9, 123.0, 121.6, 117.9, 116.5, 56.2. HRMS (ESI): calc. for $C_{12}H_{12}N_3O_3$ $[M+H]^+$: 246.0873, found: 246.0884.

***N*-(4-Fluorophenyl)-2-methoxy-6-nitroaniline (19).** Yield**:** 81%; 401.8 mg was isolated as a red oily residue. $^{1}$H NMR (400 MHz, $CDCl_3$): δ 8.22 (br. s, 1H), 7.71 (dd, *J* = 8.5, 1.4 Hz, 1H), 7.09 (dd, *J* = 8.1, 1.4 Hz, 1H), 6.99 (d, *J* = 8.3 Hz, 1H), 6.96 – 6.89 (m, 2H), 6.83 – 6.78 (m, 2H), 3.73 (s, 3H). $^{13}$C NMR (100 MHz, $CDCl_3$): δ 158.6 (d, *J* = 240.8 Hz), 152.2, 139.8, 138.4 (d, *J* = 2.7 Hz), 130.2, 120.5 (d, *J* = 8.0 Hz), 120.3, 118.0, 116.4, 115.2 (d, *J* = 22.7 Hz), 56.2. HRMS (ESI): calc. for $C_{13}H_{12}FN_2O_3$ $[M+H]^+$: 263.0826, found: 263.0823.

***N*-(4-Chlorophenyl)-2-methoxy-6-nitroaniline (20).** Yield: 83%; 515.0 mg was isolated as a red oily residue. $^{1}$H NMR (400 MHz, $CDCl_3$): δ 8.14 (br. s, 1H), 7.70 (dd, *J* = 8.3, 1.5 Hz, 1H), 7.21 – 7.13 (m, 2H), 7.11 (dd, *J* = 8.3, 1.5 Hz, 1H), 7.03 (dd, *J* = 8.3, 8.3 Hz, 1H), 6.79 – 6.67 (m, 2H), 3.76 (s, 3H). $^{13}$C NMR (100 MHz, $CDCl_3$): δ 152.5, 141.0, 140.5, 129.0, 128.6, 127.0, 121.2, 119.7, 118.0, 116.4, 56.2. HRMS (ESI): calc. for $C_{13}H_{12}ClN_2O_3$ $[M+H]^+$: 279.0531, found: 279.0538.

**2,4-Dichloro-*N*-(2-methoxy-6-nitrophenyl)aniline (21).** Yield**:** 60%; 354.7 mg was isolated as an orange solid. $^{1}$H NMR (400 MHz, $CDCl_3$): δ 8.12 (br. s, 1H), 7.71 (dd, *J* = 7.6, 2.3 Hz, 1H), 7.36 (d, *J* = 2.3 Hz, 1H), 7.18 – 7.10 (m, 2H), 7.03 (ddd, *J* = 8.7, 2.3, 0.5 Hz, 1H), 6.46 (d, *J* = 8.7 Hz, 1H), 3.79 (s, 3H). $^{13}$C NMR (100 MHz, $CDCl_3$): δ 153.0, 141.9, 137.9, 129.0, 127.2, 126.8, 126.2, 123.5, 122.6, 118.4, 118.0, 116.6, 56.4. HRMS (ESI): calc. for $C_{13}H_{11}Cl_2N_2O_3$ $[M+H]^+$: 313.0141, found: 313.0146. MP: 120 – 122 °C.

***N*-(4-Bromophenyl)-2-methoxy-6-nitroaniline (22).** Yield**:** 52%; 289.5 mg was isolated as a red oily residue. $^{1}$H NMR (400 MHz, $CDCl_3$): δ 8.11 (br. s, 1H), 7.70 (dd, *J* = 8.2, 1.5 Hz, 1H), 7.34 – 7.27 (m, 2H), 7.11 (dd, *J* =

8.2, 1.5 Hz, 1H), 7.04 (dd, *J* = 8.2, 8.2 Hz, 1H), 6.72 – 6.59 (m, 2H), 3.76 (s, 3H). $^{13}$C NMR (100 MHz, $CDCl_3$): δ 152.6, 141.5, 140.7, 131.5, 128.8, 121.3, 120.1, 118.0, 116.5, 114.4, 56.3. HRMS (ESI): calc. for $C_{13}H_{12}BrN_2O_3$ $[M+H]^+$: 323.0026, found: 323.0037.

**2-Methoxy-6-nitro-*N*-(4-(trifluoromethyl)phenyl)aniline (23).** Yield**:** 21%; 124.5 mg was isolated as a red oily residue. $^1$H NMR (400 MHz, $CDCl_3$): δ 8.10 (br. s, 1H), 7.73 (dd, *J* = 7.7, 2.1 Hz, 1H), 7.52 – 7.40 (m, 2H), 7.21 – 7.06 (m, 2H), 6.83 – 6.74 (m, 2H), 3.81 (s, 3H). $^{13}$C NMR (100 MHz, $CDCl_3$): δ 153.3, 145.5 (d, *J* = 1.4 Hz), 142.0, 127.4, 126.1 (q, *J* = 3.8 Hz), 123.5 (q, *J* = 123.2 Hz), 123.3, 122.6, 118.0, 117.4, 116.6, 56.4. HRMS (ESI): calc. for $C_{14}H_{12}F_3N_2O_3$ $[M+H]^+$: 313.0795, found: 313.0788.

***N*-(4-((*tert*-Butyldimethylsilyl)oxy)phenyl)-2-methoxy-6-nitroaniline (24).** Yield: 53%; 474.2 mg was isolated as a red oily residue. $^1$H NMR (400 MHz, $CDCl_3$): δ 8.36 (br. s, 1H), 7.71 (dd, *J* = 8.6, 1.4 Hz, 1H), 7.04 (dd, *J* = 8.0, 1.4 Hz, 1H), 6.91 (dd, *J* = 8.6, 7.9 Hz, 1H), 6.79 – 6.68 (m, 4H), 3.69 (s, 3H), 0.99 (s, 9H), 0.19 (s, 6H). $^{13}$C NMR (100 MHz, $CDCl_3$): δ 152.0, 151.5, 139.1, 136.2, 131.6, 121.1, 120.1, 119.3, 118.2, 116.4, 56.2, 25.9, 18.4, -4.3. HRMS (ESI): calc. for $C_{19}H_{27}N_2O_4Si$ $[M+H]^+$: 375.1735, found: 375.1744.

**2-Methoxy-6-nitro-*N*-(4-phenoxyphenyl)aniline (25).** Yield**:** 76%; 646.9 mg was isolated as a red oily residue. $^1$H NMR (400 MHz, $CDCl_3$): δ 8.29 (br. s, 1H), 7.73 (dd, *J* = 8.5, 1.4 Hz, 1H), 7.36 – 7.29 (m, 2H), 7.14 – 7.05 (m, 2H), 7.03 – 6.98 (m, 3H), 6.97 – 6.91 (m, 2H), 6.89 – 6.83 (m, 2H), 3.76 (s, 3H). $^{13}$C NMR (100 MHz, $CDCl_3$): δ 158.1, 152.2, 152.0, 139.7, 138.1, 130.3, 129.8, 122.8, 120.4, 120.2, 119.7, 118.1, 116.4, 56.2. Note: One $^{13}$C signal missing from aromatic region, likely due to signal overlap. HRMS (ESI): calc. for $C_{19}H_{17}N_2O_4$ $[M+H]^+$: 337.1183, found: 337.1193.

***N*$_1$,*N*$_1$-Diethyl-*N*$_4$-(2-methoxy-6-nitrophenyl)benzene-1,4-diamine (26).** Yield: 50%; 298.7 mg was isolated as a dark purple oily residue. $^1$H NMR (400 MHz, $CDCl_3$): δ 8.38 (br. s, 1H), 7.71 (dd, *J* = 8.7, 1.4 Hz, 1H), 7.02 (dd, *J* = 8.0, 1.4 Hz, 1H), 6.89 – 6.75 (m, 3H), 6.67 – 6.54 (m, 2H), 3.71 (s, 3H), 3.32 (q, *J* = 7.1 Hz, 4H), 1.15 (t, *J* = 7.1 Hz, 6H). $^{13}$C NMR (100 MHz, $CDCl_3$): δ 151.8, 144.7, 138.2, 132.4, 131.5, 121.6, 118.3, 118.3, 116.2, 112.7, 56.4, 44.8, 12.7. HRMS (ESI): calc. for $C_{17}H_{22}N_3O_3$ $[M+H]^+$: 316.1656, found: 316.1641.

**(4-((2-Methoxy-6-nitrophenyl)amino)phenyl)methanol (27).** Yield: 99%; 422.1 mg was isolated as a red oily residue. $^1$H NMR (400 MHz, $CDCl_3$): δ 8.12 (br. s, 1H), 7.69 (d, *J* = 8.2 Hz, 1H), 7.21 (d, *J* = 8.4 Hz, 2H), 7.10 (d, *J* = 8.2 Hz, 1H), 7.01 (dd, *J* = 8.2, 8.2 Hz, 1H), 6.79 (d, *J* = 8.3 Hz, 2H), 4.59 (s, 2H), 3.75 (s, 3H), 1.97 (br.

s, 1H). $^{13}$C NMR (100 MHz, $CDCl_3$): δ 152.7, 141.8, 140.5, 134.8, 129.4, 127.8, 120.8, 118.5, 118.1, 116.3, 65.2, 56.3. HRMS (ESI): calc. for $C_{14}H_{15}N_2O_4$ $[M+H]^+$: 275.1026, found: 275.1024.

***N*-(4-(2-((*tert*-Butyldimethylsilyl)oxy)ethyl)phenyl)-2-methoxy-6-nitroaniline (28)**. Yield**:** 83%; 695.1 mg was isolated as a red oily residue. $^1$H NMR (400 MHz, $CDCl_3$): δ 8.21 (br. s, 1H), 7.70 (dd, *J* = 8.5, 1.4 Hz, 1H), 7.13 – 7.05 (m, 3H), 6.97 (m, 1H), 6.78 (d, *J* = 8.5 Hz, 2H), 3.81 (t, *J* = 7.0 Hz, 2H), 3.74 (s, 3H), 2.79 (t, *J* = 7.0 Hz, 2H), 0.91 (s, 9H), 0.02 (s, 6H). $^{13}$C NMR (100 MHz, $CDCl_3$): δ 152.4, 140.4, 139.9, 133.2, 129.9, 129.3, 120.2, 118.6, 117.9, 116.2, 64.7, 56.2, 39.0, 26.0, 18.4, -5.3. HRMS (ESI): calc. for $C_{21}H_{31}N_2O_4Si$ $[M+H]^+$: 403.2048, found: 403.2061.

**2-(4-((2-Methoxy-6-nitrophenyl)amino)phenyl)ethan-1-ol (29).** Yield: 97%; 297.4 mg was isolated as a red oily residue. $^1$H NMR (400 MHz, $CDCl_3$): δ 8.10 (br. s, 1H), 7.68 (dd, *J* = 8.5, 1.4 Hz, 1H), 7.13 – 7.03 (m, 3H), 6.98 (t, *J* = 8.3 Hz, 1H), 6.76 (d, *J* = 8.4 Hz, 2H), 3.79 (t, *J* = 6.6 Hz, 2H), 3.75 (s, 3H), 2.79 (t, *J* = 6.6 Hz, 2H), 1.94 (br. s, 1H). $^{13}$C NMR (100 MHz, $CDCl_3$): δ 152.5, 140.7, 140.1, 132.4, 129.7, 129.3, 120.5, 118.7, 118.0, 116.2, 63.8, 56.3, 38.6. HRMS (ESI): calc. for $C_{15}H_{15}N_2O_4$ $[M-H]^-$: 287.1037, found: 287.1024.

**1-(4-((2-Methoxy-6-nitrophenyl)amino)phenyl)-*N*-methylmethanesulfonamide (30).** Yield**:** 46%; 228.1 mg was isolated as a red solid. $^1$H NMR (400 MHz, DMSO-$d_6$): δ 8.08 (s, 1H), 7.52 (dd, *J* = 8.3, 1.3 Hz, 1H), 7.38 (dd, *J* = 8.3, 1.4 Hz, 1H), 7.24 (dd, *J* = 8.3, 8.3 Hz, 1H), 7.11 (d, *J* = 8.5 Hz, 2H), 6.84 (q, *J* = 4.9 Hz, 1H), 6.63 (d, *J* = 8.5 Hz, 2H), 4.16 (s, 2H), 3.80 (s, 3H), 2.51 (d, *J* = 4.9 Hz, 3H). $^{13}$C NMR (100 MHz, DMSO-$d_6$): δ 154.2, 144.0, 143.8, 131.1, 125.3, 123.5, 120.9, 116.5, 116.1, 114.9, 56.4, 55.5, 28.9. HRMS (ESI): calc. for $C_{15}H_{17}N_3O_5SNa$ $[M+Na]^+$: 374.0781, found: 374.0791. MP: 156 – 158 °C.

**1-Methoxy-7-methylphenazine (32).** Yield: 83%; 265.9 mg was isolated as a yellow solid. $^1$H NMR (400 MHz, $CDCl_3$): δ 8.15 (m, 1H), 7.82 (m, 1H), 7.66 (dd, *J* = 8.9, 1.1 Hz, 1H), 7.56 (dd, *J* = 8.9, 7.5 Hz, 1H), 7.51 (dd, *J* = 8.9, 1.9 Hz, 1H), 6.86 (dd, *J* = 7.6, 1.1 Hz, 1H), 4.02 (s, 3H), 2.48 (d, *J* = 1.2 Hz, 3H). $^{13}$C NMR (100 MHz, $CDCl_3$): δ 155.1, 144.1, 143.5, 141.5, 140.9, 136.2, 133.1, 130.2, 129.6, 127.3, 121.3, 105.9, 56.4, 22.2. HRMS (ESI): calc. for $C_{14}H_{13}N_2O$ $[M+H]^+$: 225.1022, found: 225.1026. MP: 124 – 126 °C. Note: Compound has been previously reported (CAS: 13860-49-6), but no spectra were found for comparison.

**7-Ethyl-1-methoxyphenazine (33).** Yield: 97%; 294.4 mg was isolated as a yellow solid. $^1$H NMR (400 MHz, $CDCl_3$): δ 8.05 (d, *J* = 8.9 Hz, 1H), 7.70 (m, 1H), 7.52 (dd, *J* = 8.9, 1.1 Hz, 1H), 7.41 – 7.33 (m, 2H), 6.68 (dd, *J*

= 7.6, 1.1 Hz, 1H), 3.86 (s, 3H), 2.64 (qd, *J* = 7.5, 1.1 Hz, 2H), 1.12 (t, *J* = 7.6 Hz, 3H). $^{13}$C NMR (100 MHz, $CDCl_3$): δ 155.3, 147.7, 144.3, 143.9, 141.4, 136.4, 132.5, 130.5, 129.9, 126.0, 121.4, 106.2, 56.6, 29.4, 14.6. HRMS (ESI): calc. for $C_{15}H_{15}N_2O$ $[M+H]^+$: 239.1179, found: 239.1182. MP: 106 – 108 °C.

**1-Methoxy-7-propylphenazine (34).** Yield: 70%; 277.3 mg was isolated as a yellow solid. $^1$H NMR (400 MHz, $CDCl_3$): δ 8.24 (dd, *J* = 9.0, 0.6 Hz, 1H), 7.91 (dq, *J* = 1.8, 0.9 Hz, 1H), 7.74 (dd, *J* = 9.0, 1.1 Hz, 1H), 7.67 – 7.56 (m, 2H), 6.96 (dd, *J* = 7.8, 1.1 Hz, 1H), 4.10 (s, 3H), 2.81 (td, *J* = 7.5, 0.9 Hz, 2H), 1.92 – 1.52 (m, 2H), 0.96 (t, *J* = 7.3 Hz, 3H). $^{13}$C NMR (100 MHz, $CDCl_3$): δ 155.2, 146.1, 144.3, 143.7, 141.3, 136.4, 132.6, 130.4, 129.8, 126.8, 121.4, 106.1, 56.5, 38.4, 23.6, 13.9. HRMS (ESI): calc. for $C_{16}H_{17}N_2O$ $[M+H]^+$: 253.1335, found: 253.1335. MP: 70 – 72 °C.

**7-(*tert*-Butyl)-1-methoxyphenazine (35).** Yield: 94%; 363.8 mg was isolated as a yellow oily residue. $^1$H NMR (400 MHz, $CDCl_3$): 8.10 (dd, *J* = 9.2, 0.6 Hz, 1H), 7.89 (dd, *J* = 2.2, 0.6 Hz, 1H), 7.69 (dd, *J* = 9.2, 2.1 Hz, 1H), 7.53 (dd, *J* = 8.8, 1.1 Hz, 1H), 7.43 – 7.32 (m, 1H), 6.68 (dd, *J* = 7.6, 1.1 Hz, 1H), 3.86 (s, 3H), 1.22 (s, 9H). $^{13}$C NMR (100 MHz, $CDCl_3$): δ 154.8, 153.8, 143.9, 143.3, 140.7, 136.1, 129.9, 129.6, 129.2, 123.4, 120.9, 105.7, 56.1, 35.2, 30.5. HRMS (ESI): calc. for $C_{17}H_{19}N_2O$ $[M+H]^+$: 267.1492, found: 267.1502.

**6-Methoxy-1,3-dimethylphenazine (36).** Yield: 86%; 233.1 mg was isolated as a yellow solid. $^1$H NMR (400 MHz, $CDCl_3$): δ 7.91 (m, 1H), 7.75 (dd, *J* = 8.8, 1.1 Hz, 1H), 7.57 (dd, *J* = 8.8, 7.6 Hz, 1H), 7.37 (m, 1H), 6.93 (dd, *J* = 7.6, 1.1 Hz, 1H), 4.08 (s, 3H), 2.78 (dd, *J* = 1.0, 1.0 Hz, 3H), 2.49 (d, *J* = 1.0 Hz, 3H). $^{13}$C NMR (100 MHz, $CDCl_3$): δ 154.9, 143.0, 142.5, 142.0, 140.6, 136.8, 136.3, 132.9, 129.2, 126.2, 121.9, 106.2, 56.4, 22.3, 17.6. HRMS (ESI): calc. for $C_{15}H_{15}N_2O$ $[M+H]^+$: 239.1179, found: 239.1177. MP: 117 – 119 °C.

**9-Methoxy-1,2-dimethylphenazine (37).** Yield: 44%; 121.3 mg was isolated as a yellow solid. $^1$H NMR (400 MHz, $CDCl_3$): δ 7.92 (d, *J* = 8.9 Hz, 1H), 7.75 (dd, *J* = 8.8, 1.1 Hz, 1H), 7.63 (dd, *J* = 8.8, 7.5 Hz, 1H), 7.58 (d, *J* = 8.9 Hz, 1H), 6.95 (dd, *J* = 7.5, 1.1 Hz, 1H), 4.10 (s, 3H), 2.86 (s, 3H), 2.49 (s, 3H). $^{13}$C NMR (100 MHz, $CDCl_3$): δ 155.4, 143.2, 142.4, 141.7, 137.6, 136.0, 134.8, 134.7, 129.9, 126.1, 121.2, 106.3, 56.5, 20.8, 13.4. HRMS (ESI): calc. for $C_{15}H_{15}N_2O$ $[M+H]^+$: 239.1179, found: 239.1179. MP: 157 – 159 °C, lit. 165 – 168 °C. Note: $^1$H NMR tabulation and melting point match previously reported values.[49]

**1-Ethyl-9-methoxyphenazine (38).** Yield: 46%; 104.5 mg was isolated as a yellow solid. $^1$H NMR (400 MHz, $CDCl_3$): δ 8.03 (m, 1H), 7.78 (dd, *J* = 8.9, 1.2 Hz, 1H), 7.74 (dd, *J* = 8.7, 6.9 Hz, 1H), 7.68 (dd, *J* = 8.8, 7.5 Hz,

1H), 7.61 (dq, *J* = 6.9, 1.2 Hz, 1H), 6.99 (dd, *J* = 7.6, 1.1 Hz, 1H), 4.11 (s, 3H), 3.49 (q, *J* = 7.5 Hz, 2H), 1.45 (t, *J* = 7.5 Hz, 3H). $^{13}$C NMR (100 MHz, $CDCl_3$): δ 155.6, 144.1, 143.9, 143.7, 141.4, 136.2, 131.0, 130.4, 127.5, 127.2, 121.3, 106.6, 56.7, 23.8, 14.5. HRMS (ESI): calc. for $C_{15}H_{15}N_2O$ $[M+H]^+$: 239.1179, found: 239.1184. MP: 124 – 126 °C.

**6-Methoxy-1,2,3-trimethylphenazine (39).** Yield: 60%; 213.2 mg was isolated as a yellow solid. $^1$H NMR (400 MHz, $CDCl_3$): δ 7.93 (s, 1H), 7.74 (dd, *J* = 8.8, 1.1 Hz, 1H), 7.55 (dd, *J* = 8.8, 7.6 Hz, 1H), 6.89 (dd, *J* = 7.6, 1.1 Hz, 1H), 4.07 (s, 3H), 2.77 (s, 3H), 2.44 (d, *J* = 1.1 Hz, 3H), 2.32 (s, 3H). $^{13}$C NMR (100 MHz, $CDCl_3$): δ 154.9, 143.1, 142.2, 141.3, 141.2, 138.5, 135.7, 133.4, 129.0, 126.3, 121.9, 105.8, 56.3, 21.9, 16.8, 13.4. HRMS (ESI): calc. for $C_{16}H_{17}N_2O$ $[M+H]^+$: 253.1335, found: 253.1339. MP: 196 – 198 °C.

**6-Methoxypyrido[2,3-*b*]quinoxaline (40).** Yield: 42%; 49.4 mg was isolated as a yellow solid. $^1$H NMR (400 MHz, $CDCl_3$): δ 9.37 (dd, *J* = 3.9, 2.0 Hz, 1H), 8.76 (dd, *J* = 8.7, 2.0 Hz, 1H), 7.97 (dd, *J* = 8.9, 1.1 Hz, 1H), 7.84 (dd, *J* = 8.9, 7.6 Hz, 1H), 7.78 (dd, *J* = 8.7, 3.9 Hz, 1H), 7.14 (dd, *J* = 7.6, 1.1 Hz, 1H), 4.20 (s, 3H). $^{13}$C NMR (100 MHz, $CDCl_3$): δ 156.9, 155.1, 149.8, 145.9, 139.1, 137.9, 137.7, 132.2, 125.4, 122.1, 107.3, 56.7. HRMS (ESI): calc. for $C_{12}H_{10}N_3O$ $[M+H]^+$: 212.0818, found: 212.0822. MP: 141 – 143 °C. Note: Compound has been previously published (CAS: 54696-72-9), but no characterization data was reported for the isolated product.[50]

**7-Ethoxy-1-methoxyphenazine (41).** Yield: 79%; 110.0 mg was isolated as a yellow solid. $^1$H NMR (400 MHz, $CDCl_3$): δ 8.12 (d, *J* = 9.5 Hz, 1H), 7.61 (dd, *J* = 8.8, 1.4 Hz, 1H), 7.56 (dd, *J* = 8.8, 7.3 Hz, 1H), 7.35 (dd, *J* = 9.5, 2.7 Hz, 1H), 7.21 (d, *J* = 2.7 Hz, 1H), 6.84 (dd, *J* = 7.4, 1.4 Hz, 1H), 4.10 (q, *J* = 7.0 Hz, 2H), 4.02 (s, 3H), 1.40 (t, *J* = 7.0 Hz, 3H). $^{13}$C NMR (100 MHz, $CDCl_3$): δ 161.0, 155.5, 145.4, 144.2, 139.5, 135.1, 131.3, 130.6, 126.4, 120.9, 105.6, 104.9, 64.4, 56.6, 14.7. MP: 149 – 151 °C, lit. 148 – 149 °C.[51] Note: Compound has been previously reported (CAS: 58476-65-6), but only melting point was found for comparison.

**7-Chloro-1-methoxyphenazine (42).** Yield: 71%; 380.0 mg was isolated as a yellow solid. $^1$H NMR (400 MHz, $CDCl_3$): δ 8.14 (dd, *J* = 9.2, 0.6 Hz, 1H), 8.00 (dd, *J* = 2.4, 0.6 Hz, 1H), 7.64 – 7.47 (m, 3H), 6.87 (dd, *J* = 6.2, 2.4 Hz, 1H), 4.02 (s, 3H). $^{13}$C NMR (100 MHz, $CDCl_3$): δ 155.0, 144.3, 143.2, 140.3, 136.7, 136.5, 131.4, 131.3, 131.1, 127.6, 121.2, 106.6, 56.4. HRMS (ESI): calc. for $C_{13}H_{10}ClN_2O$ $[M+H]^+$: 245.0476, found:

245.0479. MP: 162 – 164 °C, lit. 164 – 165 °C.[52] Note: Compound has been previously reported (CAS: 13554-02-4), but only melting point was found for comparison.

**1,3-Dichloro-9-methoxyphenazine (43).** Yield: 15%; 10.2 mg was isolated as a yellow solid. $^1$H NMR (400 MHz, $CDCl_3$): δ 8.17 (d, *J* = 2.2 Hz, 1H), 7.92 (d, *J* = 2.2 Hz, 1H), 7.86 – 7.75 (m, 2H), 7.11 (dd, *J* = 6.5, 2.3 Hz, 1H), 4.18 (s, 3H). $^{13}$C NMR (100 MHz, $CDCl_3$): δ 155.6, 145.1, 143.7, 137.6, 136.8, 136.1, 135.0, 132.5, 130.9, 127.3, 121.1, 107.6, 56.9. HRMS (ESI): calc. for $C_{13}H_9Cl_2N_2O$ $[M+H]^+$: 279.0086, found: 279.0082. MP: 186 – 188 °C.

**Ethyl 6-methoxyphenazine-2-carboxylate (44).** Yield: 84%; 77.5 mg was isolated as a yellow solid. $^1$H NMR (400 MHz, $CDCl_3$): δ 8.97 (dd, *J* = 1.8, 0.8 Hz, 1H), 8.43 (dd, *J* = 9.1, 0.7 Hz, 1H), 8.37 (dd, *J* = 9.1, 1.8 Hz, 1H), 7.84 (dd, *J* = 8.9, 1.2 Hz, 1H), 7.77 (dd, *J* = 8.9, 7.4 Hz, 1H), 7.10 (dd, *J* = 7.4, 1.2 Hz, 1H), 4.48 (q, *J* = 7.1 Hz, 2H), 4.18 (s, 3H), 1.46 (t, *J* = 7.1 Hz, 3H). $^{13}$C NMR (100 MHz, $CDCl_3$): δ 165.9, 155.3, 145.0, 143.6, 142.8, 137.9, 132.7, 132.5, 131.3, 130.6, 129.3, 121.9, 107.6, 61.9, 56.8, 14.5. HRMS (ESI): calc. for $C_{16}H_{15}N_2O_3$ $[M+H]^+$: 305.0897, found: 305.0908. MP: 139 – 141 °C. Note: Product obtained from an acidic workup following reductive cyclization of diarylamine intermediate **23**.

**6-Methoxyphenazin-2-ol (45).** Yield: 64%; 183.0 mg was isolated as a yellow solid. $^1$H NMR (400 MHz, DMSO-$d_6$): δ 10.86 (s, 1H), 8.13 (d, *J* = 9.4 Hz, 1H), 7.77 (dd, *J* = 8.8, 7.6 Hz, 1H), 7.64 (dd, *J* = 8.8, 1.1 Hz, 1H), 7.55 (dd, *J* = 9.4, 2.6 Hz, 1H), 7.31 (d, *J* = 2.6 Hz, 1H), 7.14 (dd, *J* = 7.6, 1.1 Hz, 1H), 4.04 (s, 3H). $^{13}$C NMR (100 MHz, DMSO-$d_6$): δ 159.8, 155.2, 144.6, 143.7, 138.1, 134.1, 131.1, 130.9, 125.8, 119.9, 106.9, 105.8, 55.9. HRMS (ESI): calc. for $C_{13}H_{11}N_2O_2$ $[M+H]^+$: 249.0634, found: 249.0636. MP: 210 °C (decomp), lit. 200 °C (decomp).[53]

**1-Methoxy-7-phenoxyphenazine (46).** Yield: 71%; 388.2 mg was isolated as a yellow solid. $^1$H NMR (400 MHz, $CDCl_3$): δ 8.35 (dd, *J* = 9.5, 0.5 Hz, 1H), 7.74 – 7.61 (m, 3H), 7.49 – 7.39 (m, 2H), 7.34 (dd, *J* = 2.7, 0.5 Hz, 1H), 7.29 – 7.16 (m, 3H), 6.96 (dd, *J* = 6.2, 2.5 Hz, 1H), 4.13 (s, 3H). $^{13}$C NMR (100 MHz, $CDCl_3$): δ 160.5, 155.2, 154.7, 144.5, 144.2, 139.5, 135.5, 131.8, 130.7, 130.3, 125.4, 125.3, 121.0, 120.8, 109.9, 105.8, 56.4. HRMS (ESI): calc. for $C_{19}H_{15}N_2O_2$ $[M+H]^+$: 303.1128, found: 303.1140. MP: 163 – 165 °C. Note: TMS used for reference of $^1$H NMR spectrum (0.00 ppm).

***N*,*N*-Diethyl-6-methoxyphenazin-2-amine (47).** Yield: 89%; 88.3 mg was isolated as a red oily residue. $^{1}$H NMR (400 MHz, $CDCl_3$): δ 8.15 (d, *J* = 9.7 Hz, 1H), 7.67 – 7.57 (m, 2H), 7.49 (dd, *J* = 9.7, 2.8 Hz, 1H), 7.00 (d, *J* = 2.8 Hz, 1H), 6.87 (dd, *J* = 6.2, 2.6 Hz, 1H), 4.12 (s, 3H), 3.54 (q, *J* = 7.1 Hz, 4H), 1.28 (t, *J* = 7.1 Hz, 6H). $^{13}$C NMR (100 MHz, $CDCl_3$): δ 155.6, 149.2, 146.2, 144.9, 138.2, 133.8, 131.2, 130.2, 122.3, 120.5, 104.2, 101.3, 56.4, 45.1, 13.0. HRMS (ESI): calc. for $C_{17}H_{20}N_3O$ $[M+H]^+$: 282.1601, found: 282.1607.

**(6-Methoxyphenazin-2-yl)methanol (48).** Yield: 68%; 148.5 mg was isolated as a yellow solid. $^{1}$H NMR (400 MHz, $CDCl_3$): δ 8.35 (d, *J* = 9.0 Hz, 1H), 8.20 (d, *J* = 1.5 Hz, 1H), 7.85 – 7.72 (m, 3H), 7.07 (dd, *J* = 7.5, 1.2 Hz, 1H), 5.00 (d, *J* = 6.1 Hz, 2H), 4.18 (s, 3H), 2.57 (t, *J* = 6.1 Hz, 1H). $^{13}$C NMR (100 MHz, $CDCl_3$): δ 155.3, 144.5, 144.4, 143.6, 142.0, 136.9, 130.8, 130.6, 129.7, 125.7, 121.5, 106.6, 65.0, 56.7. HRMS (ESI): calc. for $C_{14}H_{12}N_2O_2Na$ $[M+Na]^+$: 263.0791, found: 263.0802. MP: 209 – 211 °C.

**7-(2-((*tert*-butyldimethylsilyl)oxy)ethyl)-1-methoxyphenazine (49).** Yield: 31%; 161.6 mg was isolated as a yellow oily residue. $^{1}$H NMR (400 MHz, $CDCl_3$): δ 8.25 (dd, *J* = 9.0, 0.8 Hz, 1H), 7.96 (dt, *J* = 1.9, 0.8 Hz, 1H), 7.75 (dd, *J* = 9.0, 1.2 Hz, 1H), 7.67 (dd, *J* = 8.9, 1.9 Hz, 1H), 7.65 (dd, *J* = 8.9, 7.5 Hz, 1H), 6.96 (dd, *J* = 7.7, 1.1 Hz, 1H), 4.10 (s, 3H), 3.93 (t, *J* = 6.7 Hz, 2H), 3.04 (td, *J* = 6.7, 0.8 Hz, 2H), 0.79 (s, 9H), -0.09 (s, 6H). $^{13}$C NMR (100 MHz, $CDCl_3$): δ 155.2, 144.3, 143.6, 143.1, 141.4, 136.5, 133.1, 130.4, 129.7, 128.0, 121.4, 106.2, 63.8, 56.5, 39.9, 26.0, 18.4, -5.3. HRMS (ESI): calc. for $C_{21}H_{29}N_2O_2Si$ $[M+H]^+$: 369.1993, found: 369.2009.

**2-(6-Methoxyphenazin-2-yl)ethan-1-ol (50).** Yield: 64%; 116.1 mg was isolated as a yellow solid. $^{1}$H NMR (400 MHz, $CDCl_3$): δ 8.28 (d, *J* = 8.9 Hz, 1H), 8.03 (m, 1H), 7.78 (dd, *J* = 8.9, 1.4 Hz, 1H), 7.76 – 7.67 (m, 2H), 7.05 (dd, *J* = 7.3, 1.4 Hz, 1H), 4.17 (s, 3H), 4.08 (t, *J* = 6.4 Hz, 2H), 3.16 (t, *J* = 6.4 Hz, 2H). $^{13}$C NMR (100 MHz, $CDCl_3$): δ 155.3, 144.4, 143.5, 142.5, 141.5, 136.7, 132.6, 130.8, 130.3, 128.2, 121.5, 106.5, 63.0, 56.7, 39.7. HRMS (ESI): calc. for $C_{15}H_{14}N_2O_2Na$ $[M+Na]^+$: 277.0947, found: 277.0946. MP: 148 – 150 °C.

**1-(6-Methoxyphenazin-2-yl)-*N*-methylmethanesulfonamide (51).** Yield: 73%; 71.4 mg was isolated as a yellow solid. $^{1}$H NMR (400 MHz, DMSO-$d_6$): δ 8.29 (d, *J* = 8.9 Hz, 1H), 8.24 (d, *J* = 1.6 Hz, 1H), 7.93 (dd, *J* = 9.0, 1.9 Hz, 1H), 7.88 (dd, *J* = 8.9, 7.5 Hz, 1H), 7.79 (dd, *J* = 8.9, 1.2 Hz, 1H), 7.29 (dd, *J* = 7.6, 1.1 Hz, 1H), 7.09 (q, *J* = 4.8 Hz, 1H), 4.73 (s, 2H), 4.08 (s, 3H), 2.66 (d, *J* = 4.8 Hz, 3H). $^{13}$C NMR (100 MHz, DMSO-$d_6$): δ 155.0, 143.7, 142.4, 141.1, 136.3, 134.0, 133.2, 131.5, 130.8, 129.4, 120.6, 107.4, 56.0, 55.4, 28.9. HRMS (ESI): calc. for $C_{15}H_{16}N_3O_3S$ $[M+H]^+$: 318.0907, found: 318.0917. MP: 171 – 173 °C.

**2,4-Dibromo-7-methylphenazin-1-ol (52).** Yield: 52%; 51.2 mg was isolated as a yellow solid. $^{1}$H NMR (400 MHz, $CDCl_3$): δ 8.50 (br. s, 1H), 8.21 (s, 1H), 8.17 – 8.15 (m, 1H), 8.14 (d, *J* = 9.0 Hz, 1H), 7.75 (dd, *J* = 8.9, 1.9 Hz, 1H), 2.67 (d, *J* = 1.1 Hz, 3H). $^{13}$C NMR (100 MHz, $CDCl_3$): δ 149.3, 144.4, 142.9, 140.4, 140.1, 137.1, 135.3, 133.9, 128.5, 128.4, 113.0, 102.6, 22.5. HRMS (ESI): calc. for $C_{13}H_9Br_2N_2O$ $[M+H]^+$: 368.9056, found: 368.9071. MP: 200 – 202 °C.

**2,4-Dibromo-7-ethylphenazin-1-ol (53).** Yield: 74%; 117.9 mg was isolated as a yellow solid. $^{1}$H NMR (400 MHz, $CDCl_3$): δ 8.48 (br. s, 1H), 8.19 (s, 1H), 8.15 – 8.10 (m, 2H), 7.76 (dd, *J* = 8.9, 2.0 Hz, 1H), 2.96 (qd, *J* = 7.5, 1.1 Hz, 2H), 1.42 (t, *J* = 7.5 Hz, 3H). $^{13}$C NMR (100 MHz, $CDCl_3$): δ 149.0, 148.6, 144.3, 140.4, 139.8, 136.8, 134.3, 133.6, 128.2, 126.7, 112.7, 102.4, 29.3, 14.4. HRMS (ESI): calc. for $C_{14}H_{11}Br_2N_2O$ $[M+H]^+$: 382.9213, found: 382.9302. MP: 160 – 162 °C.

**2,4-Dibromo-7-propylphenazin-1-ol (54).** Yield: 76%; 89.6 mg was isolated as a yellow solid. $^{1}$H NMR (400 MHz, $CDCl_3$): δ 8.50 (br. s, 1H), 8.20 (s, 1H), 8.17 – 8.10 (m, 2H), 7.76 (dd, *J* = 9.0, 1.9 Hz, 1H), 2.90 (td, *J* = 7.4, 0.9 Hz, 2H), 1.93 – 1.70 (m, 2H), 1.03 (t, *J* = 7.4 Hz, 3H). $^{13}$C NMR (100 MHz, $CDCl_3$): δ 149.3, 147.4, 144.5, 140.6, 140.0, 137.0, 134.7, 133.9, 128.4, 127.9, 113.0, 102.6, 38.6, 23.8, 14.0. HRMS (ESI): calc. for $C_{15}H_{13}Br_2N_2O$ $[M+H]^+$: 396.9369, found: 396.9389. MP: 139 – 141 °C.

**2,4-Dibromo-7-(*tert*-butyl)phenazin-1-ol (55).** Yield: 61%; 139.1 mg was isolated as a yellow solid. $^{1}$H NMR (400 MHz, $CDCl_3$): δ 8.50 (br. s, 1H), 8.26 (dd, *J* = 2.1, 0.6 Hz, 1H), 8.17 (s, 1H), 8.14 (dd, *J* = 9.2, 0.6 Hz, 1H), 8.01 (dd, *J* = 9.2, 2.1 Hz, 1H), 1.49 (s, 9H). $^{13}$C NMR (100 MHz, $CDCl_3$): δ 155.5, 149.3, 144.4, 140.4, 140.0, 136.9, 134.0, 132.2, 128.2, 124.8, 112.9, 102.6, 36.0, 30.9. HRMS (ESI): calc. for $C_{16}H_{15}Br_2N_2O$ $[M+H]^+$: 410.9526, found: 410.9529. MP: 176 – 178 °C.

**2,4-Dibromo-6,8-dimethylphenazin-1-ol (56).** Yield: 73%; 87.4 mg was isolated as a yellow solid. $^{1}$H NMR (400 MHz, DMSO-$d_6$): δ 11.33 (br. s, 1H), 8.32 (s, 1H), 7.85 (dt, *J* = 2.0, 1.1 Hz, 1H), 7.68 (m, 1H), 2.80 (s, 3H), 2.59 (d, *J* = 1.1 Hz, 3H). $^{13}$C NMR (100 MHz, DMSO-$d_6$): δ 150.6, 142.5, 141.6, 141.0, 137.9, 136.7, 135.7, 134.9, 133.8, 124.5, 111.9, 104.2, 21.9, 16.8. HRMS (ESI): calc. for $C_{14}H_{11}Br_2N_2O$ $[M+H]^+$: 382.9213, found: 382.9208. MP: 216 – 218 °C.

**2,4-Dibromo-8,9-dimethylphenazin-1-ol (57).** Yield: 66%; 70.7 mg was isolated as a yellow solid. $^{1}$H NMR (400 MHz, DMSO-$d_6$): δ 11.10 (s, 1H), 8.37 (s, 1H), 8.04 (d, *J* = 8.9 Hz, 1H), 7.89 (d, *J* = 8.9 Hz, 1H), 2.90 (s,

3H), 2.58 (s, 3H). $^{13}$C NMR (100 MHz, DMSO-$d_6$): δ 150.7, 141.9, 140.7, 139.5, 138.4, 136.0, 135.9, 134.3, 125.9, 111.5, 103.8, 20.3, 13.3. HRMS (ESI): calc. for $C_{14}H_9Br_2N_2O$ [M-H]$^-$: 380.9067, found: 380.9067. MP: 232 – 234 °C. Note: One $^{13}$C NMR signal missing in the aromatic region, likely due to signal overlap.

**2,4-Dibromo-9-ethylphenazin-1-ol (58).** Yield: 76%; 113.5 mg was isolated as a yellow solid. $^1$H NMR (400 MHz, $CDCl_3$): δ 8.50 (s, 1H), 8.22 – 8.19 (m, 1H), 8.21 (s, 1H), 7.85 (dd, *J* = 8.8, 6.9 Hz, 1H), 7.73 (dq, *J* = 6.9, 1.1 Hz, 1H), 3.38 (q, *J* = 7.5 Hz, 2H), 1.45 (t, *J* = 7.5 Hz, 3H). $^{13}$C NMR (100 MHz, $CDCl_3$): δ 149.2, 144.7, 142.7, 140.4, 139.7, 137.1, 133.2, 131.9, 129.9, 128.2, 113.0, 102.9, 24.4, 14.7. HRMS (ESI): calc. for $C_{14}H_9Br_2N_2O$ [M-H]$^-$: 380.9067, found: 380.9078. MP: 161 – 163 °C.

**2,4-Dibromo-6,7,8-trimethylphenazin-1-ol (59).** Yield: 84%; 83.8 mg was isolated as a yellow solid. $^1$H NMR (400 MHz, $CDCl_3$): δ 8.14 (s, 1H), 7.82 (m, 1H), 2.93 (s, 3H), 2.59 (d, *J* = 1.1 Hz, 3H), 2.50 (s, 3H). $^{13}$C NMR (100 MHz, $CDCl_3$): δ 149.0, 144.1, 142.8, 140.6, 140.1, 138.5, 135.8, 134.9, 133.4, 124.9, 113.8, 102.2, 22.3, 17.3, 13.8. HRMS (ESI): calc. for $C_{15}H_{13}Br_2N_2O$ [M+H]$^+$: 396.9369, found: 396.9389. MP: 226 – 228 °C.

**2,4-Dibromo-7-ethoxyphenazin-1-ol (60).** Yield: 88%; 48.0 mg was isolated as a yellow solid. $^1$H NMR (400 MHz, $CDCl_3$): δ 8.45 (br. s, 1H), 8.20 (s, 1H), 8.09 (dd, *J* = 9.4, 0.5 Hz, 1H), 7.57 (dd, *J* = 9.4, 2.7 Hz, 1H), 7.52 (dd, *J* = 2.7, 0.5 Hz, 1H), 4.28 (q, *J* = 7.1 Hz, 2H), 1.56 (t, *J* = 7.1 Hz, 3H). $^{13}$C NMR (100 MHz, $CDCl_3$): δ 161.8, 149.5, 146.3, 140.0, 138.8, 137.1, 132.6, 129.9, 128.6, 112.3, 105.8, 101.8, 64.9, 14.8. HRMS (ESI): calc. for $C_{14}H_{11}Br_2N_2O_2$ [M+H]$^+$: 396.9182, found: 396.9168. MP: 205 – 207 °C.

**2,4-Dibromo-7-chlorophenazin-1-ol (61).** Yield: 90%; 184.0 mg was isolated as a yellow solid. $^1$H NMR (400 MHz, DMSO-$d_6$): δ 11.62 (s, 1H), 8.43 (s, 1H), 8.36 (d, *J* = 2.3 Hz, 1H), 8.32 (d, *J* = 9.3 Hz, 1H), 8.01 (dd, *J* = 9.3, 2.3 Hz, 1H). $^{13}$C NMR (100 MHz, DMSO-$d_6$): δ 151.0, 142.7, 139.9, 139.8, 137.6, 136.8, 135.5, 132.9, 130.8, 127.7, 111.3, 104.9. HRMS (ESI): calc. for $C_{12}H_4Br_2ClN_2O$ [M-H]$^-$: 386.8363, found: 386.8356. MP: 234 – 236 °C.

**Ethyl 7,9-dibromo-6-hydroxyphenazine-2-carboxylate (62).** Yield: 35%; 23.2 mg was isolated as a yellow solid. $^1$H NMR (400 MHz, DMSO-$d_6$): δ 11.71 (s, 1H), 8.83 (d, *J* = 1.7 Hz, 1H), 8.50 (s, 1H), 8.46 (d, *J* = 9.1 Hz, 1H), 8.41 (dd, *J* = 9.1, 1.8 Hz, 1H), 4.46 (q, *J* = 7.1 Hz, 2H), 1.43 (t, *J* = 7.1 Hz, 3H). $^{13}$C NMR (100 MHz, DMSO-$d_6$): δ 164.8, 151.0, 142.6, 141.8, 140.2, 137.6, 136.5, 132.4, 131.7, 130.0, 129.8, 111.7, 105.8, 61.7, 14.1. HRMS (ESI): calc. for $C_{15}H_{11}Br_2N_2O_3$ [M+H]$^+$: 426.9111, found: 426.9128. MP: 240 – 242 °C.

**2,4-Dibromo-7-phenoxyphenazin-1-ol (63).** Yield: 55%; 37.1 mg was isolated as a yellow solid. $^{1}$H NMR (400 MHz, DMSO-$d_6$): δ 11.54 (s, 1H), 8.41 – 8.34 (m, 2H), 7.93 (dd, *J* = 9.4, 2.7 Hz, 1H), 7.59 (t, *J* = 7.7 Hz, 2H), 7.44 – 7.32 (m, 3H), 7.20 (d, *J* = 2.7 Hz, 1H). $^{13}$C NMR (100 MHz, DMSO-$d_6$): δ 160.7, 154.1, 151.1, 143.9, 139.6, 138.7, 137.0, 134.3, 131.1, 130.7, 126.9, 125.8, 120.9, 110.9, 109.5, 103.7. HRMS (ESI): calc. for $C_{18}H_{11}Br_2N_2O_2$ $[M+H]^+$: 446.9162, found: 446.9169. MP: 240 °C (decomp).

**2,4,6-Tribromo-7-(diethylamino)phenazin-1-ol (64).** Yield: 53%; 51.1 mg was isolated as a red oily residue. $^{1}$H NMR (400 MHz, $CDCl_3$): δ 8.30 (br. s, 1H), 8.20 (s, 1H), 8.05 (d, *J* = 9.5 Hz, 1H), 7.76 (d, *J* = 9.5 Hz, 1H), 3.53 (q, *J* = 7.1 Hz, 4H), 1.21 (t, *J* = 7.1 Hz, 6H). $^{13}$C NMR (100 MHz, $CDCl_3$): δ 152.7, 149.0, 143.6, 140.2, 139.4, 137.3, 132.8, 129.5, 127.6, 114.4, 113.3, 102.5, 46.7, 13.5. HRMS (DART): calc. for $C_{16}H_{15}Br_3N_3O$ $[M+H]^+$: 503.8740, found: 503.8758.

**2,4-Dibromo-7-(bromomethyl)phenazin-1-ol (65).** Yield: 73%; 78.6 mg was isolated as a yellow solid. $^{1}$H NMR (400 MHz, DMSO-$d_6$): δ 11.58 (br. s, 1H), 8.43 (s, 1H), 8.41 (d, *J* = 1.9 Hz, 1H), 8.34 (d, *J* = 9.0 Hz, 1H), 8.05 (dd, *J* = 9.0, 1.9 Hz, 1H), 5.05 (s, 2H). $^{13}$C NMR (100 MHz, DMSO-$d_6$): δ 151.0, 142.4, 142.1, 140.9, 139.7, 137.0, 135.6, 133.4, 129.5, 128.7, 111.4, 104.7, 33.4. HRMS (ESI): calc. for $C_{13}H_6Br_3N_2O$ $[M-H]^-$: 444.8016, found: 444.8013. MP: 214 – 216 °C.

**4-Bromo-7-methylphenazin-1-ol (66).** Yield: 96%; 122.6 mg was isolated as a yellow solid. $^{1}$H NMR (400 MHz, $CDCl_3$): δ 8.19 (s, 1H), 8.17 (ddd, *J* = 1.9, 1.2, 0.7 Hz, 1H), 8.12 (dt, *J* = 8.9, 0.5 Hz, 1H), 8.05 (d, *J* = 8.1 Hz, 1H), 7.72 (dd, *J* = 8.9, 1.9 Hz, 1H), 7.10 (d, *J* = 8.1 Hz, 1H), 2.67 (d, *J* = 1.2 Hz, 3H). $^{13}$C NMR (100 MHz, $CDCl_3$): δ 151.9, 144.7, 142.5, 141.0, 140.3, 134.6, 134.4, 128.5, 128.5, 112.2, 109.2, 22.5. HRMS (ESI): calc. for $C_{13}H_{10}BrN_2O$ $[M+H]^+$: 288.9971, found: 288.9978. MP: 179 – 181 °C. Note: One $^{13}$C NMR signal missing in the aromatic region, likely due to overlap.

**4-Bromo-7-ethylphenazin-1-ol (67).** Yield: 92%; 136.1 mg was isolated as a yellow solid. $^{1}$H NMR (400 MHz, $CDCl_3$): δ 8.17 (br. s, 1H), 8.11 (m, 1H), 8.04 (dd, *J* = 8.9, 0.6 Hz, 1H), 8.01 (d, *J* = 8.1 Hz, 1H), 7.68 (m, 1H), 7.06 (d, *J* = 8.1 Hz, 1H), 2.93 (qd, *J* = 7.5, 1.1 Hz, 2H), 1.40 (t, *J* = 7.5 Hz, 3H). $^{13}$C NMR (100 MHz, $CDCl_3$): δ 151.8, 148.3, 144.7, 140.8, 140.3, 134.5, 134.3, 133.7, 128.4, 126.8, 112.1, 109.1, 29.5, 14.6. HRMS (ESI): calc. for $C_{14}H_{12}BrN_2O$ $[M+H]^+$: 303.0128, found: 303.0126. MP: 96 – 98 °C.

**4-Bromo-6,8-dimethylphenazin-1-ol (68).** Yield: 82%; 56.3 mg was isolated as a yellow solid. $^{1}$H NMR (400 MHz, $CDCl_3$): δ 8.15 (br. s, 1H), 7.99 (d, *J* = 8.1 Hz, 1H), 7.75 (m, 1H), 7.53 (dd, *J* = 2.0, 1.1 Hz, 1H), 7.08 (d, *J* = 8.1 Hz, 1H), 2.91 (s, 3H), 2.60 (d, *J* = 1.1 Hz, 3H). $^{13}$C NMR (100 MHz, $CDCl_3$): δ 151.6, 142.9, 142.4, 141.8, 139.5, 138.1, 134.6, 133.6, 133.3, 124.8, 113.0, 109.3, 22.6, 17.6. HRMS (ESI): calc. for $C_{14}H_{12}BrN_2O$ $[M+H]^+$: 303.0128, found: 303.0130. MP: 180 – 182 °C.

**4-Bromo-7-chlorophenazin-1-ol (69).** Yield: 90%; 120.2 mg was isolated as a yellow solid. $^{1}$H NMR (400 MHz, DMSO-$d_6$): δ 10.98 (br. s, 1H), 8.33 (d, *J* = 2.3 Hz, 1H), 8.30 (d, *J* = 9.3 Hz, 1H), 8.16 (d, *J* = 8.2 Hz, 1H), 7.95 (dd, *J* = 9.3, 2.3 Hz, 1H), 7.13 (d, *J* = 8.2 Hz, 1H). $^{13}$C NMR (100 MHz, DMSO-$d_6$): δ 153.9, 142.7, 140.6, 139.9, 136.5, 136.4, 135.6, 132.1, 131.2, 127.5, 111.4, 110.3. HRMS (ESI): calc. for $C_{12}H_5BrClN_2O$ $[M-H]^-$: 308.9257, found: 308.9258. MP: 199 – 201 °C.

**7-(Bromomethyl)phenazin-1-ol (70).** Yield: 87%; 93.9 mg was isolated as a yellow solid. $^{1}$H NMR (400 MHz, $CDCl_3$): δ 8.24 – 8.18 (m, 2H), 8.14 (s, 1H), 7.85 (dd, *J* = 9.0, 2.1 Hz, 1H), 7.79 – 7.75 (m, 2H), 7.24 (m, 1H), 4.73 (s, 2H). $^{13}$C NMR (100 MHz, $CDCl_3$): δ 152.0, 144.4, 144.0, 141.0, 140.6, 135.1, 132.3, 131.7, 130.2, 129.2, 120.2, 109.5, 32.8. HRMS (DART): calc. for $C_{13}H_{10}BrN_2O$ $[M+H]^+$: 288.9971, found: 288.9985. MP: 160 – 162 °C. Note: Product obtained from $BBr_3$ demethylation of HP **48**. NMR spectra acquired at 40 °C.

**7-(2-Bromoethyl)phenazin-1-ol (71).** Yield: 53%; 70.3 mg was isolated as a yellow solid. $^{1}$H NMR (400 MHz, $CDCl_3$): δ 8.21 (br. s, 1H), 8.15 (dd, *J* = 8.9, 0.6 Hz, 1H), 8.07 (dt, *J* = 1.9, 0.8 Hz, 1H), 7.78 – 7.74 (m, 2H), 7.68 (dd, *J* = 8.9, 2.0 Hz, 1H), 7.22 (dd, *J* = 4.6, 3.9 Hz, 1H), 3.75 (t, *J* = 7.3 Hz, 2H), 3.46 (t, *J* = 7.3 Hz, 2H). $^{13}$C NMR (100 MHz, $CDCl_3$): δ 151.9, 144.2, 144.1, 142.0, 140.5, 134.7, 132.1, 132.1, 129.5, 128.6, 120.1, 109.0, 39.4, 31.8. HRMS (ESI): calc. for $C_{14}H_{12}BrN_2O$ $[M+H]^+$: 303.0128, found: 303.0128. MP: 155 – 157 °C. Note: Product obtained from $BBr_3$ demethylation of HP **50**.

**2,4-Dibromophenazin-1-yl 2-(2-(2-methoxyethoxy)ethoxy)acetate (75).** Yield: 63%; 53.3 mg was isolated as a yellow solid. $^{1}$H NMR (400 MHz, $CDCl_3$): δ 8.33, (m, 1H), 8.32 (s, 1H), 8.18 (m, 1H), 7.94 – 7.84 (m, 2H), 4.78 (s, 2H), 4.01 – 3.96 (m, 2H), 3.82 – 3.76 (m, 2H), 3.72 – 3.68 (m, 2H), 3.60 – 3.54 (m, 2H), 3.38 (s, 3H). $^{13}$C NMR (100 MHz, $CDCl_3$): δ 168.2, 144.6, 143.7, 143.4, 140.2, 137.4, 135.7, 132.4, 132.1, 130.1, 129.8, 122.5, 117.0, 72.1, 71.4, 70.8, 68.6, 59.2. HRMS (ESI): calc. for $C_{19}H_{19}Br_2N_2O_5$ $[M+H]^+$: 514.9636, found:

514.9630. MP: 184 – 186 °C. Note: One $^{13}$C NMR signal missing in the aliphatic region, likely due to signal overlap.

**2,4-Dibromophenazin-1-yl 3-(methylsulfonyl)-2-oxoimidazolidine-1-carboxylate (76).** Yield: >99%; 95.7 mg was isolated as a pale yellow solid. $^1$H NMR (600 MHz, $CDCl_3$): δ 8.38 – 8.35 (m, 1H), 8.36 (s, 1H), 8.27 (m, 1H), 7.97 – 7.90 (m, 2H), 4.37 – 4.28 (m, 2H), 4.11 (t, *J* = 7.9 Hz, 2H), 3.45 (s, 3H). $^{13}$C NMR (150 MHz, $CDCl_3$): δ 149.9, 147.9, 143.9, 143.8, 143.6, 140.3, 137.5, 135.6, 132.6, 132.3, 130.3, 130.0, 123.3, 117.3, 41.6, 41.0, 40.3. HRMS (ESI): calc. for $C_{17}H_{13}Br_2N_4O_5S$ $[M+H]^+$: 544.8948, found: 544.8949. MP: > 250 °C.

**2,4-Dibromo-7-chlorophenazin-1-yl (2,5,8,11-tetraoxatridecan-13-yl) carbonate (77).** Yield: 99%; 183.1 mg was isolated as a yellow solid. $^1$H NMR (400 MHz, $CDCl_3$): δ 8.35 (d, *J* = 2.3 Hz, 1H), 8.34 (s, 1H), 8.22 (d, *J* = 9.3 Hz, 1H), 7.83 (dd, *J* = 9.3, 2.3 Hz, 1H), 4.57 – 4.47 (m, 2H), 3.91 – 3.80 (m, 2H), 3.76 – 3.71 (m, 2H), 3.70 – 3.60 (m, 8H), 3.58 – 3.50 (m, 2H), 3.36 (s, 3H). $^{13}$C NMR (100 MHz, $CDCl_3$): δ 152.3, 144.5, 143.5, 141.9, 140.5, 138.4, 137.5, 136.5, 133.9, 131.2, 128.5, 122.5, 117.3, 72.1, 71.0, 70.8, 70.8, 70.8, 70.7, 69.0, 68.9, 59.2. HRMS (ESI): calc. for $C_{22}H_{23}Br_2ClN_2O_7Na$ $[M+Na]^+$: 644.9433, found: 644.9433. MP: 66 – 68 °C.

**2,4-Dibromo-7-phenoxyphenazin-1-yl (2,5,8,11-tetraoxatridecan-13-yl) carbonate (78).** Yield: 71%; 47.9 mg was isolated as a yellow solid. $^1$H NMR (600 MHz, $CDCl_3$): δ 8.29 (s, 1H), 8.25 (d, *J* = 9.4 Hz, 1H), 7.78 (dd, *J* = 9.4, 2.7 Hz, 1H), 7.49 (t, *J* = 8.0 Hz, 2H), 7.42 (d, *J* = 2.7 Hz, 1H), 7.31 (t, *J* = 7.5 Hz, 1H), 7.23 – 7.20 (m, 2H), 4.56 – 4.51 (m, 2H), 3.91 – 3.87 (m, 2H), 3.74 (dd, *J* = 5.9, 3.5 Hz, 2H), 3.72 – 3.62 (m, 8H), 3.57 – 3.54 (m, 2H), 3.37 (s, 3H). $^{13}$C NMR (150 MHz, $CDCl_3$): δ 161.8, 154.5, 152.4, 145.1, 144.7, 141.0, 140.4, 136.4, 135.9, 131.6, 130.6, 128.1, 126.0, 121.9, 121.3, 115.5, 110.0, 72.1, 71.0, 70.9, 70.8, 70.8, 70.7, 69.0, 68.9, 59.2. HRMS (ESI): calc. for $C_{28}H_{29}Br_2N_2O_8$ $[M+H]^+$: 681.0267, found: 681.0275. MP: 49 – 51 °C.

**((2,4-Dibromophenazin-1-yl)oxy)methyl (2-(2-(2-methoxyethoxy)ethoxy)ethyl) carbonate (80).** Yield: 54%; 43.4 mg was isolated as a yellow solid. $^1$H NMR (400 MHz, $CDCl_3$): δ 8.37 (m, 1H), 8.32 (s, 1H), 8.28 (m, 1H), 7.97 – 7.89 (m, 2H), 6.26 (s, 2H), 4.34 – 4.29 (m, 2H), 3.73 – 3.68 (m, 2H), 3.62 (d, *J* = 5.5 Hz, 6H), 3.56 – 3.51 (m, 2H), 3.37 (s, 3H). $^{13}$C NMR (100 MHz, $CDCl_3$): δ 154.7, 149.7, 143.5, 143.0, 140.7, 138.4, 136.5, 132.3, 132.0, 130.2, 129.8, 120.5, 116.8, 92.4, 72.1, 70.9, 70.8, 70.8, 68.9, 67.8, 59.3. HRMS (ESI): calc. for $C_{21}H_{23}Br_2N_2O_7$ $[M+H]^+$: 574.9848, found: 574.9821. MP: 116 – 118 °C.

**((2,4-Dibromophenazin-1-yl)oxy)methyl (2,2-dimethyl-3,3-diphenyl-4,7,10,13-tetraoxa-3-silapentadecan-15-yl) carbonate (81).** Yield: 69%; 38.2 mg was isolated as a yellow oily residue. $^{1}$H NMR (400 MHz, $CDCl_3$): δ 8.36 (m, 1H), 8.30 (s, 1H), 8.27 (m, 1H), 7.96 – 7.88 (m, 2H), 7.68 (dt, *J* = 6.5, 1.7 Hz, 4H), 7.44 – 7.33 (m, 6H), 6.25 (s, 2H), 4.33 – 4.28 (m, 2H), 3.80 (t, *J* = 5.4 Hz, 2H), 3.71 – 3.66 (m, 2H), 3.66 – 3.56 (m, 10H), 1.04 (s, 9H). $^{13}$C NMR (100 MHz, $CDCl_3$): δ 154.7, 149.7, 143.5, 143.0, 140.7, 138.4, 136.4, 135.8, 133.9, 132.3, 132.0, 130.2, 129.8, 127.8, 120.5, 116.7, 92.3, 72.6, 70.9, 70.9, 70.9, 70.8, 68.9, 67.8, 63.6, 27.0, 19.4. HRMS (ESI): calc. for $C_{38}H_{43}Br_2N_2O_8Si$ $[M+H]^+$: 843.1134, found: 843.1147. Note: One $^{13}$C NMR signal missing in the aromatic region, likely due to signal overlap.

**2-((2-(((((2,4-Dibromophenazin-1-yl)oxy)methoxy)carbonyl)oxy)ethyl)disulfaneyl)ethyl benzoate (85).** Yield: 60%; 69.8 mg was isolated as a yellow solid. $^{1}$H NMR (400 MHz, $CDCl_3$): δ 8.35 (m, 1H), 8.30 (s, 1H), 8.27 (m, 1H), 8.03 (m, 2H), 7.93 (ddd, *J* = 5.6, 4.7, 3.1 Hz, 2H), 7.54 (m, 1H), 7.42 (t, *J* = 7.7 Hz, 2H), 6.26 (s, 2H), 4.56 (t, *J* = 6.5 Hz, 2H), 4.43 (t, *J* = 6.6 Hz, 2H), 3.05 (t, *J* = 6.5 Hz, 2H), 2.95 (t, *J* = 6.6 Hz, 2H). $^{13}$C NMR (100 MHz, $CDCl_3$): δ 166.5, 154.5, 149.6, 143.5, 142.9, 140.7, 138.3, 136.4, 133.3, 132.4, 132.0, 130.2, 130.0, 129.9, 129.7, 128.6, 120.5, 116.7, 92.4, 66.3, 62.9, 37.5, 37.1. HRMS (ESI): calc. for $C_{25}H_{20}Br_2N_2O_6S_2Na$ $[M+Na]^+$: 690.9002, found: 690.8986. MP: 123 – 125 °C.

**((2,4-Dibromophenazin-1-yl)oxy)methyl((2,4,5-trimethyl-3,6-dioxocyclohexa-1,4-dien-1-yl)methyl) carbonate (86).** Yield: 13%; 9.1 mg was isolated as a yellow solid. $^{1}$H NMR (500 MHz, $CDCl_3$): δ 8.36 (m, 1H), 8.28 (s, 1H), 8.28 (m, 1H), 7.95 – 7.89 (m, 2H), 6.27 (s, 2H), 5.12 (s, 2H), 2.10 (s, 3H), 2.04 (m, 3H), 2.02 (m, 3H). $^{13}$C NMR (125 MHz, $CDCl_3$): δ 187.3, 185.5, 154.4, 149.6, 145.6, 143.5, 143.0, 141.3, 141.0, 140.7, 138.3, 136.4, 135.7, 132.4, 132.0, 130.2, 129.8, 120.5, 116.7, 92.5, 61.1, 12.8, 12.7, 12.6. HRMS (ESI): calc. for $C_{24}H_{19}Br_2N_2O_6$ $[M+H]^+$: 590.9586, found: 590.9577. MP: 181 – 183 °C.

**((2,4-dibromo-7-chlorophenazin-1-yl)oxy)methyl((2,4,5-trimethyl-3,6-dioxocyclohexa-1,4-dien-1-yl)methyl) carbonate (87).** Yield: 8%; 15.0 mg was isolated as a yellow solid. $^{1}$H NMR (500 MHz, $CDCl_3$): δ 8.38 (d, *J* = 2.3 Hz, 1H), 8.30 (s, 1H), 8.23 (d, *J* = 9.2 Hz, 1H), 7.85 (dd, *J* = 9.2, 2.3 Hz, 1H), 6.23 (s, 2H), 5.11 (s, 2H), 2.11 (s, 3H), 2.04 (m, 3H), 2.03 (m, 3H). $^{13}$C NMR (125 MHz, $CDCl_3$): δ 187.3, 185.5, 154.4, 149.7, 145.6, 143.3, 141.4, 141.4, 141.0, 141.0, 138.4, 138.2, 137.1, 135.6, 133.8, 131.0, 128.6, 120.5, 117.1, 92.5, 61.1, 12.8, 12.7, 12.6. HRMS (ESI): calc. for $C_{24}H_{18}Br_2ClN_2O_6$ $[M+H]^+$: 624.9195, found: 624.9190. MP: 179 – 181 °C.

**II.c) HP Complex Formation with Fe(II).** The rates of phenazine-iron(II) complex formation were independently evaluated via UV-vis spectrometry following addition of 0.5 equivalents ammonium iron(II) sulfate hexahydrate to stirring solutions of HP **57**, **58**, **61**, or **86** (5 mM, 5 mL) in dimethyl sulfoxide. Aliquots (20 µL) were removed from each stirring solution and added to 980 µL dimethyl sulfoxide in a cuvette. Spectral scanning was performed from 300 to 700 nm in 2 nm increments. The $\lambda_{max}$ value was determined to be 374 nm for all HP analogues tested herein. A loss of absorbance at 374 nm corresponds to a loss of free hydroxyphenazine and apparent formation of a phenazine-iron(II) complex.

**II.d) Spectrophotometric Determination of Prodrug Stability in LB Media.** Into 1.5 mL Eppendorf tubes was added 750 µL of LB at 37 °C. To this solution was added 7.5 µL of test compound (10 mM DMSO stock). Tubes were briefly vortexed, then incubated for up to 48 hours. At the indicated time points, 750 µL ethyl acetate was added to the LB solution and the tubes were vigorously vortexed. From the organic layer was drawn 500 µL, which was added to 1.5 mL of 1.33 mM triethylamine in ethyl acetate in a quartz cuvette (due to overlapping absorbance spectra for prodrugs and the respective HP, triethylamine was added as a reporter to generate the HP anions, which fortunately presented spectra distinct from those of the prodrugs). Spectral scans were taken from 200 to 700 nm at 2 nm increments. Results were plotted using GraphPad Prism.

**III) Biology.** This biology section includes the following items, in order: (a) MIC susceptibility assay protocols, (b) Calgary Biofilm Device (CBD) assay protocol, (c) LIVE/DEAD staining of MRSE 35984 biofilms protocol, (d) hemolysis assay protocol, (e) lactate dehydrogenase (LDH) assay protocol, (f) prodrug serum stability assay protocol and (g) agar diffusion assay protocol.

**III.a) Minimum Inhibitory Concentration (MIC) Susceptibility Assay (in 96-well plate).**[11,12,15,54] The minimum inhibitory concentration (MIC) for each phenazine analogue was determined by the broth microdilution method as recommended by the Clinical and Laboratory Standards Institute (CLSI). In a 96-well plate, eleven two-fold serial dilutions of each compound were made in a final volume of 100 µL Lysogeny Broth. Each well was inoculated with ~$10^5$ bacterial cells at the initial time of incubation, prepared from a fresh log phase culture ($OD_{600}$ of 0.5 to 1.0 depending on bacterial strain). The MIC was defined as the lowest concentration of compound that prevented bacterial growth after incubating 16 to 18 hours at 37 °C (MIC values were supported by spectrophotometric readings at $OD_{600}$). The concentration range tested for each phenazine analogue/antibacterial during this study was 0.10 to 100 µM. DMSO served as our vehicle and

negative control in each microdilution MIC assay. DMSO was serially diluted with a top concentration of 1% v/v. All compounds were tested in three independent experiments.

**III.b) MIC Assay for *Mycobacterium tuberculosis*.**[11,12,15] *M. tuberculosis* H37Ra (ATCC 25177) was inoculated in 10 mL Middlebrook 7H9 medium and allowed to grow for two weeks. The culture was then diluted with fresh medium until an $OD_{600}$ of 0.01 was reached. Aliquots of 200 µL were then added to each well of a 96-well plate starting from the second column. Test compounds were dissolved in DMSO at final concentration of 10 mM. 7.5 µL of each compound along with DMSO (negative control) and streptomycin (positive control-40mg/ml stock solution) were added to 1.5 mL of the Mycobacterium diluted cultures, resulting in 50 µM final concentration of each halogenated phenazine analogues and 340 µM for streptomycin. The final DMSO concentration was maintained at 0.5%. Aliquots of 400 µl were added to wells of the first column of the 96-well plate and serially diluted two-fold (200 µl) per well across the plate to obtain final concentrations that ranges from 0.024 to 50 µM for the test compounds and 0.16 to 340 µM for streptomycin. Three rows were reserved for each compound. The plates were then incubated at 37°C for seven days. Minimum inhibitory concentrations are reported as the lowest concentration at which no bacterial growth was observed. $OD_{600}$ absorbance was recorded using SpectraMax M5 (Molecular Devices). Data obtained from three independent experiments were analyzed using Excel.

**III.c) Calgary Biofilm Device (CBD) Experiments.**[11,12,15] Biofilm eradication experiments were performed using the Calgary Biofilm Device to determine MBC/MBEC values for various compounds of interest (Innovotech, product code: 19111). The Calgary device (96-well plate with lid containing pegs to establish biofilms on) was inoculated with 125 µL of a mid-log phase culture diluted 1,000-fold in tryptic soy broth with 0.5% glucose (TSBG) to establish bacterial biofilms after incubation at 37 °C for 24 hours. The lid of the Calgary device was then removed, washed and transferred to another 96-well plate containing 2-fold serial dilutions of the test compounds (the “challenge plate”). The total volume of media with compound in each well in the challenge plate is 150 µL. The Calgary device was then incubated at 37 °C for 24 hours. The lid was then removed from the challenge plate and MBC/MBEC values were determined using different final assays. To determine MBC values, 20 µL of the challenge plate was transferred into a fresh 96-well plate containing 180 µL TSBG and incubated overnight at 37 °C. The MBC values were determined as the concentration giving a lack of visible bacterial growth (i.e., turbidity). For determination of MBEC values, the Calgary device lid (with

attached pegs/treated biofilms) was transferred to a new 96-well plate containing 150 µL of fresh TSBG media in each well and incubated for 24 hours at 37 °C to allow viable biofilms to grow and disperse resulting in turbidity after the incubation period. MBEC values were determined as the lowest test concentration that resulted in eradicated biofilm (i.e., wells that had no turbidity after final incubation period). All compounds were tested in a minimum of three independent experiments. In select experiments, both treated and untreated pegs from the Calgary Biofilm Device were removed from active HP biofilm eradicators after final incubation, sonicated for 30 minutes in PBS and plated out to determine biofilm cell killing (see supporting information for data).

**III.d) Live / Dead staining (Fluorescence Microscopy) of MRSE 35984 biofilms:** A mid-log culture of MRSE 35894 was diluted 1:1,000-fold and 500 µL was transferred to each compartment of a 4 compartment CELLview dish (Greiner Bio-One 627871). The dish was then incubated for 24 hours at 37 °C. After this time, the cultures were removed and the plate was washed with 0.9% saline. The dish was then treated with the compounds in fresh media at various concentrations. DMSO was used as our negative control in this assay. The dish was incubated with the compound for 24 hours at 37 °C. After this time, the cultures were removed and the dish was washed with 0.9% saline for 2 minutes. Saline was then removed and 500 µL of the stain (Live/Dead BacLight Viability Kit, Invitrogen) were added for 15 minutes and left in the dark. After this time, the stain was removed and the dish was washed twice with 0.9% saline. Then the dish was fixed with 500 µL 4% paraformaldehyde in PBS for 30 minutes. Images of remaining MRSE biofilms were then taken with a fluorescence microscope. All data were analyzed using Image J software from three independent experiments.

**III.e) Hemolysis Assay with Red Blood Cells:** Freshly drawn human red blood cells (hRBC with ethylenediaminetetraacetic acid (EDTA) as an anticoagulant) were washed with Tris-buffered saline (0.01M Tris-base, 0.155 M sodium chloride (NaCl), pH 7.2) and centrifuged for 5 minutes at 3,500 rpm. The washing was repeated three times with the buffer. In 96-well plate, test compounds were added to the buffer from DMSO stocks. Then 2% hRBCs (50 µL) in buffer were added to test compounds to give a final concentration of 200 µM. The plate was then incubated for 1 hour at 37 °C. After incubation, the plate was centrifuged for 5 minutes at 3,500 rpm. Then 80 µL of the supernatant was transferred to another 96-well plate and the optical density (OD) was read at 405 nm. DMSO served as our negative control (0% hemolysis) while Triton X served

as our positive control (100% hemolysis). The percent of hemolysis was calculated as ($OD_{405}$ of the compound-$OD_{405}$ DMSO) / ($OD_{405}$ Triton X- $OD_{405}$ buffer) from three independent experiments.

**III.f) LDH Release Assay for HeLa Cytotoxicity Assessment:** HeLa cytotoxicity was assessed using the LDH release assay described by CytoTox96 (Promega G1780). HeLa cells were grown in Dulbecco's Modified Eagle Medium (DMEM; Gibco) supplemented with 10% Fetal Bovine Serum (FBS) at 37°C with 5% $CO_2$. When the HeLa cultures exhibited 70-80% confluence, halogenated phenazines were then diluted by DMEM (10% FBS) at concentrations of 25, 50 and 100 μM and added to HeLa cells. Triton X-100 (at 2% v/v) was used as the positive control for maximum lactate dehydrogenate (LDH) activity in this assay (i.e., complete cell death) while "medium only" lanes served as negative control lanes (i.e., no cell death). DMSO was used as our vehicle control. HeLa cells were treated with compounds for 24 hours and then 50 μL of the supernatant was transferred into a fresh 96-well plate where 50 μL of the reaction mixture was added to the 96-well plate and incubated at room temperature for 30 minutes. Finally, Stop Solution (50 μL) was added to the incubating plates and the absorbance was measured at 490 nm. Results are on the next page and are from three independent experiments.

**III.g) Prodrug Serum Stability Assay:** *In vitro* serum stability assays were performed according to previously reported procedures with minor modifications.[55] First, human serum was temperature-equilibrated at 37 °C and then 200 μL of the serum solution was allocated into 1.5 mL Eppendorf tubes. To each tube was added 7.5 μL of the prodrug analyte (from 10 mM DMSO stocks) and 7.5 μL of internal standard. The serum analyte solutions were vortex-mixed for 5 seconds and then incubated for 1 minute to 60 minutes. At the end of each incubation interval, 400 μL of acetonitrile (0.5% formic acid) was added to precipitate serum proteins. The tubes were then centrifuged for 5 minutes at 1500 rcf and the supernatant was removed and evaporated to dryness under reduced pressure. Samples were reconstituted in 400 μL acetonitrile (0.5% formic acid) and analyzed via LC-MS using a Shimadzu Prominence HPLC system, AB Sciex 3200 QTRAP spectrometer and a Kinetex C18 column (50 mm × 2.1 mm × 2.6 μm) with a 35-minute linear gradient from 10-65% acetonitrile in 0.5% formic acid at a flow rate of 0.25 mL/min. Formation of active HPs from prodrugs was quantified by comparison of observed ratios of HPs to internal standard with previously generated standard curves.

**III.h) Agar Diffusion Assay:** Agar diffusion assays for prodrug evaluation were performed according to the standard Kirby-Bauer disk diffusion susceptibility test protocol with some minor modifications.[56] First, 100 μL of

MRSA BAA-1707 ($OD_{600}$ = 0.7, ~$10^8$ CFU) was spread on lysogeny broth (LB) agar plates. The plates were dried for 10 min, and 20 µL of test compound from 10 mM DMSO stocks was gently pipetted directly onto the plate. The plates were incubated at 37°C for 16 h, images were taken, and zones of bacterial clearance were measured (as areas of growth inhibition) and recorded in $cm^2$ using ImageJ software (NIH), similar to a previously described reference.[57]

**Acknowledgements:**

We would like to acknowledge the University of Florida for providing start-up funds and seed funds (UF Opportunity Fund, Emerging Pathogens Institute Seed Grant) to support this work. We thank Faika Başoğlu for assistance with MIC assays. A.T.G. has been awarded a University of Florida Graduate School Fellowship. We also thank the National Science Foundation through the National High Magnetic Field Laboratory, which supported a portion of our NMR studies at the Advanced Magnetic Resonance Imaging and Spectroscopy (AMRIS) Facility in the McKnight Brain Institute of the University of Florida. High-resolution mass spectra (HRMS) were obtained from the Mass Spectrometry facility (Chemistry Department) at the University of Florida (Funded by NIH S10 OD021758-01A1).

**Keywords:** halogenated phenazines ● chemical synthesis ● antibiotic resistance ● biofilm eradication ● drug discovery

**Associated Content:**

**Supporting Information**

The Supporting Information (SI) is available free of charge on the ACS Publications website at DOI: **insert DOI here.**

NMR spectra ($^1H$ and $^{13}C$ NMR) for new compounds, select images of biological assays, biofilm cell counts from select HPs in CBD assays, synthetic procedures, full characterization data (NMR, high-resolution mass spectra, melting points for solids, observed color and state of compounds), UV-vis (metal-chelation determination), procedures for biological investigations (antibacterial assays, biofilm eradication assays, HeLa cell cytotoxicity in LDH release assays, hemolytic assays with red blood cells, serum stability assays) (PDF)

Molecular formula strings file (CSV)

**Author Information:**

Corresponding author

*E-mail: rhuigens@cop.ufl.edu. Phone: (352) 273-7718.

Notes

The authors declare no competing financial interest.

**Abbreviations Used:**

CBD, Calgary biofilm device; CCCP, Carbonyl Cyanide *m*-Chlorophenylhydrazine; EDTA, ethylenediaminetetraacetic acid; HP, halogenated phenazine; $IC_{50}$, half maximal inhibitory concentration; LDH, lactate dehydrogenase; MBEC, minimum biofilm eradication concentration; MIC, minimum inhibitory concentration; μM, micromolar; MRSA, methicillin-resistant *Staphylococcus aureus*; MRSE, methicillin-resistant *Staphylococcus epidermidis*; NAC, *N*-Acetyl Cysteine; $t_{1/2}$, half-life; TPEN, *N,N,N',N'*-tetrakis(2-pyridinylmethyl)-1,2-ethanediamine); VRE, vancomycin-resistant *Enterococcus faecium*; QAC-10, quaternary ammonium cation-10.

**References:**


(1) Clatworthy, A. E.; Pierson, E.; Hung, D. T. Targeting Virulence: A New Paradigm for Antimicrobial Therapy. *Nat. Chem. Biol.* **2007**, *3*, 541–548.

(2) Wood, T. K.; Knabel, S. J.; Kwan, B. W. Bacterial Persister Cell Formation and Dormancy. *Appl. Environ. Microbiol.* **2013**, *79*, 7116–7121.

(3) Wood, T. K. Combatting Bacterial Persister Cells. *Biotechnol. Bioeng.* **2016**, *113*, 476–483.

(4) Lewis, K. Persister Cells. *Annu. Rev. Microbiol.* **2010**, *64*, 357–372.

(5) Wolcott, R.; Dowd, S. The Role of Biofilms: Are We Hitting the Right Target? *Plast. Reconstr. Surg.* **2011**, *127*, 28S–35S.

(6) Worthington, R. J.; Richards, J. J.; Melander, C. Small Molecule Control of Bacterial Biofilms. *Org. Biomol. Chem.* **2012**, *10*, 7457–7474.

(7) Garrison, A. T.; Huigens III, R. W. Eradicating Bacterial Biofilms with Natural Products and Their Inspired Analogues That Operate Through Unique Mechanisms. *Curr. Top. Med. Chem.* **2017**, *17*, 1954–1964.

(8) Machan, Z. A.; Pitt, T. L.; White, W.; Watson, D.; Taylor, G. W.; Cole, P. J.; Wilson, R. Interaction between *Pseudomonas aeruginosa* and *Staphylococcus aureus*: Description of an Antistaphylococcal Substance. *J. Med. Microbiol.* **1991**, *34*, 213–217.

(9) Price-Whelan, A.; Dietrich, L. E. P.; Newman, D. K. Rethinking “Secondary” Metabolism: Physiological Roles for Phenazine Antibiotics. *Nat. Chem. Biol.* **2006**, *2*, 71–78.

(10) Dietrich, L. E. P.; Okegbe, C.; Price-Whelan, A.; Sakhtah, H.; Hunter, R. C.; Newman, D. K. Bacterial Community Morphogenesis Is Intimately Linked to the Intracellular Redox State. *J. Bacteriol.* **2013**, *195*, 1371–1380.

(11) Garrison, A. T.; Abouelhassan, Y.; Kallifidas, D.; Bai, F.; Ukhanova, M.; Mai, V.; Jin, S.; Luesch, H.; Huigens III, R. W. Halogenated Phenazines That Potently Eradicate Biofilms, MRSA Persister Cells in Non-Biofilm Cultures, and *Mycobacterium tuberculosis*. *Angew. Chemie Int. Ed.* **2015**, *54*, 14819–

14823.

(12) Garrison, A. T.; Abouelhassan, Y.; Norwood IV, V. M.; Kallifidas, D.; Bai, F.; Thu Nguyen, M.; Rolfe, M.; Burch, G. M.; Jin, S.; Luesch, H.; Huigens III, R. W. Structure−Activity Relationships of a Diverse Class of Halogenated Phenazines That Targets Persistent, Antibiotic-Tolerant Bacterial Biofilms and *Mycobacterium tuberculosis*. *J. Med. Chem.* **2016**, *59*, 3808–3825.

(13) Young, D. B.; Perkins, M. D.; Duncan, K.; Barry, C. E. Confronting the Scientific Obstacles to Global Control of Tuberculosis. *J. Clin. Invest.* **2008**, *118*, 1255–1265.

(14) Evangelopoulos, D.; McHugh, T. D. Improving the Tuberculosis Drug Development Pipeline. *Chem. Biol. Drug Des.* **2015**, *86*, 951–960.

(15) Yang, H.; Abouelhassan, Y.; Burch, G. M.; Kallifidas, D.; Huang, G.; Yousaf, H.; Jin, S.; Luesch, H.; Huigens, R. W. A Highly Potent Class of Halogenated Phenazine Antibacterial and Biofilm-Eradicating Agents Accessed Through a Modular Wohl-Aue Synthesis. *Sci. Rep.* **2017**, *7*, 2003.

(16) Pachter, I. J.; Kloetzel, M. C. The Wohl-Aue Reaction. I. Structure of Benzo [a] Phenazine Oxides and Syntheses of 1,6-Dimethoxyphenazine and 1,6-Dichlorophenazine1. *J. Am. Chem. Soc.* **1951**, *73*, 4958–4961.

(17) Kwast, A.; Stachowska, K.; Trawczyński, A.; Wróbel, Z. N-Aryl-2-Nitrosoanilines as Intermediates in the Synthesis of Substituted Phenazines from Nitroarenes. *Tetrahedron Lett.* **2011**, *52*, 6484–6488.

(18) Cross, B.; Williams, P. J.; Woodall, R. E. The Preparation of Phenazines by the Cyclisation of 2-Nitrodiphenylamines. *J. Chem. Soc. C Org.* **1971**, *11*, 2085–2090.

(19) Laha, J. K.; Tummalapalli, K. S. S.; Gupta, A. Palladium-Catalyzed Domino Double *N*-Arylations (Inter- and Intramolecular) of 1,2-Diamino(hetero)arenes with *O, O'*-Dihalo(hetero)arenes for the Synthesis of Phenazines and Pyridoquinoxalines. *European J. Org. Chem.* **2013**, *2013*, 8330–8335.

(20) Yu, L.; Zhou, X.; Wu, D.; Xiang, H. Synthesis of Phenazines by Cu-Catalyzed Homocoupling of 2-Halogen Anilines in Water. *J. Organomet. Chem.* **2012**, *705*, 75–78.

(21) Seth, K.; Raha Roy, S.; Chakraborti, A. K.; Meyer, F.-M.; Gaunt, M. J.; Baran, P. S.; Himmel, H. J.;

Bunz, U. H. F. Synchronous Double C–N Bond Formation via C–H Activation for a Novel Synthetic Route to Phenazine. *Chem. Commun.* **2016**, *52*, 922–925.

(22) Lian, Y.; Hummel, J. R.; Bergman, R. G.; Ellman, J. A. Facile Synthesis of Unsymmetrical Acridines and Phenazines by a Rh(III)-Catalyzed Amination/Cyclization/Aromatization Cascade. *J. Am. Chem. Soc.* **2013**, *135*, 12548–12551.

(23) Challand, S. R.; Herbert, R. B.; Holliman, F. G. A New Phenazine Synthesis. The Synthesis of Griseoluteic Acid, Griseolutein A, and Methyl Diacetylgriseolutein B. *J. Chem. Soc. D Chem. Commun.* **1970**, *21*, 1423–1425.

(24) Borrero, N. V; Bai, F.; Perez, C.; Duong, B. Q.; Rocca, J. R.; Jin, S.; Huigens III, R. W. Phenazine Antibiotic Inspired Discovery of Potent Bromophenazine Antibacterial Agents against *Staphylococcus aureus* and *Staphylococcus epidermidis*. *Org. Biomol. Chem.* **2014**, *12*, 881–886.

(25) Paciaroni, N. G.; Borrero, N. V; Rocca, J. R.; Huigens III, R. W. Rapid Synthesis of Phenazine-1-Carboxylic Acid Derived SmallMolecules from Diverse Anilines: Privileged Structures for Discovery. *Res. Rev. J. Med. Org. Chem.* **2015**, *2*, 67–76.

(26) Ruiz-Castillo, P.; Buchwald, S. L. Applications of Palladium-Catalyzed C–N Cross-Coupling Reactions. *Chem. Rev.* **2016**, *116*, 12564–12649.

(27) Enthaler, S.; Company, A. Cross Coupling Reactions in Organic Synthesis Themed Issue Palladium-Catalysed Hydroxylation and Alkoxylationw. *Chem. Soc. Rev. Chem. Soc. Rev* **2011**, *40*, 4912–4924.

(28) Zheng, Z.; Dian, L.; Yuan, Y.; Zhang-Negrerie, D.; Du, Y.; Zhao, K. PhI(OAc) 2 -Mediated Intramolecular Oxidative Aryl-Aldehyde C Sp 2 –C Sp 2 Bond Formation: Metal-Free Synthesis of Acridone Derivatives. *J. Org. Chem.* **2014**, *79*, 7451–7458.

(29) Shiu, Y.-J.; Cheng, Y.-C.; Tsai, W.-L.; Wu, C.-C.; Chao, C.-T.; Lu, C.-W.; Chi, Y.; Chen, Y.-T.; Liu, S.-H.; Chou, P.-T. Pyridyl Pyrrolide Boron Complexes: The Facile Generation of Thermally Activated Delayed Fluorescence and Preparation of Organic Light-Emitting Diodes. *Angew. Chemie Int. Ed.* **2016**, *55*, 3017–3021.

(30) Safaei-Ghomi, J.; Akbarzadeh, Z.; Khojastehbakht-Koopaei, B.; Li, L.; Zhang, H.; Stranks, S. D.; Bharti,

V.; Chand, S.; Gaur, J.; Mohanty, D. C–N Cross-Coupling Reaction Catalysed by Reusable $CuCr_2O_4$ Nanoparticles under Ligand-Free Conditions: A Highly Efficient Synthesis of Triarylamines. *RSC Adv.* **2015**, *5*, 28879–28884.

(31) Błaziak, K.; Danikiewicz, W.; Mąkosza, M. How Does Nucleophilic Aromatic Substitution Really Proceed in Nitroarenes? Computational Prediction and Experimental Verification. *J. Am. Chem. Soc.* **2016**, *138*, 7276–7281.

(32) Bunnett, J. F.; Zahler, R. E. Aromatic Nucleophilic Substitution Reactions. *Chem. Rev.* **1951**, *49*, 273–412.

(33) Chen, Z.; Zeng, H.; Gong, H.; Wang, H.; Li, C.-J. Palladium-Catalyzed Reductive Coupling of Phenols with Anilines and Amines: Efficient Conversion of Phenolic Lignin Model Monomers and Analogues to Cyclohexylamines. *Chem. Sci.* **2015**, *6*, 4174–4178.

(34) Fischer, C.; Koenig, B. Palladium-and Copper-Mediated N-Aryl Bond Formation Reactions for the Synthesis of Biological Active Compounds. *Beilstein J. Org. Chem* **2011**, *7*, 59–74.

(35) Rewcastle, G. W.; Denny, W. A. Unequivocal Synthesis of Phenazine-1-Carboxylic Acids: Selective Displacement of Fluorine During Alkaline Borohydride Reduction of *N*-(2-Fluorophenyl)-3-Nitroanthranilic Acids. *Synth. Commun.* **1987**, *17*, 1171–1179.

(36) Kolb, H. C.; Finn, M. G.; Sharpless, K. B. Click Chemistry: Diverse Chemical Function from a Few Good Reactions. *Angew. Chemie Int. Ed.* **2001**, *40*, 2004–2021.

(37) Moses, J. E.; Moorhouse, A. D.; Mocharla, V. P.; Lin, R. J.; Phelps, M. E.; Kolb, H. C.; Tseng, H.-R.; Finn, M. G.; Sharpless, K. B.; Elder, J. H.; Fokin, V. V. The Growing Applications of Click Chemistry. *Chem. Soc. Rev.* **2007**, *36*, 1249–1262.

(38) Garrison, A. T.; Bai, F.; Abouelhassan, Y.; Paciaroni, N. G.; Jin, S.; Huigens III, R. W. Bromophenazine Derivatives with Potent Inhibition, Dispersion and Eradication Activities against *Staphylococcus aureus* Biofilms. *RSC Adv.* **2014**, *5*, 1120–1124.

(39) Abouelhassan, Y.; Garrison, A. T.; Burch, G. M.; Wong, W.; Norwood IV, V. M.; Huigens III, R. W. Discovery of Quinoline Small Molecules with Potent Dispersal Activity against Methicillin-Resistant

*Staphylococcus aureus* and *Staphylococcus epidermidis* Biofilms Using a Scaffold Hopping Strategy. *Bioorganic Med. Chem. Lett.* **2014**, *24*, 5076–5080.

(40) Ceri, H.; Olson, M. E.; Stremick, C.; Read, R. R.; Morck, D.; Buret, A. The Calgary Biofilm Device: New Technology for Rapid Determination of Antibiotic Susceptibilities of Bacterial Biofilms. *J. Clin. Microbiol.* **1999**, *37*, 1771–1776.

(41) Harrison, J. J.; Stremick, C. A.; Turner, R. J.; Allan, N. D.; Olson, M. E.; Ceri, H. Microtiter Susceptibility Testing of Microbes Growing on Peg Lids: A Miniaturized Biofilm Model for High-Throughput Screening. *Nat. Protoc.* **2010**, *5*, 1236–1254.

(42) Teitelbaum, A. M.; Meissner, A.; Harding, R. A.; Wong, C. A.; Aldrich, C. C.; Remmel, R. P. Synthesis, pH-Dependent, and Plasma Stability of Meropenem Prodrugs for Potential Use against Drug-Resistant Tuberculosis. *Bioorg. Med. Chem.* **2013**, *21*, 5605–5617.

(43) Festa, R. A.; Helsel, M. E.; Franz, K. J.; Thiele, D. J. Exploiting Innate Immune Cell Activation of a Copper-Dependent Antimicrobial Agent during Infection. *Chem. Biol.* **2014**, *21*, 977–987.

(44) Sandford, C.; Aggarwal, V. K. Stereospecific Functionalizations and Transformations of Secondary and Tertiary Boronic Esters. *Chem. Commun.* **2017**, *53*, 5481–5494.

(45) Gao, W.; Xing, B.; Tsien, R. Y.; Rao, J. Novel Fluorogenic Substrates for Imaging β-Lactamase Gene Expression. *J. Am. Chem. Soc.* **2003**, *125*, 11146–11147.

(46) Phelan, R. M.; Ostermeier, M.; Townsend, C. A. Design and Synthesis of a β-Lactamase Activated 5-Fluorouracil Prodrug. *Bioorg. Med. Chem. Lett.* **2009**, *19*, 1261–1263.

(47) Kwan, B. W.; Chowdhury, N.; Wood, T. K. Combatting Bacterial Infections by Killing Persister Cells with Mitomycin C. *Environ. Microbiol.* **2015**, *17*, 4406–4414.

(48) Arts, I. S.; Gennaris, A.; Collet, J.-F. Reducing Systems Protecting the Bacterial Cell Envelope from Oxidative Damage. *FEBS Lett.* **2015**, *589*, 1559–1568.

(49) Tracy, M.; Acton, E. M. Synthesis of Tetrahydrobenzo[b]phenazines as Anthracyclinone N-Isosteres. *J. Org. Chem.* **1984**, *49*, 5116–5124.

(50) Bacon, R. G. R.; Hamilton, S. D. Metal Ions and Complexes in Organic Reactions. Part XVII. Iron(II)-Promoted Conversions of Nuclear-Substituted Anilinopyridines into Pyridoquinoxalines. *J. Chem. Soc. Perkin Trans. 1* **1974**, 1965–1969.

(51) Vivian, D. L.; Hartwell, J. L.; Waterman, H. C. Phenazine Syntheses. III. 1. Miscellaneous Phenazines. *J. Org. Chem.* **1954**, *19*, 1641–1645.

(52) Yosioka, I.; Ashikawa, R. Studies on Phenazines. XXII. *Yakugaku Zasshi* **1959**, *79*, 896–899.

(53) Mohr, R.; Hertel, H. Verfahren Zur Herstellung von Phenazinen. Patent (Germany): 1197462, Jul 29, 1965.

(54) *Methods for dilution antimicrobial susceptibility tests for bacteria that grow aerobically; approved standards,* 8th ed. (M7-M8); Clinical and Laboratory Standards Institute: Wayne, PA, 2009.

(55) Chen, Q.-Y.; Liu, Y.; Cai, W.; Luesch, H. Improved Total Synthesis and Biological Evaluation of Potent Apratoxin S4 Based Anticancer Agents with Differential Stability and Further Enhanced Activity. *J. Med. Chem.* **2014**, *57*, 3011–3029.

(56) Furtado, G. L.; Medeiros, A. A. Single-Disk Diffusion Testing (Kirby-Bauer) of Susceptibility of *Proteus mirabilis* to Chloramphenicol: Significance of the Intermediate Category. *J. Clin. Microbiol.* **1980**, *12*, 550–553.

(57) Blanchard, C.; Brooks, L.; Beckley, A.; Colquhoun, J.; Dewhurst, S.; Dunman, P. M. Neomycin Sulfate Improves the Antimicrobial Activity of Mupirocin-Based Antibacterial Ointments. *Antimicrob. Agents Chemother.* **2016**, *60*, 862-872.

**Figures:**

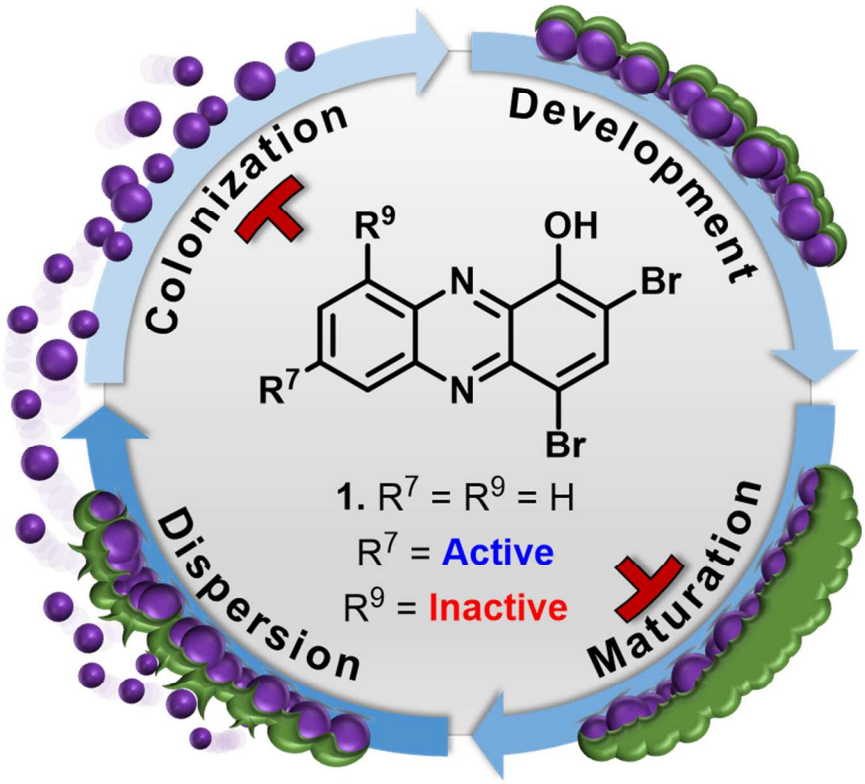


**Figure 1.** Halogenated phenazine analogues exhibit antibacterial activity against antibiotic-susceptible planktonic cells and eradication activity against antibiotic-tolerant bacteria within mature biofilms.

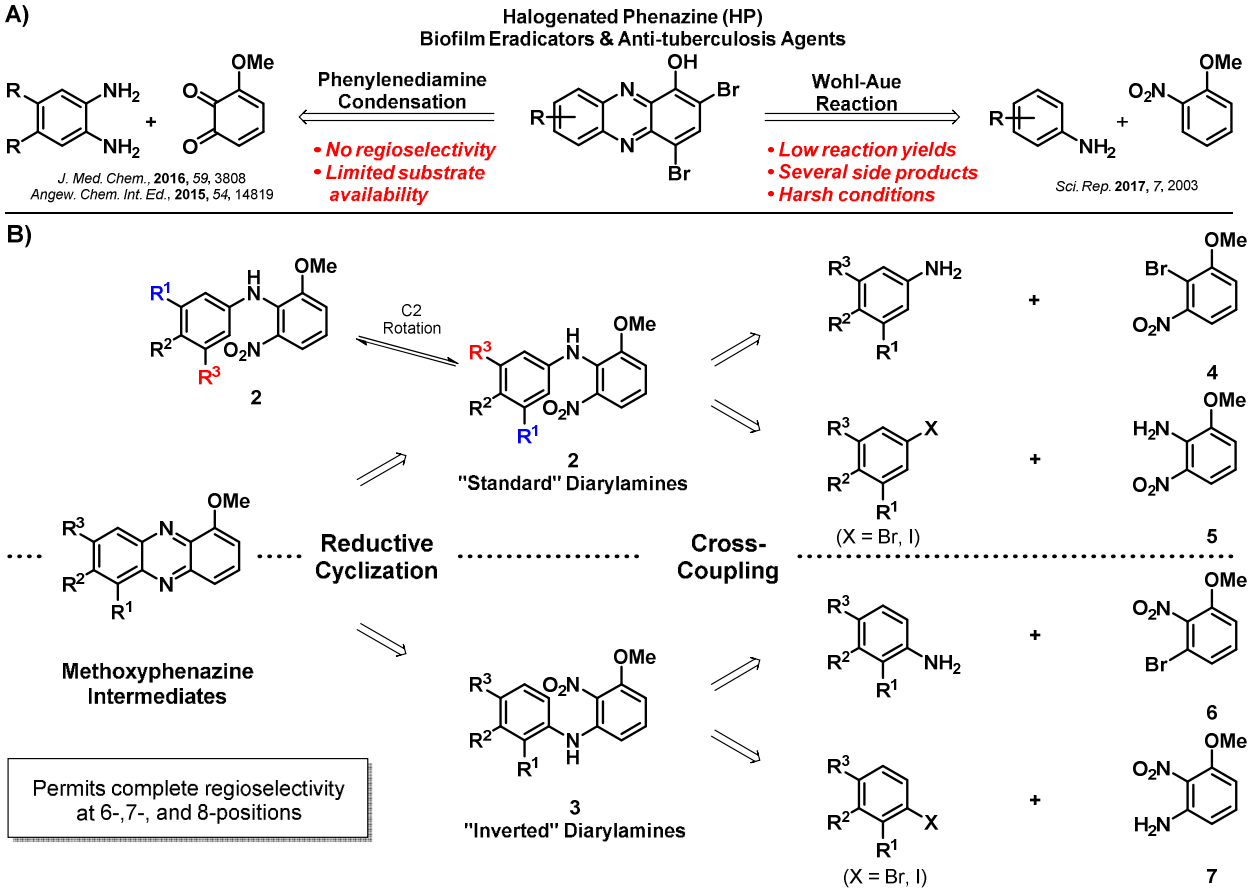


**Figure 2**. A) Phenazine syntheses previously utilized by our group along with the associated shortcomings. B) Synthetic strategy and theoretical substrate scope of cross-coupling/reductive cyclization using varied orientations of coupling starting materials.

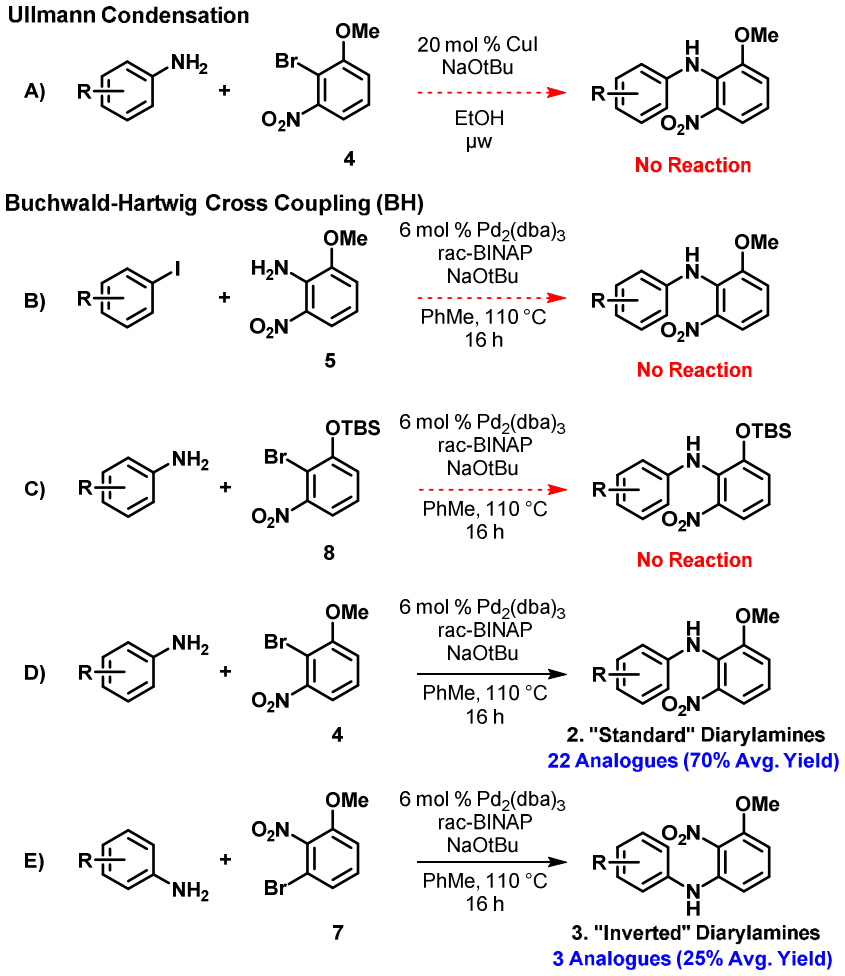


**Figure 3.** Investigation into coupling conditions for diarylamine intermediate synthesis.

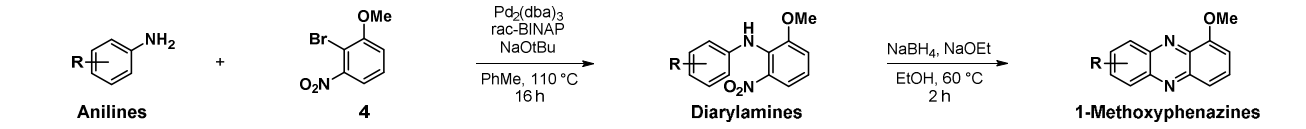


| Aniline | Diarylamine | 1-Methoxyphenazine | Aniline | Diarylamine | 1-Methoxyphenazine |
|---|---|---|---|---|---|
|  | 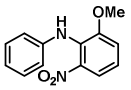 **9** (81%) | 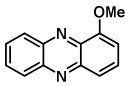 **31** (80%) | 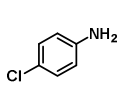 | 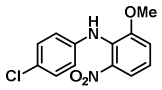 **20** (83%) | 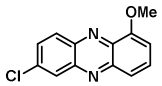 **42** (71%) |
| 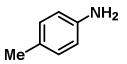 | 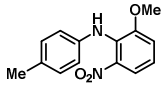 **10** (94%) | 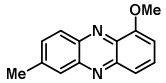 **32** (83%) | 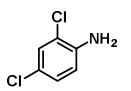 | 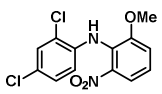 **21** (60%) | 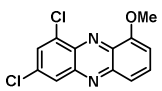 **43** (15%) |
| 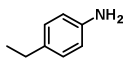 | 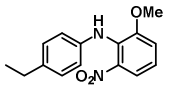 **11** (71%) | 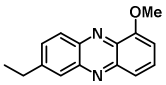 **33** (97%) | 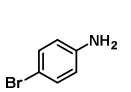 | 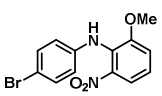 **22** (83%) | 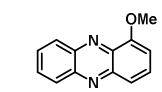 **31** (71%) |
| 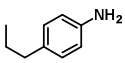 | 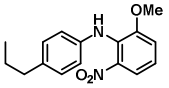 **12** (71%) | 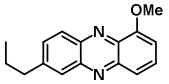 **34** (70%) | 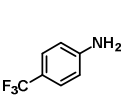 | 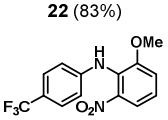 **23** (38%) | 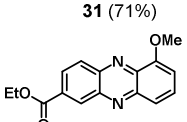 **44** (84%) |
| 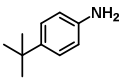 | 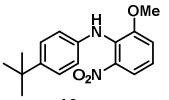 **13** (63%) | 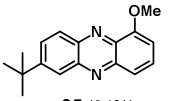 **35** (94%) | 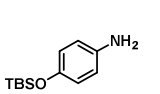 | 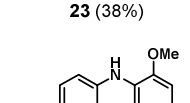 **24** (53%) | 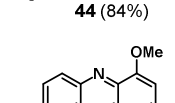 **45** (64%) |
| 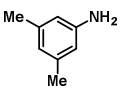 | 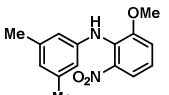 **14** (67%) | 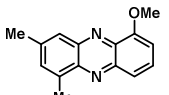 **36** (86%) | 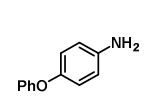 | 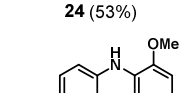 **25** (75%) | 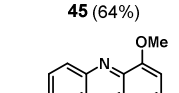 **46** (71%) |
| 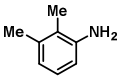 | 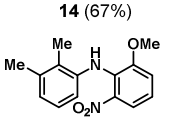 **15** (65%) | 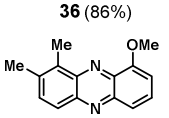 **37** (44%) |  |  **26** (50%) |  **47** (89%) |
|  |  **16** (60%) |  **38** (46%) |  |  **27** (66%, 2 steps) |  **48** (68%) |
|  |  **17** (91%) |  **39** (60%) |  |  **28** (83%) |  **49** (31%) |
|  |  **18** (76%) |  **40** (42%) |  |  **29** (81%, 2 steps) |  **50** (64%) |
|  |  **19** (81%) |  **41** (79%) |  |  **30** (47%) |  **51** (74%) |

**Average Buchwald-Hartwig (BH) Cross-Coupling Yield: 70%** **Average Reductive Cyclization (RC) Yield: 68%**

**Figure 4**. 1-Methoxyphenazine syntheses starting from key building block **4** and indicated anilines with each intermediate diarylamine shown.

A)

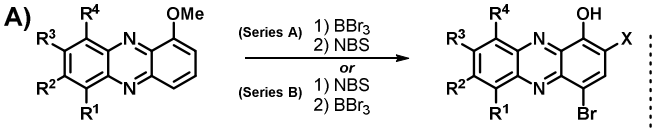


| 1-OMe Phenazine | $R^1$ | $R^2$ | $R^3$ | $R^4$ | X | $BBr_3$ Yield | NBS Yield | Series[a] | HP |
|---|---|---|---|---|---|---|---|---|---|
| **32** | H | Me | H | H | Br | 91% | 52% | **A** | **52** |
| **33** | H | Et | H | H | Br | 93% | 74% | **A** | **53** |
| **34** | H | Pr | H | H | Br | 88% | 76% | **A** | **54** |
| **35** | H | *t*-Bu | H | H | Br | 80% | 61% | **A** | **55** |
| **36** | Me | H | Me | H | Br | 89% | 73% | **A** | **56** |
| **37** | H | H | Me | Me | Br | 83% | 66% | **A** | **57** |
| **38** | H | H | H | Et | Br | 90% | 76% | **A** | **58** |
| **39** | Me | Me | Me | H | Br | 89% | 84% | **A** | **59** |
| **41** | H | OEt | H | H | Br | 88% | 88% | **A** | **60** |
| **42** | H | Cl | H | H | Br | 92% | 95% | **A** | **61** |
| **44** | H | COOEt | H | H | Br | 85% | 35% | **A** | **62** |
| **46** | H | OPh | H | H | Br | 88% | 55% | **A** | **63** |
| **47** | H[b] | $NEt_2$ | H | H | Br | 94% | 53% | **A** | **64** |
| **48**[c] | H | $CH_2Br$ | H | H | Br | 87% | 73% | **A** | **65** |
| **32** | H | Me | H | H | H | 96% | 88% | **B** | **66** |
| **33** | H | Et | H | H | H | 92% | 83% | **B** | **67** |
| **36** | Me | H | Me | H | H | 82% | 55% | **B** | **68** |
| **42** | H | Cl | H | H | H | 90% | 96% | **B** | **69** |

**Average Demethylation Yield: 89%  Average Bromination Yield: 71%**

B)

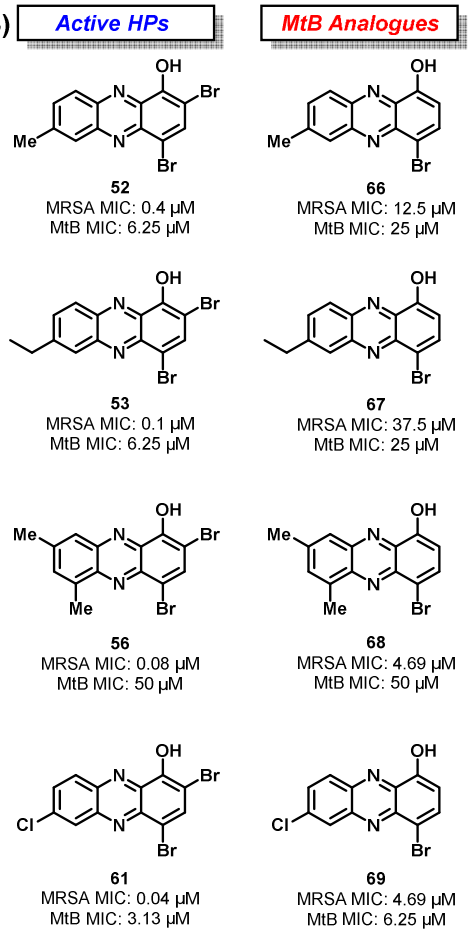


**Figure 5**. A) Synthesis of the halogenated phenazine library with corresponding demethylation and bromination yields. Note: [a] Series A analogues were synthesized to target MRSA, MRSE, and VRE while Series B analogues were synthesized to target MtB. [b] $R^1$ = Br following bromination reaction. [c] Primary bromide obtained following demethylation of **48**. B) SAR of anti-MtB (H37Ra) analogues relative to the corresponding dibrominated counterparts (MRSA = MRSA BAA-1707).

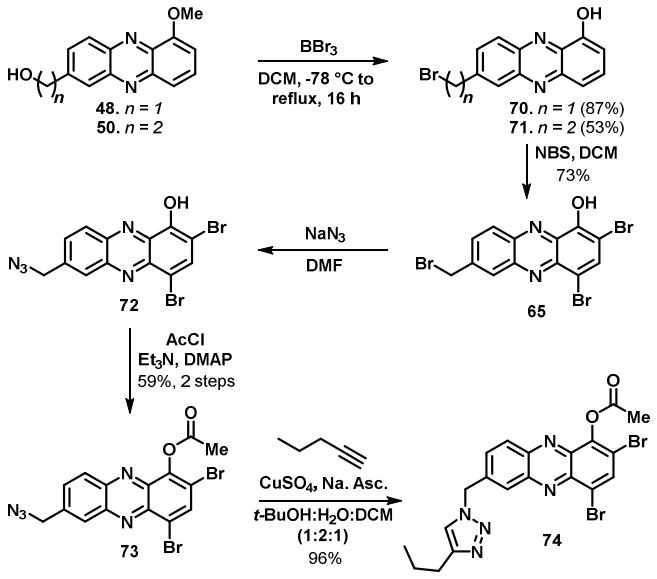


**Figure 6.** Chemical synthesis of triazole-HP **74** from 1-methoxyphenazine **48**.

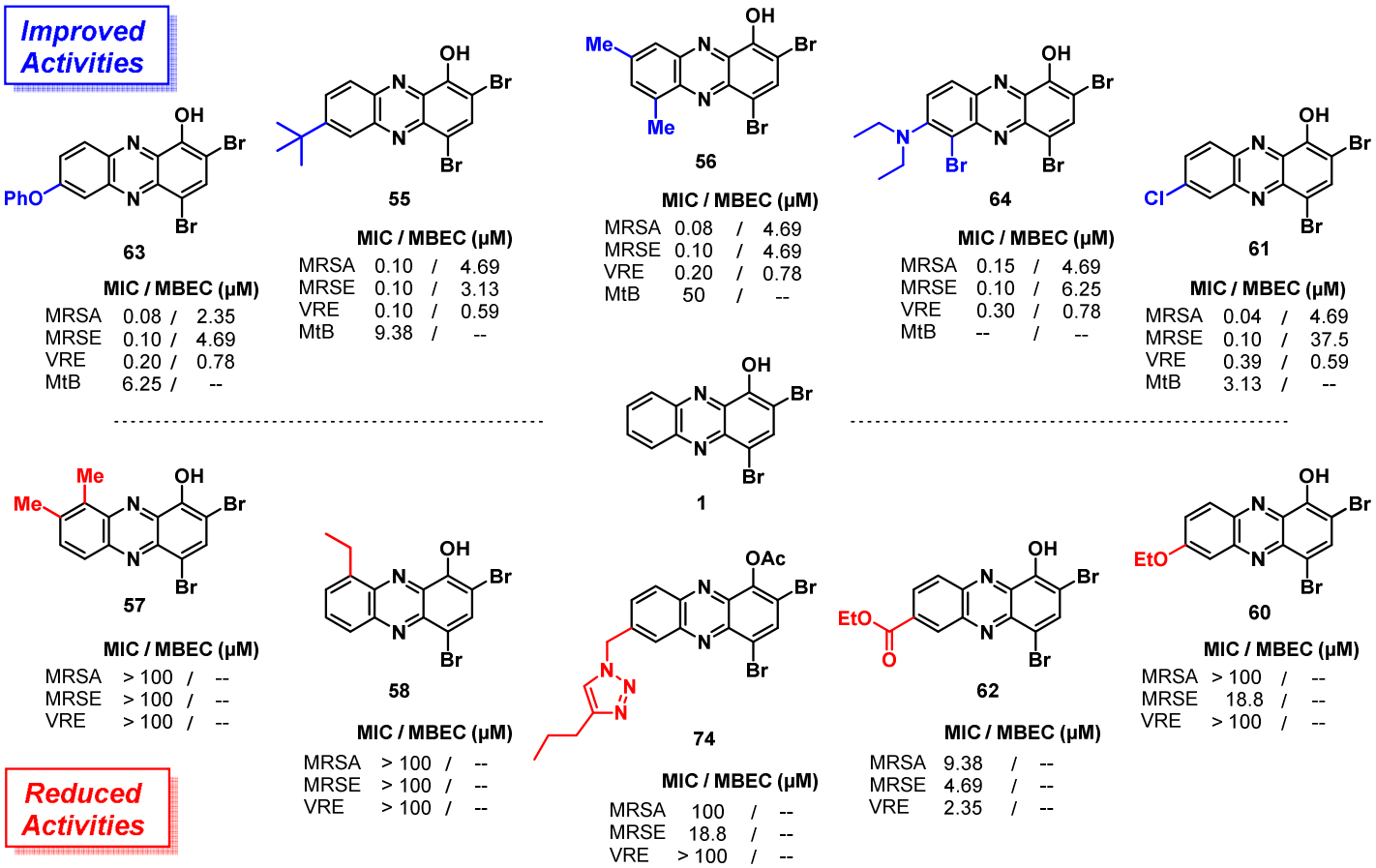


**Figure 7**. Activity profiles for select HP analogues relative to parent HP **1**. *Note:* The MRSA data in this figure is from our MRSA BAA-1707 results.

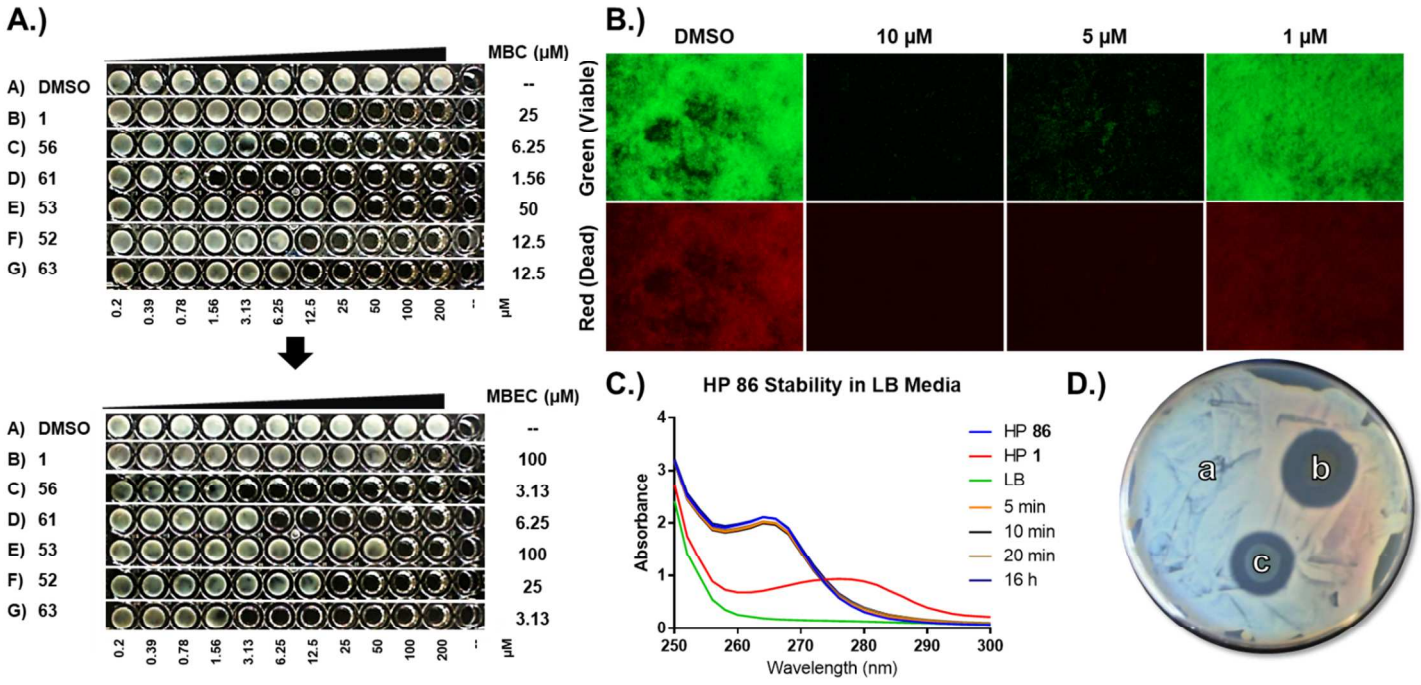


**Figure 8.** A.) Calgary Biofilm Device (CBD) assay for MBC/MBEC determination of select HPs against MRSA BAA-1707. B.) Live/dead fluorescence imaging of MRSE biofilms following treatment with HP **61.** C.) UV-Vis evaluation of QuAOCOM **86** stability in LB media. D.) MRSA BAA-1707 agar diffusion assay with HP **61** and HP QuAOCOM **87**: a) DMSO, b) HP **61**, c). HP QuAOCOM **87** (prodrug). Zones of inhibition (area) are 4.25 ± 0.3 $cm^2$ and 2.86 ± 0.2 $cm^2$ for **61** and **87**, respectively.

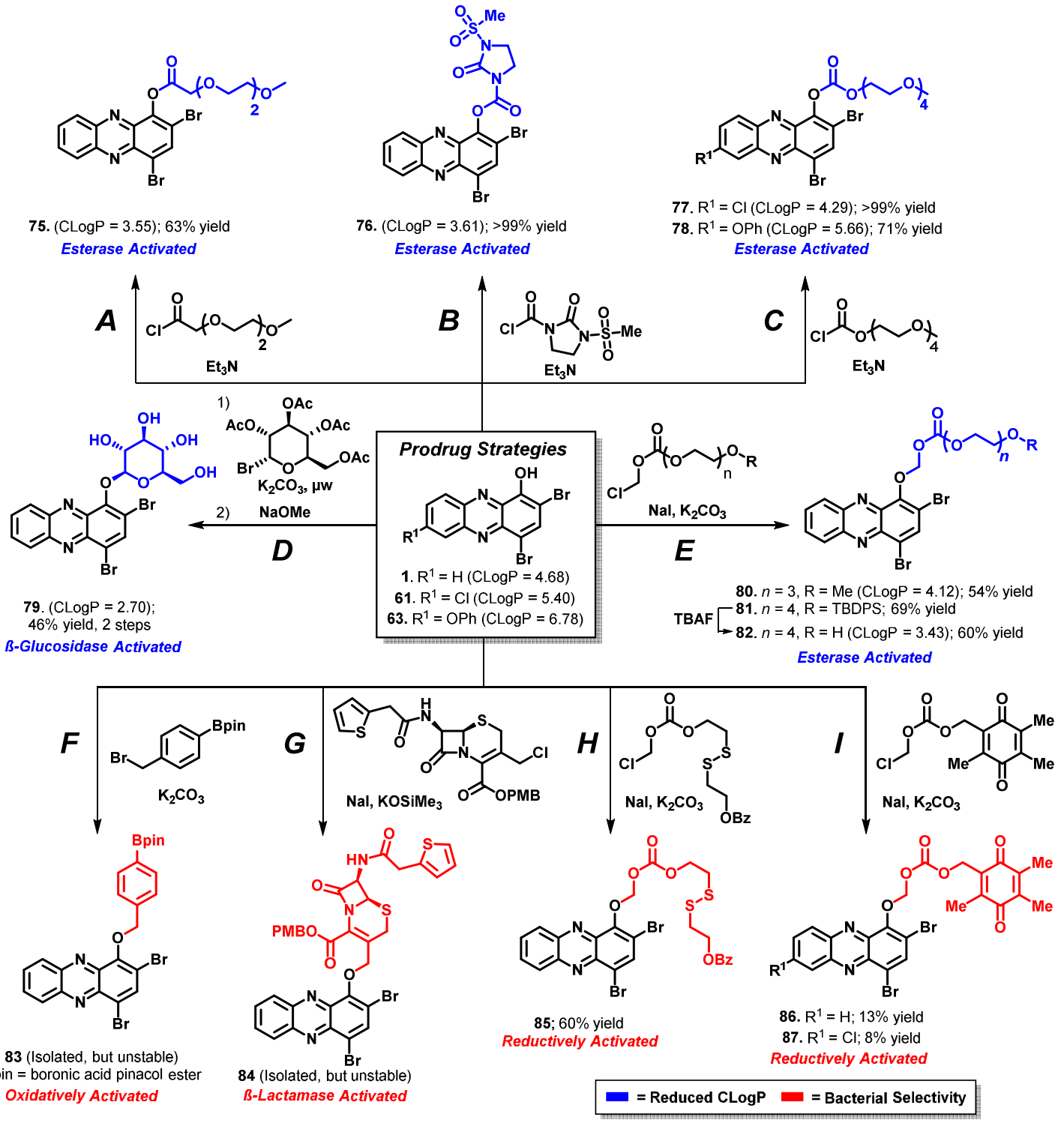


**Figure 9**. Summary of phenolic prodrug strategies used to attain improved water solubility or bacterial selectivity and proposed mechanisms of prodrug activation (CLogP values determined by ChemDraw).

## Tables:

**Table 1.** Summary of Gram-positive antibacterial activities (MIC values reported) and HeLa cell cytotoxicity of HP analogues and comparator compounds, including several antibiotics. All biological results are reported in micromolar (μM) concentrations.

| Compound | MRSA-1707 MIC | MRSA-2 MIC | MRSE 35984 MIC | VRE 700221 MIC | MtB H37Ra MIC | HeLa cell Cytotoxicity $IC_{50}$ | Selectivity Index |
|---|---|---|---|---|---|---|---|
| **1** | 1.17[a] | 1.56 | 1.17[a] | 6.25 | 25 | > 100 | > 109 |
| **52** | 0.39 | -- | 0.3[a] | 2.35[a] | 6.25 | > 100 | > 256 |
| **53** | 0.1 | 0.59[a] | 0.1 | 2.35[a] | 6.25 | > 50 | > 500 |
| **54** | 0.1 | -- | 0.15[a] | 3.13 | -- | > 50 | > 500 |
| **55** | 0.1 | 0.1 | 0.1 | 0.1 | 9.38[a] | > 100 | > 1,000 |
| **56** | 0.075[a] | 0.3[a] | 0.1 | 0.2 | 50 | > 100 | > 1,333 |
| **57** | > 100 | -- | > 100 | > 100 | -- | -- | -- |
| **58** | > 100 | -- | > 100 | > 100 | -- | -- | -- |
| **59** | 0.59[a] | -- | 0.1 | 4.69[a] | -- | > 100 | > 169 |
| **60** | > 100 | -- | 18.8[a] | > 100 | -- | -- | -- |
| **61** | 0.038[a] | 0.1 | 0.1 | 0.39 | 3.13 | > 100 | > 2,632 |
| **62** | 9.38[a] | 18.8[a] | 4.69[a] | 2.35[a] | -- | -- | -- |
| **63** | 0.075[a] | 0.39 | 0.1 | 0.2 | 6.25 | > 100 | > 1,333 |
| **64** | 0.15[a] | 0.3[a] | 0.1 | 0.3[a] | -- | > 100 | > 667 |
| **66** | 12.5 | -- | 12.5 | 25 | 25 | > 100 | > 8 |
| **67** | 37.5[a] | -- | 9.38[a] | 12.5 | 25 | > 100 | > 3 |
| **68** | 4.69[a] | -- | 2.35[a] | 9.38[a] | 50 | > 100 | > 21 |
| **69** | 4.69[a] | -- | 18.8[a] | 25 | 6.25 | > 100 | > 21 |
| **74** | 100 | -- | 18.8[a] | > 100 | -- | -- | -- |
| **QAC-10** | 4.69[a] | 3.13 | 2.35[a] | 2.35[a] | -- | -- | -- |
| **EDTA** | 25 | -- | -- | -- | -- | -- | -- |
| **TPEN** | 50 | -- | -- | -- | -- | -- | -- |
| **Vancomycin** | 0.39 | 0.59[a] | 0.78 | > 100 | -- | -- | -- |
| **Daptomycin** | 3.13 | 4.69[a] | -- | -- | -- | -- | -- |
| **Linezolid** | 12.5 | 3.13 | -- | -- | -- | -- | -- |
| **Rifampin** | -- | 0.1[b] | 0.1[b] | -- | -- | -- | -- |

| | | | | | | | |
|---|---|---|---|---|---|---|---|
| **Streptomycin** | -- | -- | -- | -- | 1.32 | -- | -- |

**Note:** [a] Midpoint value for independent experiments that yielded a 2-fold range. [b] Corresponds to the lowest concentration tested. MIC values were obtained from a minimum of three independent experiments. HPs were tested against HeLa cells at 25, 50 and 100 μM in three independent experiments. Selectivity Index was calculated by dividing the cytotoxicity $IC_{50}$ by the MIC against MRSA-1707.

**Table 2.** Summary of biofilm eradication studies against MRSA, MRSE and VRE biofilms. All biological results are reported in micromolar (μM) concentrations.

| Compound | MRSA-1707 MBC / MBEC | MRSA-2 MBC / MBEC | MRSA BAA-44 MBC / MBEC | MRSE 35984 MBC / MBEC | VRE 700221 MBC / MBEC | % Hemolysis at 200 μM |
|---|---|---|---|---|---|---|
| **1** | 37.5[a] / 150[a] | 50 / 100 | 37.5[a] / 150[a] | 50[b] / 100[b] | 23.5[a] / 9.38[a] | ≤ 1 |
| **52** | 18.8[a] / 37.5[a] | -- | -- | 18.8[a] / 37.5[a] | 12.5 / 3.13 | ≤ 1 |
| **53** | 75[a] / 150[a] | 75[a] / 150[a] | 75[a] / 75[a] | 50[b] / 75[a] | 50[b] / 2.35[a] | 3.0 |
| **54** | 37.5[a] / 75[a] | -- | -- | 25 / 37.5[a] | 25[b] / 18.8[a] | 2.1 |
| **55** | 4.69[a] / 4.69[a] | 3.13 / 3.13 | 18.8[a] / 9.38[a] | 6.25 / 3.13 | 1.56[b] / 0.59[a] | ≤ 1 |
| **56** | 9.38[a] / 4.69[a] | 9.38[a] / 37.5[a] | 37.5[a] / 37.5[a] | 4.69[a] / 4.69[a] | 1.17[a] / 0.78 | 2.2 |
| **59** | 150[a] / 75[a] | -- | -- | 25 / 25[b] | 4.69[a] / 1.17[a] | 1.3 |
| **61** | 1.17[a] / 4.69[a] | 6.25 / 25 | 6.25[a] / 18.8[a] | 6.25 / 37.5[a] | 1.56[b] / 0.59[a] | ≤ 1 |
| **63** | 9.38[a] / 2.35[a] | 4.69[a] / 4.69[a] | 25 / 18.8[a] | 9.38[a] / 4.69[a] | 2.35[a] / 0.78 | ≤ 1 |
| **64** | 9.38[a] / 4.69[a] | -- | -- | 9.38[a] / 6.25[b] | 2.35[a] / 0.78 | ≤ 1 |
| **CCCP** | -- | 31.3 / 1000 | -- | 31.3 / 93.8[a] | -- | -- |
| **NAC** | -- | > 2000 / > 2000 | -- | > 2000 / > 2000 | > 2000 / > 2000 | -- |
| **QAC-10** | 93.8[a] / 93.8[a] | 31.3[b] / 125 | -- | 31.3 / 31.3 | 3.0[a] / 3.0[a] | > 99 |
| **Pyrazinamide** | -- | > 2000 / > 2000 | -- | -- | -- | -- |
| **Vancomycin** | 3.9 / > 2000 | 3.0[a] / > 2000 | 7.8 / > 2000 | 3.0[a] / > 2000 | > 200 / 150[a] | ≤ 1 |
| **Daptomycin** | 125 / > 2000 | 62.5[b] / > 2000 | -- | -- | -- | 1.7 |
| **Linezolid** | 31.3 / > 2000 | 15.6 / > 2000 | -- | -- | 4.69[b] / 1.56 | ≤ 1 |
| **Doxycycline** | -- | 2.0 / 46.9[a] | -- | -- | -- | -- |
| **Rifampin** | -- | 2.0 / 46.9[a] | -- | 3.0[a] / 15.6[b] | -- | -- |
| **EDTA** | > 2000 / > 2000 | 2000 / > 2000 | -- | 1000 / > 2000 | -- | 3.0 |
| **TPEN** | 250 / > 2000 | -- | -- | -- | 188[a] / > 2000 | ≤ 1 |

**Note:** [a] Midpoint value for independent experiments that yielded a 2-fold range. [b] Corresponds to a 4-fold range in independent experiments. MBC/MBEC values were obtained from three to six independent experiments.

**Table 3.** Summary of biological investigations with HP prodrugs (entries for HPs **1**, **61** and **63** are included, all prodrugs were synthesized from these three parent HPs). All biological results are reported in micromolar (μM) concentrations.

| Compound | MRSA BAA-1707 MIC | MRSA BAA-1707 MBC / MBEC | MRSE 35984 MIC | MRSE 35984 MBC / MBEC | VRE 700221 MIC | VRE 700221 MBC / MBEC | HeLa $IC_{50}$ | % Hemo. at 200 μM | Serum Stability $t_{1/2}$ (min) |
|---|---|---|---|---|---|---|---|---|---|
| **1** | 1.17[a] | 18.8 / 150[a] | 1.17 | 50[b] / 100[b] | 6.25 | 23.5[a] / 9.38[a] | > 100 | ≤ 1 | n.a. |
| **61** | 0.038[a] | 1.17[a] / 4.69[a] | 0.1 | 6.25 / 37.5[a] | 0.39 | 1.56[b] / 0.59[a] | > 100 | ≤ 1 | n.a. |
| **63** | 0.075[a] | 9.38[a] / 2.35[a] | 0.1 | 9.38[a] / 4.69[a] | 0.2 | 2.35[a] / 0.78 | > 100 | ≤ 1 | n.a. |
| **75** | 0.59[a] | 18.8[a] / 75[a] | 0.59[a] | 9.38[a] / 37.5[a] | 3.13 | 6.25 / 4.69[a] | > 100 | 1.2 | < 1 |
| **76** | 0.59[a] | 37.5[a] / 75[a] | 1.56 | 18.8[a] / 37.5[a] | 3.13 | 9.38[a] / 9.38[a] | > 100 | ≤ 1 | < 1 |
| **77** | 0.0005[a] | 6.25[b] / 9.38[a] | 0.038[a] | 9.38[a] / 18.8[a] | 0.1 | 1.17[a] / 0.59[a] | > 100 | 1.1 | < 1 |
| **78** | 0.1 | 18.8[a] / 4.69[a] | 0.075[a] | 9.38[a] / 1.56 | 0.3[a] | 0.78 / 1.17[a] | -- | ≤ 1 | < 1 |
| **79** | > 100 | -- | > 100 | -- | > 100 | -- | -- | ≤ 1 | > 260 |
| **80** | > 100 | -- | > 100 | -- | > 100 | -- | -- | 1.4 | 15.8 ± 0.9 |
| **82** | > 100 | -- | > 100 | -- | > 100 | -- | > 100 | 2.7 | 7.3 ± 3.6 |
| **85** | > 100 | -- | > 100 | -- | > 100 | -- | > 100 | 1.3 | -- |
| **86** | 2.35[a] | 25 / 75[a] | 2.35[a] | 37.5[a] / 150[a] | 9.38[a] | 12.5 / 9.38[a] | -- | ≤ 1 | 6.3 ± 3.3 |
| **87** | 0.15[a] | 6.25 / 12.5 | 0.39 | 12.5 / 25 | 1.56 | 3.13[b] / 3.13[b] | > 100 | 2.7 | 11.4 ± 2.8 |
| **Vanco.** | 0.39 | 3.9 / > 2000 | 0.78 | 3.0[a] / > 2000 | > 100 | > 200 / 150[a] | -- | ≤ 1 | -- |

**Note:** [a] Midpoint value for independent experiments that yielded a 2-fold range. [b] Midpoint value for independent experiments that yielded a 4-fold range. "n.a." not applicable due to compound being a non-prodrug HP (comparator). "--" HP prodrug not tested. All values were obtained from three to six independent experiments (e.g., MIC, MBEC, HeLa cytotoxicity, RBC hemolysis, serum half-lives).

**Table of Contents Graphic.**

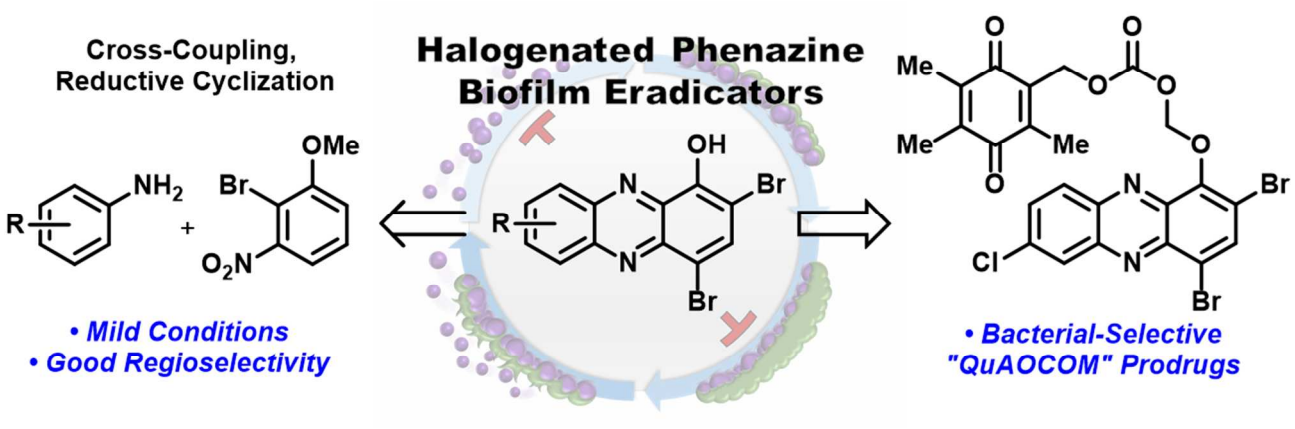

# An Efficient Buchwald-Hartwig/Reductive Cyclization for the Scaffold Diversification of Halogenated Phenazines: Potent Antibacterial Targeting, Biofilm Eradication and Prodrug Exploration

Corresponding author: Robert W. Huigens III
E-mail: rhuigens@cop.ufl.edu

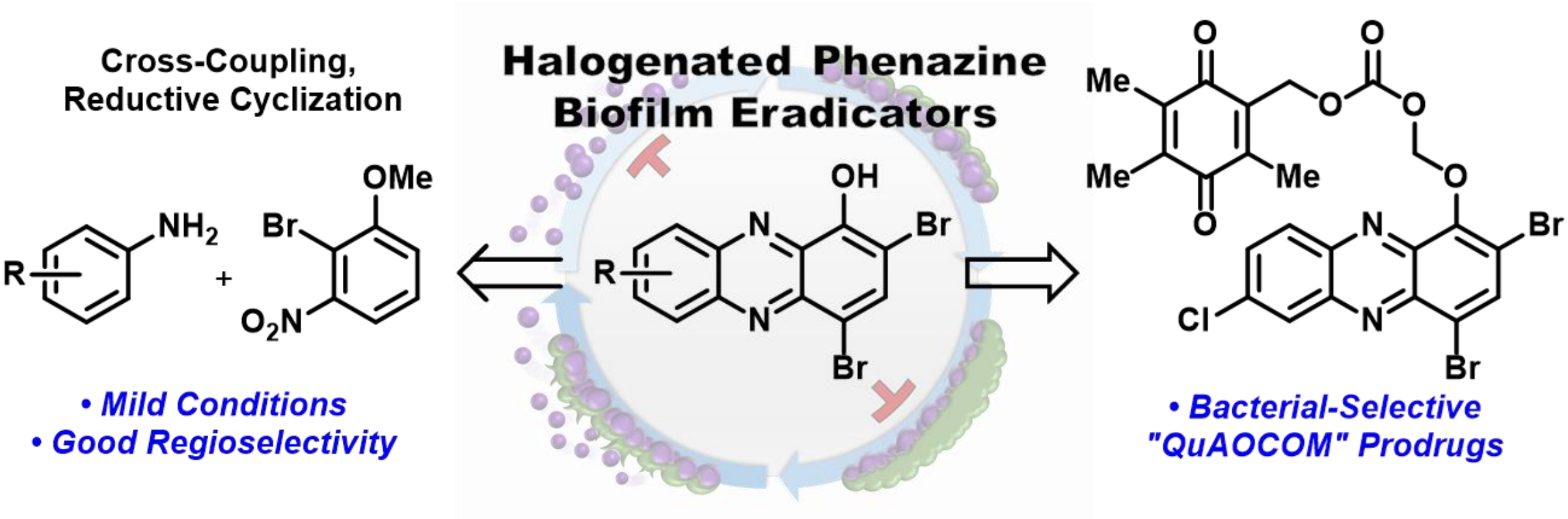


• Bacterial-Selective "QuAOCOM" Prodrugs